

CRANIAL AND MANDIBULAR OSTEOLOGY OF THE EARLY TRIASSIC ARCHOSAURIFORM *OSMOLSKINA CZATKOWICENSIS* FROM POLAND

MAGDALENA BORSUK-BIAŁYNICKA and SUSAN E. EVANS

Borsuk-Białynicka, M. and Evans, S.E. 2009. Cranial and mandibular osteology of the Early Triassic archosauriform *Osmolskina czatkowicensis* from Poland. *Palaeontologia Polonica* **65**, 235–281.

The basal archosauriform *Osmolskina czatkowicensis* Borsuk-Białynicka *et* Evans, 2003 from the Early Olenekian karst deposits of Czatkowice near Kraków (southern Poland) shares a unique mosaic of skull character states with the African Anisian genus *Euparkeria*. This is considered, with reservation, as a basis for including them in the family Euparkeriidae Huene, 1920. A provisional diagnosis is given for this family, but no unique derived character states have been identified to support its monophyly. *Osmolskina* and *Euparkeria* differ primarily in snout structure. The vertical orientation of the basisphenoid, and the postero-ventral position of the entry foramina for cerebral branches of the internal carotid artery place both genera crownward of the proterosuchids. Lack of ossification of the medial wall of the otic capsule and the partial retention of pterygoid teeth exclude them from crown-group Archosauria, while they also lack erythrosuchid autapomorphies (including extremely short cervical vertebrae).

Key words: Early Triassic, Poland, basal Archosauriformes, euparkeriids.

Magdalena Borsuk-Białynicka [borsuk.b@twarda.pan.pl], Institut Paleobiologii PAN, Twarda 51/55, PL-00-818 Warszawa, Poland.

Susan E. Evans [ucgasue@ucl.ac.uk], Research Department of Cell and Developmental Biology, UCL, University College London, Gower Street, London, WC1E 6BT, UK.

Received 20 April 2005, accepted 29 May 2008



INTRODUCTION

Osmolskina is a small Early Triassic euparkeriid-grade archosauriform, known from the karst fissure deposits of Czatkowice near Kraków (southern Poland, Czatkowice 1 locality). *Osmolskina* is the largest and most common component of a diverse small vertebrate assemblage from these deposits including a small prolacertiform-grade reptile (Borsuk-Białynicka and Evans 2009), two basal lepidosauromorphs (Evans and Borsuk-Białynicka 2009a), including a basal kuehneosaurid (Evans 2009), procolophonids (Borsuk-Białynicka and Lubka 2009) and temnospondyls (Szyszkin and Sulej 2009). A tiny stem-frog, *Czatkobatrachus polonicus* (Evans and Borsuk-Białynicka 1998, 2009b; Borsuk-Białynicka and Evans 2002), and some fish, also belong to this fauna.

The Early Triassic archosauriforms are crucial to an understanding of the incompletely known section of phylogeny preceding the split between the crocodylian and dinosaur/avian lineages. Terrestrial faunas of this age have been recorded from all over the world, beginning with the most complete assemblages of eastern European Russia (Ochev and Shishkin 1985, 1989; Shishkin and Ochev 1993), through the Lower and Middle Germanic Buntsandstein (Induan-Olenekian in age), the North American Wupatki Member (the basal member of Moenkopi Formation, Morales 1987), the upper part of the Chinese Guodikeng Formation (Jimsarian, Fuguan, and probably Ordosian faunachrons, Lucas 1993), to the Gondwanan formations: the African Karoo (*Lystrosaurus* and *Cynognathus* zones), the Antarctic Fremouw, Indian Panchet, and Australian Arcadia formations.

The Early Triassic fauna was not as uniform over Pangaea as was that of the Permian. Therapsids were present in the Gondwanan assemblages along with large temnospondyls, basal archosauriforms, and procolophonians, but were absent from Laurasian assemblages, except for those of the Induan period (Battail 1993). Small non-archosauriform reptiles and other microvertebrates were distributed more randomly. If the Czatkowice 1 fauna is correctly dated to the earliest Late Olenekian (Szyszkin and Sulej 2009), this is the first terrestrial vertebrate assemblage of this age recorded from Euramerica outside the Cis-Urals and East European Platform.

The objective of the present paper is to give a detailed description of the cranial morphology of *Osmolskina czatkowicensis*. The systematic position of *Osmolskina*, its relationships with *Euparkeria*, and the status of the Euparkeriidae, as well as the information value of cranial characters at this stage of evolution, are also discussed.

Institutional acronyms. — BPS, Bayerische Staatssammlung für Paläontologie und Historische Geologie, München, Germany; GPIT, Institute und Museum für Geologie und Paläontologie, Universität Tübingen, Germany; MZ, Museum of the Earth, Polish Academy of Sciences, Warsaw, Poland; PIN, Paleontological Institute, Russian Academy of Sciences, Moscow, Russia; SAM, South African Museum, Cape Town, Republic of South Africa; SMNS, Staatliches Museum für Naturkunde, Stuttgart, Germany; ZPAL, Institute of Paleobiology, Polish Academy of Sciences, Warsaw, Poland.

Acknowledgements. — We are indebted to Józef Wieczorek and Mariusz Paszkowski (Jagiellonian University, Kraków) who discovered the Czatkowice 1 breccia, and kindly offered it for study. Our warmest thanks go to Teresa Maryńska (Museum of the Earth) and the late Halszka Osmólska (Institute of Paleobiology), both from the Polish Academy of Sciences, who generously offered the Czatkowice material to us. MBB expresses her warmest thanks to following persons and institutions that allowed her to study archosauriform material in their collections: Rupert Wild at the Staatliches Museum für Naturkunde, Stuttgart, Michael Maisch at the Institut und Museum für Geologie und Palaeontologie, Universität Tübingen, and Helmut Mayr at the Bayerische Staatssammlung für Paläontologie und Historische Geologie, München. We are grateful to the referees who greatly helped in improving the manuscript. Thanks are also due to the following staff members of the Institute of Paleobiology, Polish Academy of Sciences in Warsaw: Ewa Hara for preparation of the material, Cyprian Kulicki, and Janusz Błaszcyk for SEM microphotographs, and Aleksandra Hołda-Michalska for preparing computer illustrations. The work of MBB was partly supported by the State Committee of Scientific Research, KBN grant No 6 PO4D 072 19.

GEOLOGICAL SETTING

Czatkowice 1 was the largest of several sediment infilled caves developed in the Early Carboniferous limestone quarry. (Paszkowski and Wieczorek 1982). Paszkowski (2009) gives a more detailed account of the geological setting of Czatkowice 1 locality. As a result of economic exploitation of the quarry, the Czatkowice 1 fissure no longer exists. The original age determination of the assemblage, as Early Olenekian on the basis of *Gnathorhiza* (Dipnoi) teeth and procolophonian material (Borsuk-Białynicka *et al.* 2003), has been revised to earliest Late Olenekian on the basis of temnospondyl material (Shishkin and Sulej 2009). This suggests Czatkowice 1 karst deposits are slightly younger than the upper part of the Vetlugian Superhorizon of the East European biozonation (Shishkin *et al.* 1995, 2000; Shishkin and Ochev 1985; Ochev and Shishkin 1989). According to Ochev (1993), and Shishkin and Ochev (1993), the locality must have been within the xeric circumequatorial belt occurring at this latitude in Northern Pangaea. The vertebrate assemblage from Czatkowice 1, including both terrestrial and amphibious animals and some fish (Borsuk-Białynicka *et al.* 1999), indicates that the material was deposited primarily in a freshwater pool, probably developed within an oasis in an otherwise arid Central European Scythian environment. At a higher taxonomic level, the assemblage corresponds to others in Laurasia, but it differs dramatically in the size of the animals included (see below) and was probably taphonomically biased. The taphonomy of the Czatkowice 1 locality has recently been studied by Cook and Trueman (2009). The authors suggest that the diagenetic pathways included reworking of the skeletal remains, originally incorporated into sediments at the bottom of ephemeral lakes and pools, and their redeposition in nearby cave systems after a short fast transport during periods of stormy weather and flooding.

MATERIAL AND METHODS

General comments. — The material is completely disarticulated, and often broken into pieces, both before deposition and in preparation. Chemical breakdown of the matrix by acetic acid is the only method of preparation for this material. Freshly dissociated pieces may sometimes be matched with one another and glued together. The bones are mostly white, orange or dark brown, and are generally preserved three-dimensionally. Most of them show relatively little abrasion. To date, about 100 specimens have been catalogued, but there are hundreds of other specimens. The materials are stored at the Museum of the Earth and the Institute of Paleobiology, Polish Academy of Sciences, Warsaw.

Attribution of osteological elements. — The primary criteria for the attribution of disarticulated bones to particular species are size ranges and relative frequency of particular morphotypes in the samples. Robustness of elements, sculpture, articular facet fit, and phylogenetically relevant characters are the next criteria. The composition of fossil assemblages is biased by the differential preservational potential of particular elements belonging to the same animal, and those of different animals. Nonetheless, the relative percentage of elements in a fossil sample seems to be fairly consistent for each member of the assemblage. The largest (20 mm dentary length) and most frequent remains belong to Archosauriformes and are generally considered conspecific. Some less common bones exceeding the normal variability range of the genus have been excluded as representing a separate taxon, their attribution being relegated to future studies. Next in size in the assemblage is a prolacertiform-grade reptile (Borsuk-Białynicka and Evans 2009a), but the dimensions overlap. The remaining material is a mixture of medium-sized procolophonids, and tiny bones (up to a few mm in length) including two rarer lepidosauromorphs (Evans and Borsuk-Białynicka 2009a; Evans 2009), tiny temnospondyls (Shishkin and Sulej 2009), and the stem frog *Czatkobatrachus polonicus* (Evans and Borsuk-Białynicka 1998, 2009b; Borsuk-Białynicka and Evans 2002). The dimensions of these animals do not overlap the range of *Osmolskina czatkowicensis*.

Reconstruction (Fig. 1A, B). — Based on counts of the best preserved bone fragments, such as frontals, quadrates and articulars, the number of *Osmolskina* individuals of the Czatkowice 1 taphocoenosis amounts to several hundred. Some more fragile bones are represented by single specimens. The reconstruction of the whole skull on the basis of such material requires some scaling of elements. The shape of paired premaxillae in the horizontal plane (Fig. 2A₁) is conclusive for the horizontal outline of the skull as a whole, while the

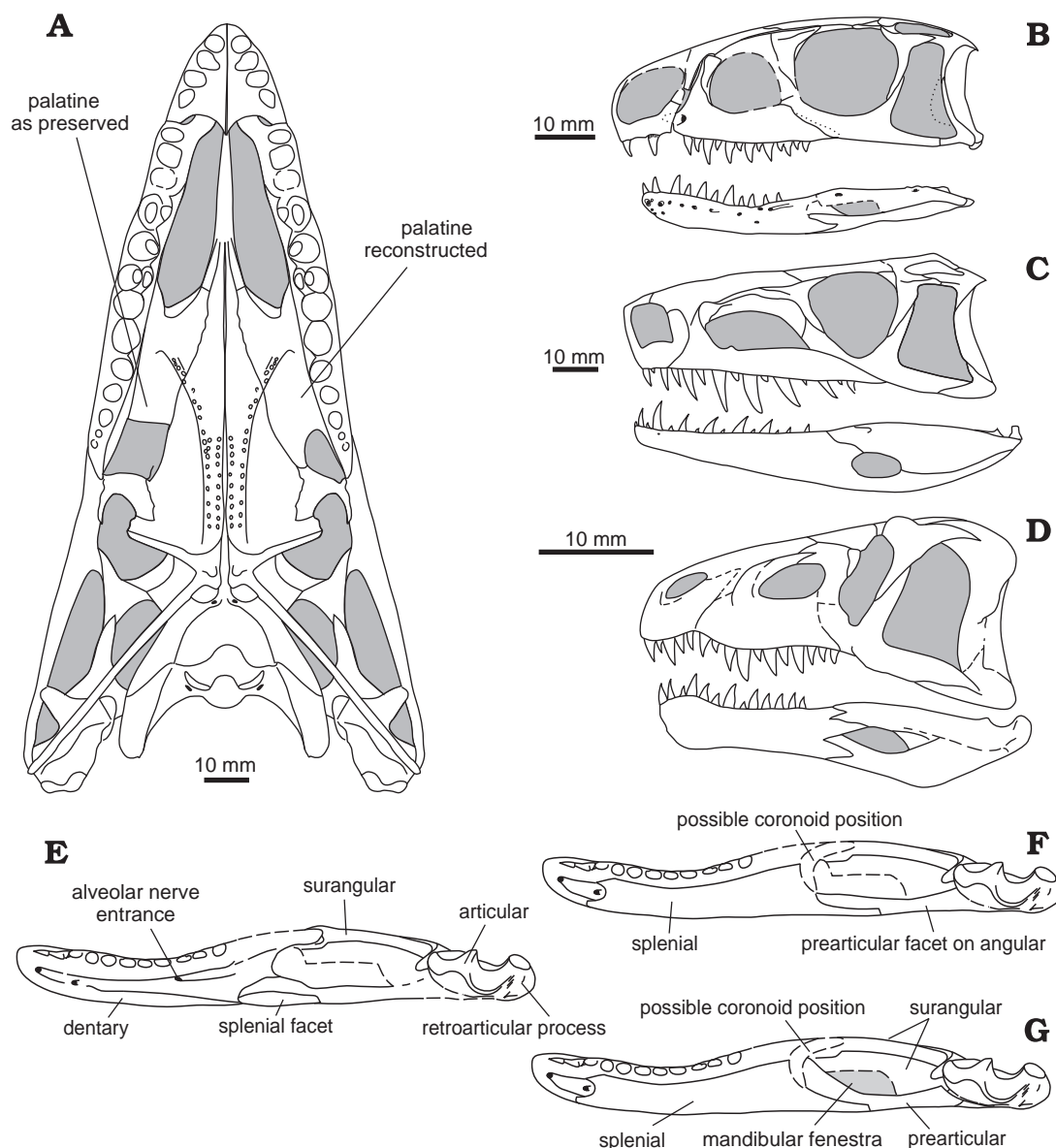


Fig. 1. *Osmolskina czatkowicensis* Borsuk-Białynicka *et* Evans, 2003, Early Triassic of Czatkowice 1, Poland. Reconstructions: A. Skull. B. Skull with mandible. E–G. Mandibles, different views of mandibular bones; without splenial and prearticular (E), without prearticular (F), complete (G); out of scale. C. *Euparkeria capensis* Broom, 1913, skull with mandible (from Ewer 1965, fig. 2). D. *Erythrosuchus africanus* Broom, 1905, skull with mandible (from Gower 2003, fig. 1). Ventral (A), left lateral (B–D), and medial (E–G) views.

profile of the nasal process of the premaxilla (Fig. 2B₂, D₁) affects that of the skull in a sagittal plane. The length of skull roof bones should correspond to that of the maxilla articulated with the jugal and quadratojugal, whereas the gap between the skull roof bones and the ventral profile of the skull should match the size of the quadrate, which closes the skull outline from behind. These interdependent dimensions help to correct the relative sizes of missing parts, especially those of the maxillae. There are no complete specimens of the maxilla. The posterior parts of the maxillae preserved as separate pieces (Figs 5B, 14D, E) are tentatively considered as belonging to the same species if they match the size and thecodont tooth implantation of the anterior fragments. The length of the maxilla has been deduced on the basis of the gap left between the jugal and the anterior part of the maxilla. Among other problematic elements, the pterygoids barely fit within the space outlined by the maxillae and jugals (Fig. 1A) unless aligned obliquely with the dentigerous fields descending ventro-laterad to produce a V-shaped concave palate open ventrally.

In spite of a poor ossification of the walls of the braincase, the component bones are fairly well preserved and allow a reconstruction of the whole element and of its details (Figs 17, 25).

The braincase structure of the basal archosauriforms *Sarmatosuchus*, *Erythrosuchus*, and *Euparkeria*, and of the basal crurotarsians *Batrachotomus* and *Stagonolepis* (Gower and Sennikov 1997, Gower 1997, Gower 2002, Gower and Weber 1998, and Gower and Walker 2002, respectively) has been used as a reference. Nonetheless, the complex nature of this part of the skeleton, and preservation problems, substantiate the use of extant comparative material. Lizards, although more distantly related to archosauriforms than crocodiles, have a less specialized skull structure than the latter group. Hence, lizard skulls have been used as the basis of structural interpretations, and the terminology of Oelrich (1956) has been applied.

Several points contribute to the reconstruction of the structure and the proper life position of the mandible. Most informative is the mandibular symphysis, which determines the alignment of the dentaries and their inclination to one another.

Individual age and size. — The braincase specimens show poor ossification of the internal surface, with almost no finished bone (except for the passage of nerve canals) suggesting that they are immature. The rarity of fully attached teeth may further suggest that much of the material is immature. However, cervical vertebrae, that match the size of the skull bones, have neurocentral suture closed which is a criterion of maturity in crocodiles and, most probably, in crocodylian relatives (Brochu 1996). The most abundant vertebrae of *Osmolskina*, with neural arches fused, are about the size of those of an adult individual of the lizard *Heloderma suspectum* (ZPAL RV/26) used for comparison. This specimen has a skull 60 mm in length, which corresponds to the average skull length reconstructed for *Osmolskina*. The closure of the neurocentral sutures does not necessarily mean a complete stoppage of growth (Brochu 1996).

The term “grade” used herein refers to taxa that share the same combination of primitive and derived characters but no unique synapomorphies.

SYSTEMATIC BACKGROUND

The Archosauriformes (*sensu* Gauthier 1986) correspond to what Romer (1956) designated as Archosauria. They belong to the diapsid subgroup Archosauromorpha (Gauthier, 1986) along with rhynchosaurs, “prolacertiforms” and a number of isolated genera which stand as plesions (Evans 1988). According to Gauthier’s definition, Archosauria is restricted to the two extant groups, Aves and Crocodylia, their most recent common ancestor and all its descendants, and thus correspond to the “crown group Archosauria” of *e.g.*, Benton and Clark (1988), or to Avesuchia of Benton (1999). Archosauriformes is a more-inclusive taxon encompassing a series of taxa on the archosaurian stem. Phylogenetic relationships within this assemblage have been studied by many authors (Benton and Clark 1988; Gauthier 1986; Sereno and Arcucci 1990; Sereno 1991; Parrish 1993; Juul 1994; Gower and Sennikov 1996; Gower 1997; Gower and Walker 2002). Gower and Wilkinson (1996) demonstrated a substantial agreement in the general topology of cladograms resulting from those studies, all supporting the monophyly of Archosauria *sensu* Gauthier (1986). The semistrict reduced consensus cladogram of those analyses (Gower and Wilkinson 1996, fig. 4) is a framework (Fig. 31) for discussion in the present paper. According to this tree, proterochampsids, euparkeriids, erythrosuchids, and proterosuchids are consecutive outgroups of Archosauria. The exclusion of these taxa from the Archosauria is based mainly on the retention of a palatal dentition (lacking in Archosauria *sensu* Gauthier 1986) and a virtually transverse construction of the tarsus, rather than the posteriorly deflected calcaneum of archosaurs (Juul 1994, p. 38). It is also supported by braincase data, most notably by a lateral position of the entrances of the cerebral branches of the internal carotid arteries into the parbasiphonoid (Gower and Weber 1998).

Proterosuchids are the most basal of the non-crown-group archosauriforms, including the medium-sized *Archosaurus* from the Late Permian of Russia (Tatarinov 1960; Sennikov 1995; Gower and Sennikov 2000), *Proterosuchus* from the Early Triassic (*Lystrorhynchus* Zone) of South Africa (Cruickshank 1972), *Fugusuchus hejiapanensis* from the Early Triassic of China (Cheng 1980; Gower and Sennikov 1997), and the Mid Triassic Russian *Sarmatosuchus otschevi* (Gower and Sennikov 1997).

Erythrosuchids are large archosauriform predators recorded from the Late Olenekian through Ladinian of Russia, China, Argentina, and South Africa, and reviewed by Parrish (1992; see also Gower 2003). *Euparkeria* from the Anisian of the South African Karoo Formation (*Cynognathus* Zone), the only adequately known

euparkeriid genus, was roughly contemporaneous with *Erythrosuchus* in South Africa (Mid Triassic, early Anisian, *Cynognathus* Zone; Hancox *et al.* 1995; Shishkin *et al.* 1995), but is much smaller in size.

Euparkeria capensis Broom, 1913 became the type genus of the family Euparkeriidae Huene, 1920. *Browniella africana* (Broom, 1913) from exactly the same site as *Euparkeria capensis* is currently considered conspecific with the latter (Haughton 1922; Ewer 1965). Among four Chinese genera assigned to the family, *Wangisuchus* Young, 1964, from the Upper Ehrmayng Formation (early Mid Triassic), *Xilousuchus* Wu, 1981 (Early Triassic, Heshanggou Fm), and *Halazhaisuchus* Wu, 1982 (Early Triassic, Lower Ermaying Fm; Lucas 1993) are of doubtful affinity (Gower and Sennikov 2000). Sennikov (1989) added a new possible euparkeriid, *Dorosuchus neoetus*, from the Anisian Donguz Formation to this list (Gower and Sennikov 2000). *Turfanosuchus* Young, 1973 from the late Early Triassic Lower Ehrmayng Formation, originally regarded as an euparkeriid (Young 1973), is more probably a crurotarsian (Parrish 1993 and Gower and Sennikov 2000, *contra* Wu and Russell 2001).

The Mid through Late Triassic Proterochampsidae (Sill 1967; Romer 1971, 1972a) includes medium-sized, lightly built semiaquatic crocodile-like animals from South and North America. Their highly distinctive anatomy is poorly documented.

SYSTEMATIC PALEONTOLOGY

Clade Archosauromorpha Huene, 1946

Clade Archosauriformes Gauthier, 1986

Family **Euparkeriidae** Huene, 1920

Provisional diagnosis. — Basal archosauriforms differing from crown-group Archosauria in the lateral orientation of the calcaneal tuber and the unossified medial wall of the otic capsule. They share a vertical orientation of the basisphenoid and the absence of an astragalocalcaneal canal with all archosauriforms except proterosuchids. They differ from erythrosuchids in the lighter construction of the skeleton, relatively smaller skull, and generally more elongate cervical vertebrae (centrum length/depth usually around 1.4–1.6 instead of 0.4–1.0 in erythrosuchids).

Generic composition. — *Euparkeria* Broom, 1913, *Osmolskina* Borsuk-Białynicka *et* Evans, 2003, most probably *Dorosuchus* Sennikov, 1989.

Occurrence. — Olenekian to Anisian of Pangaea (localities in Europe and South Africa).

Genus *Osmolskina* Borsuk-Białynicka *et* Evans, 2003

Diagnosis. — As for the species.

Osmolskina czatkowicensis Borsuk-Białynicka *et* Evans, 2003

Holotype: The fragmentary maxilla ZPAL RV/77 (Borsuk-Białynicka and Evans 2003, fig. 2A; and Fig. 5 herein).

Type horizon: Early Late Olenekian.

Type locality: Czatkowice 1, southern Poland.

Occurrences. — Type locality only.

Emended diagnosis. — An euparkeriid similar to *Euparkeria*, but smaller, having a modal skull length of about 60 mm, modal femur and tibia length about 40 mm and 30 mm, respectively. Differs from *Euparkeria* in having a slightly overhanging premaxilla (but less so than in proterosuchids) that has a deeper body (maximum length to depth 10:3 in *Osmolskina*, *versus* 10:4 in *Euparkeria*), a more oblique posterolateral process (sloping at an angle of 50° *versus* almost 90° in *Euparkeria*). The posterolateral process was weakly attached to the maxilla (with no peg and socket articulation developed), and was probably separated from it by a slit-like additional antorbital space. *Osmolskina* differs from *Euparkeria* in having a subquadrangular nasal process of the maxilla, and a barely recessed antorbital fenestra. The preorbital part of the skull is less elongated than in *Euparkeria*. The maximum maxilla length to depth is 5:1 in *Osmolskina czatkowicensis*, *versus* 7:1 in *Euparkeria capensis*. The estimated tooth count is 13 in both species, but the teeth are less compressed in *O.*

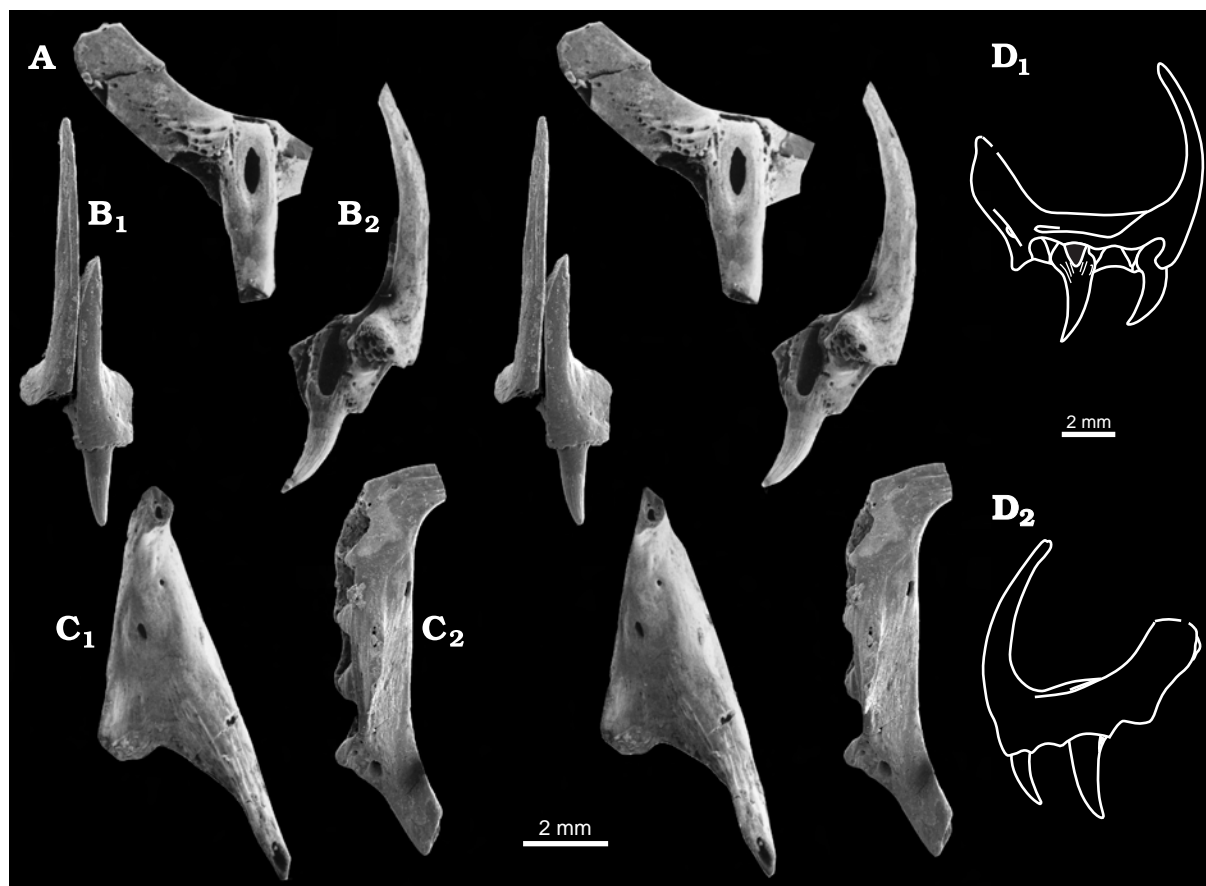


Fig. 2. *Osmolskina czatkowicensis* Borsuk-Białynicka *et* Evans, 2003, Early Triassic of Czatkowice 1, Poland. Premaxillae. **A.** The posterolateral process ZPAL RV/83, in medial view. **B.** Articulated ZPAL RV/88a and 88b, in anterior (**B₁**) and right lateral (**B₂**) views. **C.** ZPAL RV/31, in dorsal (**C₁**) and medial (**C₂**) views. **D.** Reconstructions of premaxillae, in medial (**D₁**) and lateral (**D₂**) views. A–C, SEM stereo-pairs.

czatkowicensis. In *Osmolskina* the ventral bordering of the orbit is smoothly concave, and the orbit more rounded while tapering ventrally in *Euparkeria*. The mandible of *Osmolskina* does not increase in depth posteriorly unlike that of *Euparkeria*. *Osmolskina* differs from *Euparkeria* in the shorter humerus; more twisted femur (distal to proximal end angle is about 55° in *Osmolskina*, 32° in *Euparkeria*), and the extremely anterior position of the coracoid foramen or notch. Compared to *Dorosuchus* (femur about 90 mm, tibia about 70 mm in length, femur twist about 40°) *Osmolskina* is smaller and has the femur more twisted.

Material. — About 100 catalogued skull bones, including isolated braincase and mandibular elements, and several hundred less complete cranial elements.

SKULL ROOF

Premaxilla. — The premaxilla is robust and has three processes (Fig. 2). The main body is swollen to include four deep alveoli (Fig. 3A₂, D) medially separated by interdental plates. A ventrally directed tubercle borders the tooth row. The posteriormost part of the bone is blunt, and more or less fits a concavity produced by the medially inclined anterior process of the maxilla (Fig. 3B, C₂) just anterior to the exit of the superior alveolar canal, but the contact is by no means precise. The posterolateral process passes obliquely backwards at an angle of about 50° to the long axis of the body. Distally, the medial surface of the process is sculptured by oblique (anteroventral) ridges (Fig. 2A) that are possibly for ligaments connecting the premaxilla to the nasal. The configuration of bones in this region suggests that the former overlapped the latter, but the overlapping parts are never preserved in the material. The posterior margin of the posterolateral process is acute and does not show any facets for the maxilla. The medial process of the premaxilla forms a triangular flange. Its medial border bears a symphyseal surface. The processes of both sides fill the space between the articulated premaxillae and

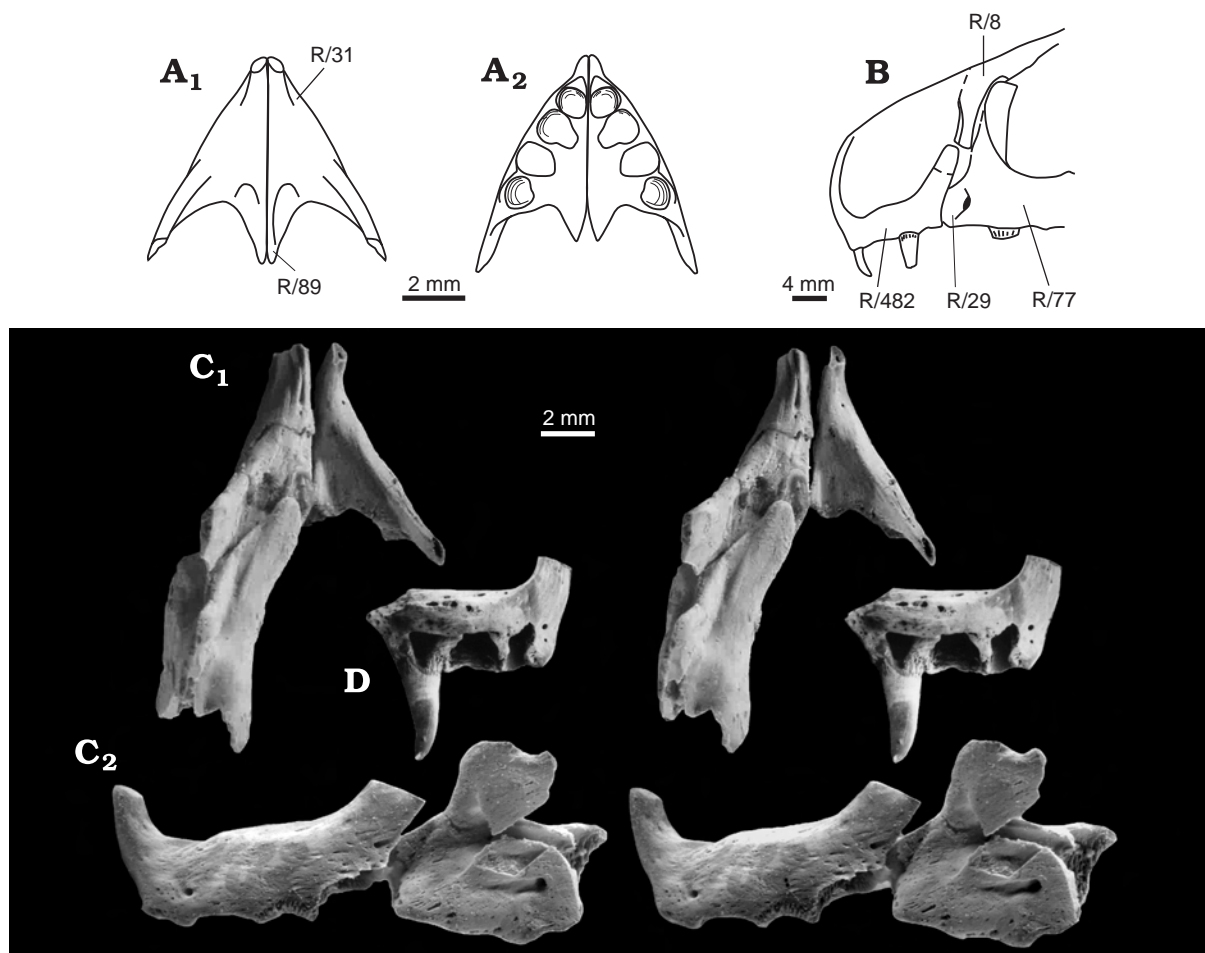


Fig. 3. *Osmolskina czatkowicensis* Borsuk-Białynicka *et* Evans, 2003, Early Triassic of Czatkowice 1, Poland. **A.** Reconstruction of articulated premaxillae, in dorsal (A_1) and ventral (A_2) views. **B.** Reconstruction of anterior part of skull, in left lateral view. **C.** Premaxillae: ZPAL RV/30 (left) and 31 (right) combined with anterior part of maxilla ZPAL RV/29, in dorsal (C_1) and left lateral (C_2) views. **D.** Left premaxilla ZPAL RV/78, in medial view. C, D SEM stereo-pairs. Shortened catalogue numbers indicate the specimens on which the reconstruction is based.

protrude posteromedially. They leave no space for the entrance of the vomer (Figs 2C₁, 3A₁, A₂). On each side, a slight dorsal concavity received the underside of the anterior process of the maxilla (Fig. 3C₁). The premaxilla was probably held in place mainly by connective tissue.

The anterior (nasal) process is very tall, thin (Fig. 2B), and posteriorly concave. In transverse section, it is medially flat and laterally evenly convex. It suggests the external nares were fairly large. It tapers distally and becomes sub-tetrahedric at about 1/4 of its height, with the anterior and lateral surfaces flat, the former being narrower than the latter. The lateral surface probably served for the nasal contact. In anterior view, the articulated premaxillae are very slender. A longitudinal furrow follows the symphysis line on each side (Fig. 2B₁).

The length of the premaxilla body varies from ca. 7 to 10 mm. Smaller specimens have more slender proportions and the angle of the posterior process to the horizontal is more acute. This variability is tentatively ascribed to allometric growth.

Maxilla. — There is no complete specimen. Usually, the maxilla breaks into four pieces that are difficult to match to one another. The central section (Fig. 4A) is usually sub-triangular but it develops dorsally into a tall, narrow sub-quadrangular nasal process (Fig. 6) and posteriorly into a horizontal tooth bearing ramus (ca. 30% the total height of the maxilla Fig. 6A, D–F). The borders of the nasal process are almost vertical, but become more oblique ventrally as the process broadens out. The lateral surface of the central portion is flat. Together with the curvature of the premaxilla (see above) and the position of the nasal (see below) it suggests that the snout was deep. Only the posterodorsal border of the maxilla curves slightly medially. The ventral border of the

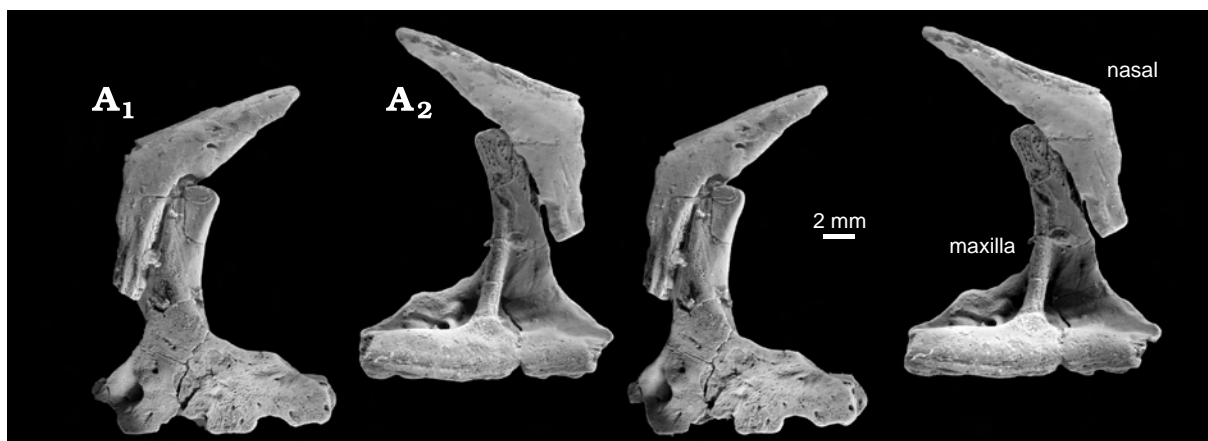


Fig. 4. *Osmolskina czatkowicensis* Borsuk-Białynicka *et* Evans, 2003, Early Triassic of Czatkowice 1, Poland. Anterior fragment of the holotype maxilla ZPAL RV/77 combined with a fragmentary nasal ZPAL RV/8, in lateral (A₁) and medial (A₂) views. SEM stereo-pairs.

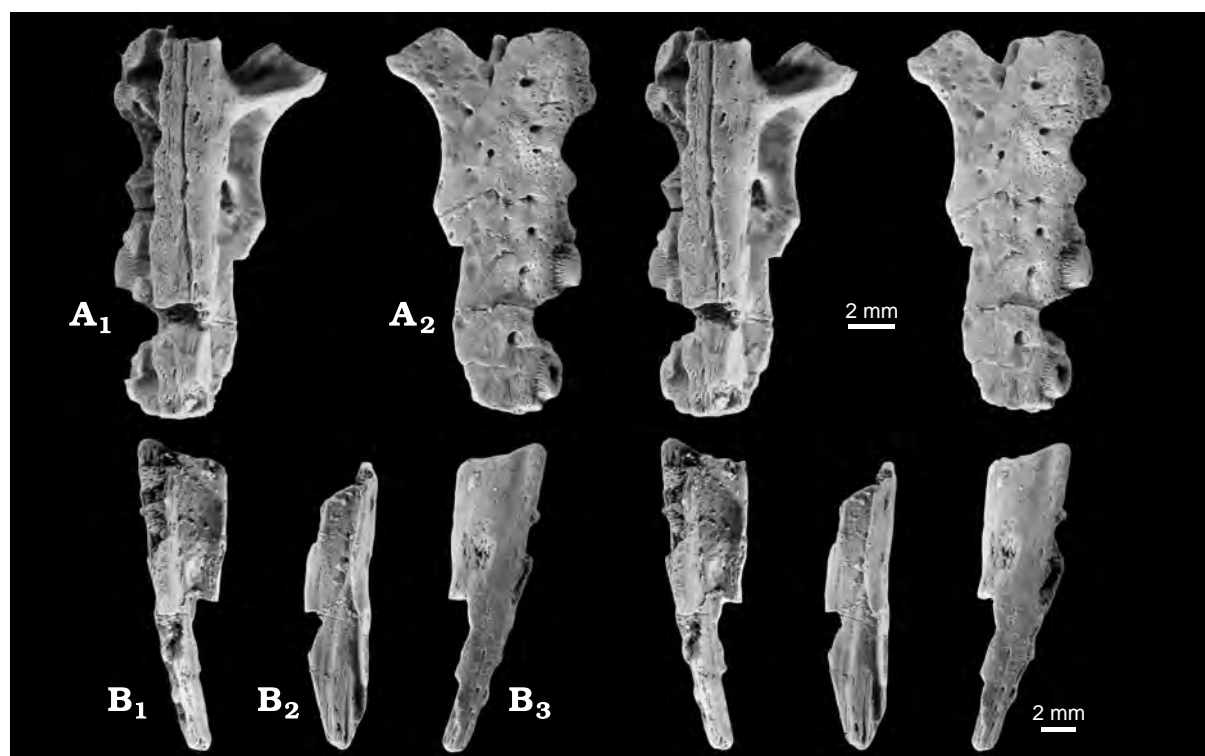


Fig. 5. *Osmolskina czatkowicensis* Borsuk-Białynicka *et* Evans, 2003, Early Triassic of Czatkowice 1, Poland. **A.** Middle part of right maxilla ZPAL RV/81, in lingual (A₁) and labial (A₂) views. **B.** Posterior fragment of right maxilla ZPAL RV/160, in lingual (B₁), dorsal (B₂), and labial (B₃) views. SEM stereo-pairs.

maxilla is straight (Fig. 6A, C). A large exit foramen for the superior alveolar canal opens on the labial surface at the base of the premaxillary process (Figs 4A₁, 6A₁). The estimated number of alveoli is 13.

In the type specimen, ZPAL RV/77, the anterior border of the nasal process is damaged but the losses seem to be insignificant. The medial surface of the anterior border bears a longitudinal furrow descending almost half way down the total height of the maxilla. This groove is the posterior part of the nasal facet. Behind it the medial surface of the nasal process bears a pattern of sub-vertical ridges and furrows (Fig. 4A₂) marking the position of the lacrimal. The posterior border of the nasal process crosses the dorsal margin of the maxilla to extend onto the medial surface. The dorsal margin of the horizontal ramus continues over the lateral face of the nasal process as an oblique crest ascending anterodorsally. The crest forms the anterior border of the weak antorbital recess.

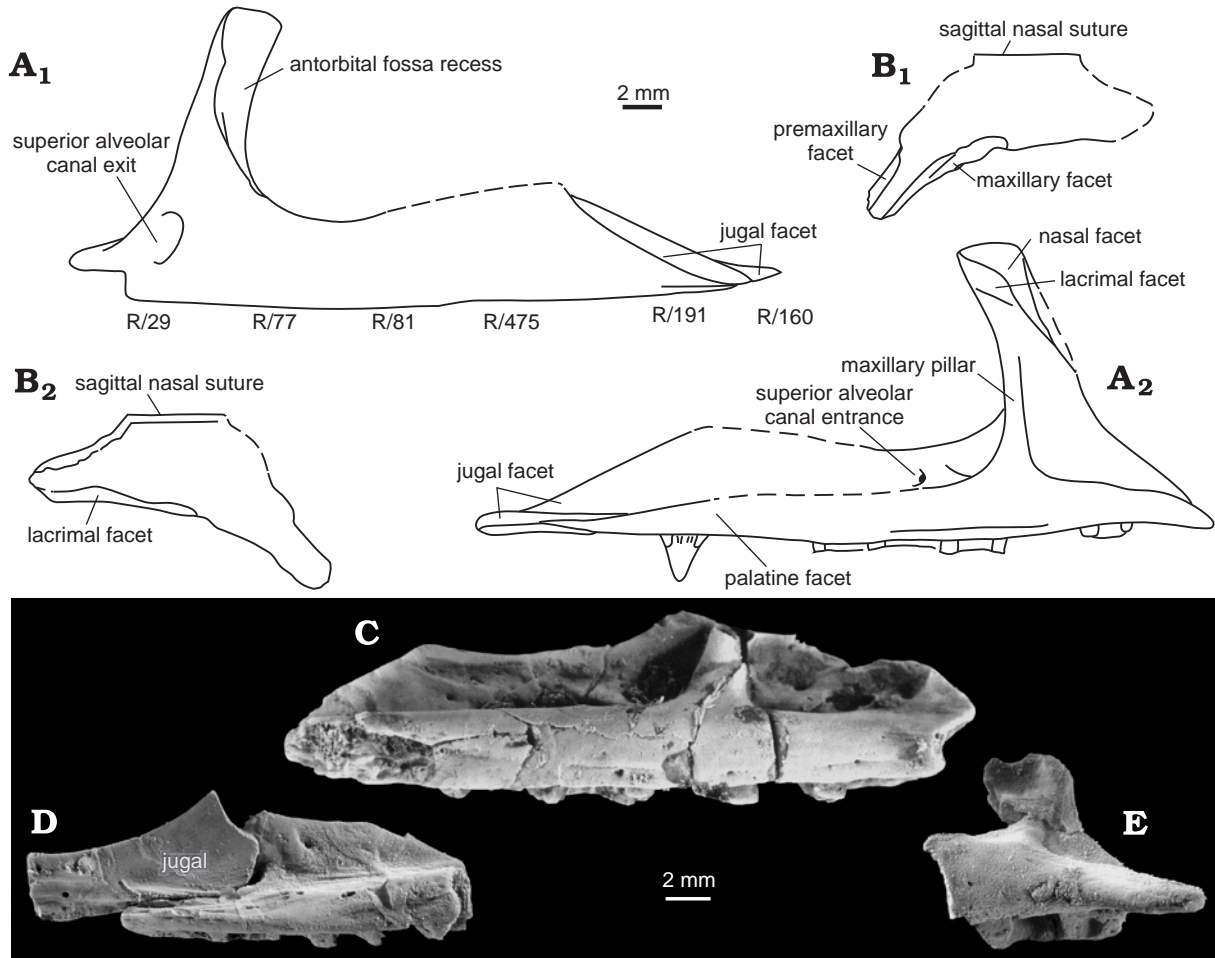


Fig. 6. *Osmolskina czatkowicensis* Borsuk-Białynicka *et* Evans, 2003, Early Triassic of Czatkowice 1, Poland. **A**. Reconstruction of the left maxilla, in lateral (**A₁**) and medial (**A₂**) views. **B**. Left nasal ZPAL RV/8, in lateral (**B₁**) and medial (**B₂**) views. **C**. Central part of maxilla ZPAL RV/81, in medial view. **D**. Posterior fragment of maxilla ZPAL RV/484 combined with the anterior part of the jugal ZPAL RV/281, in medial view (right side bones reversed). **E**. Anterior part of maxilla ZPAL RV/29, in medial view. C–E SEM micrographs. Shortened catalogue numbers indicate the specimens on which the reconstruction is based.

The premaxillary process curves medially. It is an anteromedial pyramidal extension of the alveolar margin and corresponds to what Gow (1970) called an anterior median flange. There is no discrete articular facet for the premaxilla along the acute anterior border of the maxilla, nor is there any space between the nasal and maxilla for the posterior process of the premaxilla that probably fitted the anterior surface of the nasal. The contact between the processes of the premaxilla and maxilla was probably quite loose, possibly leaving an accessory antorbital fenestra. There are also no traces of a lateral overlap between the body of the maxilla and that of premaxilla. The bones probably only touched each other in this region, while the faintly sculptured ventral surface of the premaxillary process of the maxilla probably overlapped the dorsal surface of the medial process of the premaxilla in the anteriormost part of the palate (Fig. 3A). Articulated in such a way, the premaxilla slightly overhangs the maxilla (Fig. 3A₂, C), although the posterior premaxillary teeth are level with the maxillary tooth-row.

The medial face of the premaxillary process bears a sub-horizontal longitudinal furrow on the dorsal surface of the superior alveolar shelf. In articulated bones, this furrow is in line with the vascular foramen piercing the posterior margin of the premaxilla. It probably served for the neurovascular supply of the premaxilla from the superior alveolar canal. Faint sculpture on the lateral face of the premaxillary process, directly behind the anterior margin, may reflect the presence of ligaments that attached the premaxilla. Directly behind the nasal process, the dorsal border of the horizontal ramus is slightly concave, but the profile of the more posterior part is poorly known. It clearly sloped posteroventrally at the tip.

The medial surface of the main body of the maxilla (Figs 4A₂, 5A₁) displays a very deep, medially swollen alveolar part, and a sub-vertical pillar inclined anterodorsally and buttressing the fragile nasal process. Both the alveolar part and the pillar are sub-circular in transverse section, but the pillar is much smaller in diameter. The alveolar part is separated from the main lamina of the maxilla by a longitudinal furrow. A few millimetres posterior to the pillar base, and usually roofed by an oblique blade of bone (Fig. 6A₂), is the entrance of the superior alveolar canal for the maxillary artery and superior alveolar branch of the maxillary nerve passing from the palatine. This opening (posterior alveolar foramen of Oelrich 1956) should correspond in position with the infraorbital foramen of the palatine. The palatine facet consists of a sub-perpendicular surface extending along the medial border of the alveolar edge between roughly the fifth to ninth alveolus, and tapering both anteriorly (Figs 5A₁, 6A₂) and posteriorly (Fig. 14D). The deepest part, facing obliquely dorsomedially at the level of about the sixth to seventh tooth, was probably received into a longitudinal concavity on the maxillary process of the palatine (see below). As a result, the anteromedial part of the palatine slightly overlapped the dorsal surface of the alveolar part of the maxilla.

As in the premaxilla, the maxillary alveoli are bordered by interdental plates situated slightly medial to the lingual side of the dentigerous margin. Labially the interdental plates pass into interdental septa. The alveolar part becomes flatter posteriorly (Fig. 6F), as the alveoli become shallower, and its dorsal wall bears numerous irregular perforations (possible reason for its poor preservation). The dorsal overlap of the jugal on the maxilla is fairly long (see *e.g.*, Figs 5B₂, 6D).

Nasal. — The nasal is represented by a single damaged right specimen, ZPAL RV/8 (Figs 4, 6B), and some fragments. It is a transversally curved bone blade turning anterolaterally into a long process that descends obliquely down the lateral face of the snout. The posterior process, sub-triangular shape, allow for reconstruction of the U-shaped incision between joint nasals. The incision probably received the anteriorly protruding part of the frontal (Fig. 8B). An elongated wavy medial facet (Fig. 6B₂) extending along approximately posterior one half of the preserved ventral border of the nasal should have received the lacrimal, but this bone has not yet been identified. The sagittal suture is straight and simple. The maxillary facet begins anterior to the lacrimal one and runs down the posterolateral border of the anterolateral process. As preserved, the process is rounded at the top and tapers ventrally. The anterior border of the process bears remnants of a premaxillary facet (Fig. 6B₁).

Frontal. — The frontals (Fig. 7A–C) are represented by many specimens. They are flat, paired and strongly built, and ca. 3.5 times as long as wide. The sagittal suture is straight along the anterior third of its length, becoming increasingly sinuous posteriorly. The frontonasal suture is broadly U-shaped (Fig. 8B) with anterolateral corners retracted, and bearing a dorsal nasal facet. Anterolaterally and posterolaterally the frontal joins the prefrontal and postfrontal respectively, so that it borders the orbit for only about one quarter of its length (the second quarter from the rear). The prefrontal facet incises the dorsal surface of the frontal obliquely (Fig. 8A₁) at the level of the second quarter of the frontal from the front. The facet protrudes slightly laterally from the main body of the frontal. It is convex in transverse section and longitudinally ridged, which suggests a rather rigid junction permitting no mobility in the transverse plane. The postfrontal facet incises the posterior quarter of the lateral frontal margin, but is usually little exposed in dorsal view. Between the prefrontal and postfrontal, the orbital margin of the frontal is slightly concave. The ventral surface of each frontal bears a strong, laterally concave sub-olfactory process (Fig. 8A₂). The longitudinal concavity of the olfactory canal deepens at both ends. The posterolateral part of each frontal is slightly dorsally concave (Fig. 7B). It bears posterior and medial parietal facets facing ventrally (Fig. 8C), and a ventrolateral postfrontal facet (Fig. 8A₂, D). However, the medial border of the process also bears a dorsal facet (Fig. 7B), and was probably overlapped by a thin superficial sheet of the parietal. The posterior border of the combined frontals is U-shaped.

The total length of frontals varies between roughly 15 and 22 mm. The posterior width is 100–118% of the anterior width. This variability affects the shape of the lateral border, which varies from almost straight to concave. Some larger specimens do not fit into the variability range of the majority form. They are relatively shorter and stouter (in ZPAL RV/96 posterior width attains ca. 155% of the anterior one), while the postfrontal facet invades the dorsal surface of the frontal. The large type is much less numerous in the assemblage. Whether it is a variant of the majority form or belongs to another animal cannot be resolved at the present time. The frontals of the majority variant are usually longer and more slender than those of *Euparkeria* (Ewer 1965), but the topography of the bones in the frontal region, including the suture structure, is exactly the same.

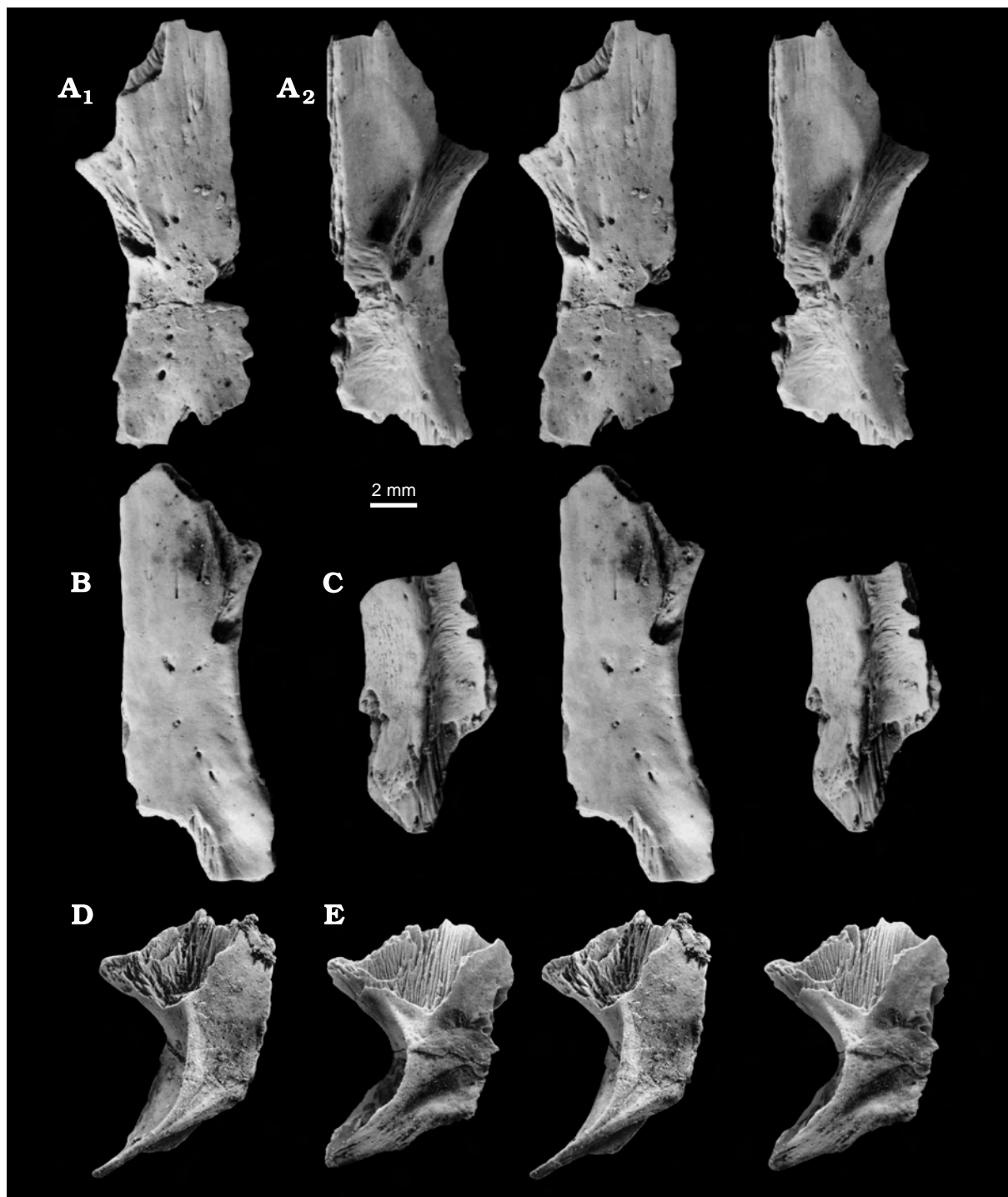


Fig. 7. *Osmolskina czatkowicensis* Borsuk-Białynicka *et* Evans, 2003, Early Triassic of Czatkowice 1, Poland. **A.** Left frontal ZPAL RV/91, in dorsal (A_1) and ventral (A_2) views. **B.** Right frontal ZPAL RV/1370, in dorsal view. **C.** Posterior fragment of the right frontal ZPAL RV/250, in ventral view. **D.** Left parietal ZPAL RV/293, in dorsal view. **E.** Left parietal ZPAL RV/285, in dorsal view. SEM stereo-pairs.

Parietal. — The parietals (Figs 7D, E, 8B) are paired and there is no trace of a parietal foramen. By comparison with the frontal, the parietal is short (roughly about half the frontal length in sagittal axis). As a whole, the sagittal suture is interdigitating. The anterior half of the suture surface bears V-shaped ridges and differs from the posterior one, which is vertically ridged. The posterior part becomes thinner and more susceptible to damage. When the anterior parts are articulated, the posterior parts leave a long incision between them, which combined with the suture morphology is suggestive of the presence of an interparietal. This

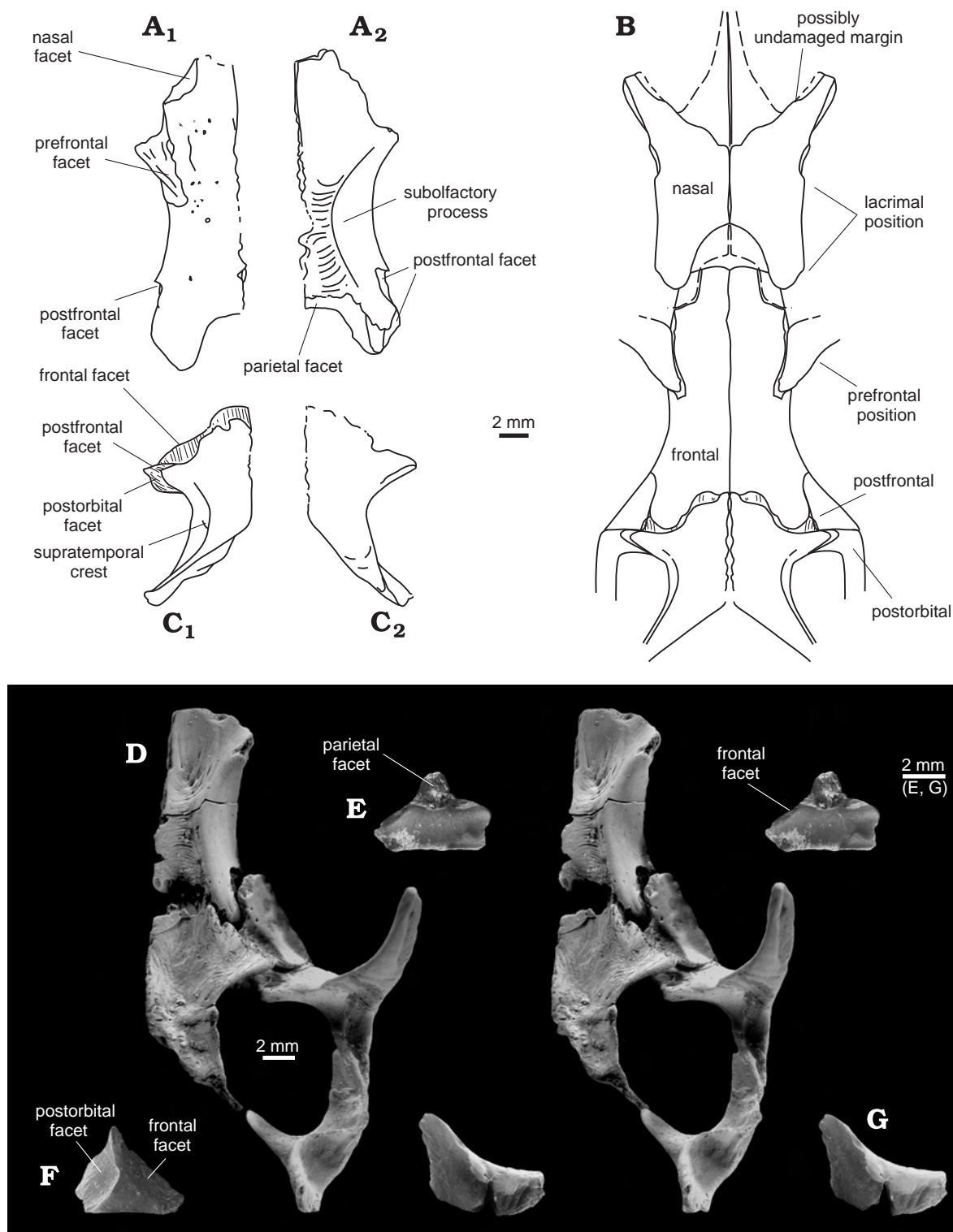


Fig. 8. *Osmolskina czatkowicensis* Borsuk-Białynicka *et* Evans, 2003, Early Triassic of Czatkowice 1, Poland. **A.** Right frontal, in dorsal (A_1) and ventral (A_2) views. **B.** Skull roof, in dorsal view. **C.** Right parietal, in dorsal (C_1) and ventral (C_2) views. **D.** Combined left side skull roof bones of different individuals, in ventral view: frontal ZPAL RV/259, ZPAL RV/291 parietal, ZPAL RV/547 postfrontal, postorbital ZPAL RV/315, and squamosal ZPAL RV/134. **E.** Right postfrontal ZPAL RV/544, in ventral view. **F.** Right postfrontal ZPAL RV/543, in dorsal view. **G.** Left prefrontal ZPAL RV/66, in lateral view. A–C, reconstructions; E–G, SEM micrographs; D, E, G, stereo-pairs.

would be consistent with the structure of this region in the other basal archosauriforms (Ewer 1965, Gower 2003), but is not supported by actual preservation of the interparietal. The anterior part of the parietal bears a strong faceted flange that is wavy in transverse section (Fig. 7D, E). It accommodated the frontal medially, and the postfrontal and postorbital laterally (Fig. 8B₁, D). The central part is convex and swollen dorsally, and protrudes anteriorly to fit the overlapping frontal. Laterally a longitudinal groove receives the rear of the descending crest of the frontal. The facet is longitudinally split to prevent lateral dislocation. The lateral wing of the parietal is oriented anterolaterally, and accommodates the combined postorbital-postfrontal. Its dorsal surface is convex. The ventral surface, correspondingly concave and roughened, may have received the dorsal part of the laterosphenoid. The lateral margin of the parietal bears an oblique surface for the origin of the temporal muscles. It faces dorsolaterally, is overhung by the supratemporal crest, and continues onto the lateral surface of the squamosal process.

In length, the squamosal processes probably exceeded that of the parietal body (see reconstruction Fig. 8D), but they are usually incomplete distally. Their posteromedial surfaces (sites of neck muscle attachment) are triangular, concave in transverse section, and are overhung by crests. They taper medially. The parietal and supraoccipital must have been connected by connective tissue. The ventral surface of the parietal has three concavities (Fig. 8D) matching the convexities of the dorsal surface: anteromedial, anterolateral (possibly receiving the laterosphenoid, see above), and posterior (extending approximately half the length of the squamosal process). In the distal half, the ventral surface of the process is more or less flattened, and probably fitted the end of the paroccipital process. A slit-like posttemporal fenestra perhaps separated the proximal parts.

The parietals are fairly uniform in overall shape, while differing in size (from about 8 to 13 mm in sagittal length). The supratemporal crests vary in strength.

Prefrontal. — The prefrontal forms a roughly semilunar conch (Fig. 8G) tapering both posteriorly and anteroventrally in the life position, and having a strongly concave ventromedial surface. The flat triangular and superficially ornamented dorsal wall of the bone (oriented to the left in Fig. 8G) overlaps the ridged prefrontal facet of the frontal (Figs 7A₁, 8A₁), and contributes to the skull table. Externally, the suture between the two bones is finely sinuous and extends along a parasagittal plane. Anteriorly the prefrontal becomes thinner and is rarely preserved intact, so that both its anterior extent and its contact with the lacrimal are poorly known. An elongated step-like surface preserved at the anterior border of ZPAL RV/66 (Fig. 8G, right lower angle of the specimen as oriented in the figure) is a fragment of the lacrimal facet.

Postfrontal. — The postfrontal is a small roughly triangular bone (Fig. 8E, F) that is wedged in between the parietal, frontal and postorbital (Fig. 8B, D). Its dorsal surface is a regular smooth triangle, the orbital border forming the longest side. Two ridged surfaces extend along the anterior and posterior sides of the triangle to contact the frontal and postorbital respectively. Both face mainly dorsally. The frontal facet is narrower and extends slightly onto the ventral side of the bone. The postorbital facet is larger and is not evident in ventral aspect. Between the two facets, there is a tiny triangular articular surface that is concave and ridged. This faces ventrally and slightly medially and contributes to the postorbital-postfrontal complex that overlaps the dorsal surface of the parietal. The orbital border of the postfrontal forms a smooth wall that is elongate in the parasagittal plane, but is only slightly concave longitudinally. In life position it faces ventrally and only slightly laterally.

Postorbital. — The postorbital is a triradiate bone (Fig. 9A–C). The axes of the posterior and ventral processes extend approximately at right angles to each other, but the processes themselves are connected by a more or less extensive blade of bone. This is laterally flat and medially concave. The posterior process fits into a groove on the squamosal to produce the upper temporal arcade. The medial process ascends slightly anteromedially (at ca. 130° to the ventral process). Its stout tip bears an ovoid concave parietal facet facing ventromedially, and this combines with the adjacent surface of the postfrontal to overlap the parietal (Fig. 8D). More anterior and lateral in position is an elongated postfrontal facet. The elongated, tapering ventral process is bent anteriorly at about half its length. It is sub-triangular in transverse section with its lateral surface flat. The anterior surface contributes to the curved posterior orbital border. It faces directly anteriorly and is separated from the posterior surface by a sharp crest. The posterior surface is concave in transverse section and faces posteromedially. The slit-like jugal facet extends onto this surface along the distal half of the lateral border.

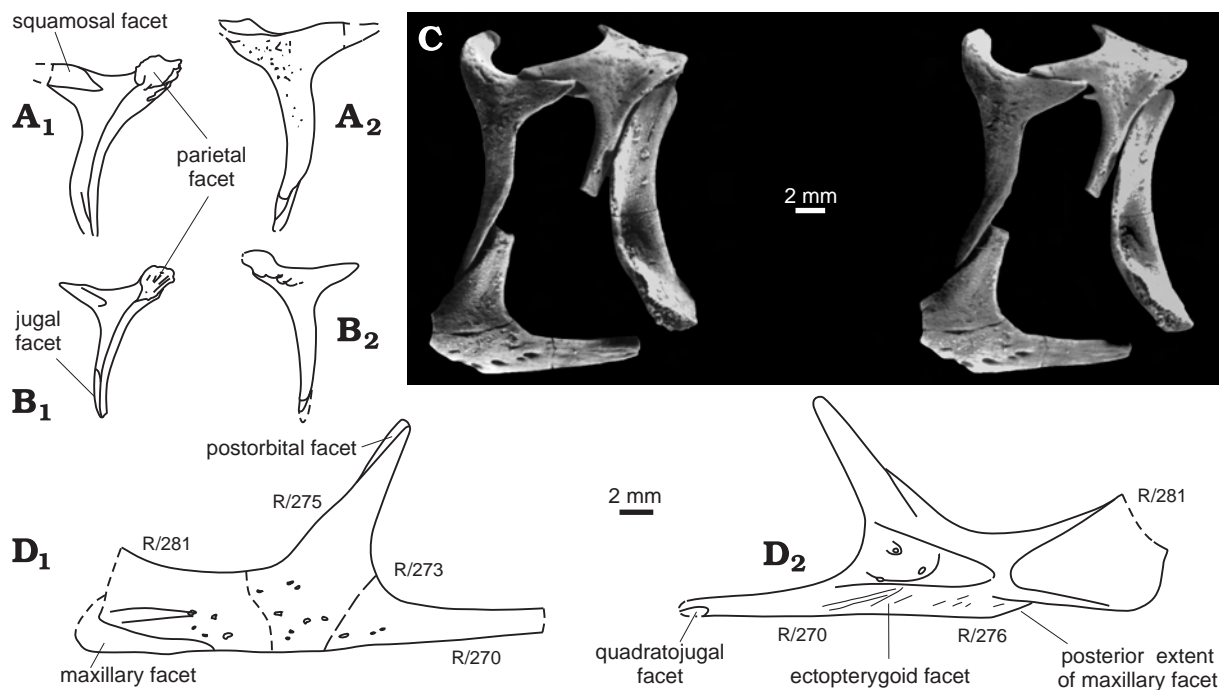


Fig. 9. *Osmolskina czatkowicensis* Borsuk-Białynicka *et* Evans, 2003, Early Triassic of Czatkowice 1, Poland. **A**, **B**. Right postorbitals, two ontogenetic stages: ZPAL RV/318 (**A**) and ZPAL RV/319 (**B**). **C**. Left posterior skull fragment combined from different individual bones: jugal fragment ZPAL RV/273, postorbital ZPAL RV/319, squamosal ZPAL RV/871, and quadrate ZPAL RV/872. **D**. Reconstruction of the left jugal, mostly on the basis of the specimens illustrated in Fig. 11 (shortened catalogue numbers around). Medial (**A**₁, **B**₁, **D**₂) and lateral (**A**₂, **B**₂, **C**, **D**₁) views. **C**, SEM stereo-pair.

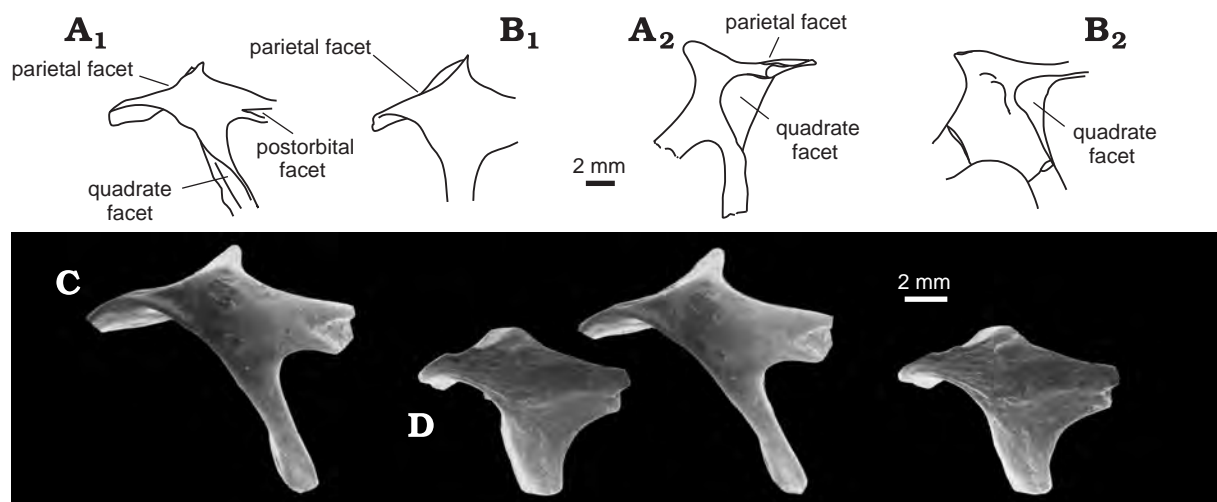


Fig. 10. *Osmolskina czatkowicensis* Borsuk-Białynicka *et* Evans, 2003, Early Triassic of Czatkowice 1, Poland. Right squamosals: ZPAL RV/398 (**A**), ZPAL RV/399 (**B**), and ZPAL RV/27 (**D**). **C**. Left squamosal ZPAL RV/27. Lateral (**A**₁, **B**₁, **C**, **D**) and ventromedial (**A**₂, **B**₂) views. **C**, **D**, SEM stereo-pairs.

There is some variability in the postorbitals, in size, thickness, angulation between the anterior and posterior processes, and transverse section of the processes (more or less flattened laterally). However, the interesting parameters are difficult to measure accurately due to imperfect preservation.

Squamosal. — The squamosal is a quadriradiate bone that consists of a bulky rhomboid body with processes extending from each of its corners (Figs 9C, 10). The anterior process is stouter in lateral aspect than the posterior one, and bears a deep triangular socket on its lateral surface to receive the postorbital. The posterior one is twisted medially to overhang the quadrate, which makes its lateral wall more slender and posteri-

only tapering. Both processes extend in line with the diagonal of the main body. This diagonal was oriented approximately horizontally as is the resulting supratemporal arcade. The posterior and medial processes contribute to an elongate rough parietal facet which generally faces posteromedial, but becomes more dorsal in orientation on the medial process. Ventrally, the squamosal extends into a long, slender process. Its lateral surface is flat and tapers to a point. A deep concavity between the posterior and ventral process received the quadrate head, while the lateral quadrate flange lay against the posterior wall of the ventral process.

There is variation in the size and proportions of the body of the squamosal, its shape and curvature, and in the angle between the postorbital and quadratojugal processes, but this cannot be quantified, partly because of differences in preservation. There seem to be two morphotypes, but they grade into one another. The smaller morphotype (width of the quadratojugal process: 1.0–2.1 mm, $n = 7$) is rhomboid in shape and the length of the body greatly exceeds its width (Fig. 10A₁, C). The quadratojugal process extends anteroventrad at an angle much less than 90° to the postorbital processes. The larger morphotype (Fig. 10B₁, D) (width of the quadratojugal process: 2–3.5 mm $n = 7$) is squarer in outline, with a quadratojugal process that is relatively stouter and flatter, as well as almost vertical in orientation, but this may be just a matter of size and individual age.

As illustrated by Ewer (1965, fig. 2), the anterior and ventral processes of the squamosal in *Euparkeria* enclose an angle of about 90°. In contrast, the same angle in *Sarmatosuchus* is 115° (Gower and Sennikov 1997, p. 63, fig. 3C).

Quadrate. — The quadrate (Fig. 11) has a pillar-like body arched in the parasagittal plane and posteriorly concave. The proximal head is simply a small rounded termination of the central pillar. The medial wing is triangular with its apex situated in the upper one third of the bone, and the base extending down to the lower one third of the pillar. The less extensive lateral wing is triangular with its apex more dorsally positioned, at about one quarter the quadrate height from the top. It is separated from the lower extremity of the bone by a deep notch that contributes to the quadratojugal foramen (Fig. 11A₁). The wings extend from the body in anteromedial and anterolateral directions, the anterior surface of the bone thus enclosing a widely open V-shaped concavity in transverse section. The lower part of the anterior face, depressed for the articulation with the pterygoid, is separated from the upper part by an oblique crest (pterygoid crest on Fig. 11A₁, B₂) extending ventrolaterad along the lower margin of the medial wing toward the quadratojugal articulation. This crest marks an abrupt change in orientation of the anterior surface of the bone. At the distal end of the pillar, there is a heavy medial condyle for the mandibular articulation (Fig. 11A₁). The lateral condyle protrudes laterad from the shaft. It is less developed than the medial one and is separated from the latter by a shallow smooth concavity. Both extend onto the anterior face of the bone, suggesting a posteroventral inclination of the bone in life (Fig. 11A₃, A₄). Given an approximately horizontal life position of the mandibular articulation, the upper concavity of the shaft faced anteriorly and the lower one anteroventrad (Fig. 11A₃, A₄). The lower border of the medial wing should have been sub-horizontal in life position. The ventrolateral margin of the bone bears a narrow oval facet for the quadratojugal (Fig. 11A₁, C), while a row of tubercles, perhaps for ligaments, parallels this surface on the posterior face of the bone.

The height of the quadrate varies from 11 to 24 mm with a modal value of about 16 mm. One of the largest specimens is ZPAL RV/37. Allowing for differences in size, the quadrate of *Osmolskina czatkowiensis* is very similar to that of *Sarmatosuchus otschevi* (Gower and Sennikov 1997, p. 63, fig. 5).

Quadratojugal. — The quadratojugal (Fig. 12F) consists of two limbs enclosing an angle of ca. 40°, and contributing to a sub-triangular posteriorly rounded body. The body is medially concave to fit the ventrolateral extremity of the quadrate, exactly as in *Euparkeria* (Ewer 1965). The horizontal limb is a simple bar tapering anteriorly to fit the quadratojugal facet on the medial side of the jugal. The vertical limb is complicated by the addition of a medial lamina (or ridge). It closes the quadratojugal foramen laterally, and it is twisted just above it.

Jugal. — The jugal is a triradiate bone (Figs 9D, 12A–D). The middle part, including the postorbital process (Fig. 12C), is usually the best preserved, whereas the anterior and posterior rami are generally broken off. A number of anterior fragments may readily be combined with the middle parts, but only three specimens have been preserved with the base of the posterior ramus that demonstrates the existence of the lower temporal arcade (Fig. 9C).

The main part of bone is straight and sub-horizontal, but ascends anteriorly to overlap the maxilla along an oblique line (Fig. 6D). The lateral surface is convex with a smooth sub-orbital part facing slightly dorso-

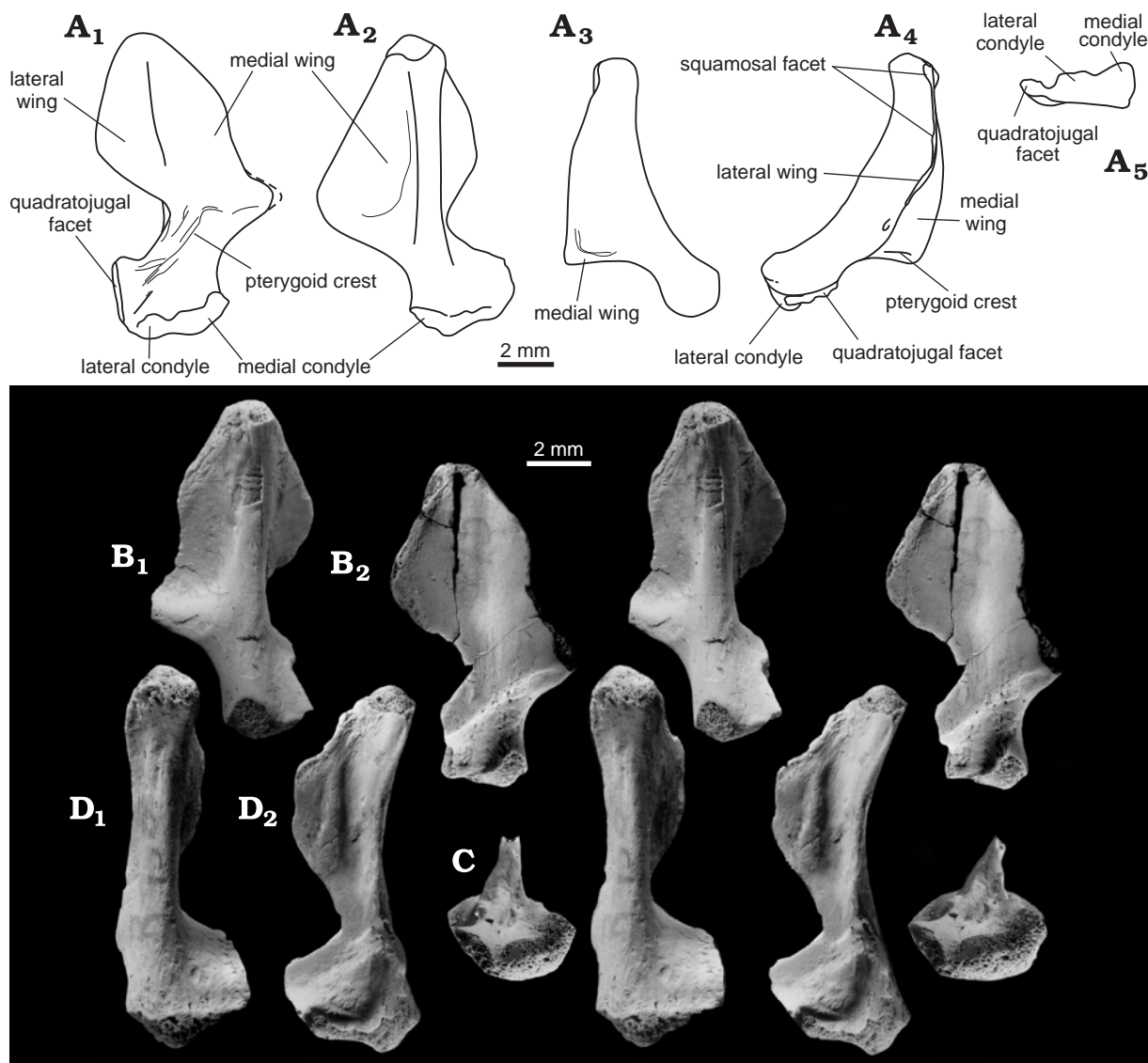


Fig. 11. *Osmolskina czatkowicensis* Borsuk-Białynicka *et* Evans, 2003, Early Triassic of Czatkowice 1, Poland. **A.** Right quadrate reconstructed on the basis of the specimens illustrated below, in anterior (A_1), posterior (A_2), medial (A_3), lateral (A_4), and distal (A_5) views. **B.** Right quadrate ZPAL RV/38, in posterior (B_1) and anterior (B_2) views. **C.** Right quadrate ZPAL RV/39, in distal view. **D.** Right quadrate ZPAL RV/39, in posterior (D_1) and anteromedial (D_2) views. B–D, SEM stereo-pairs.

laterally and a strongly pitted ventral part facing ventrolaterally (Fig. 12A). The maxillary facet is complex. The main part of the facet is elongate and faces laterally but is set off from the main lateral surface of the bone (Fig. 12A). It must have been received into the furrow-like posteromedial surface of the maxilla (Fig. 6D). The posterior border of the main maxillary facet is always damaged. The same is true of the anterior extremity of the jugal, and hence the contact with the prefrontal and lacrimal remains unknown. The posterior process (Figs 9D, 12D, E) is long and narrow. As preserved, it makes up 58% of the reconstructed length of the bone. The quadratojugal facet is a long V-shaped incision in the ventromedial surface of the distal end (Fig. 12E). The postorbital process forms a triangle with a large base, and an apex directed posterodorsally with the slope of its axis at about 52° to 65° to the long axis of the bone.

The postorbital facet is a slit-like furrow extending on the anterior margin of the process, and, more dorsally, onto its medial side (Figs 12C, D). Medially, the quadratojugal and postorbital processes are separated from each other by a deep concavity extending sub-horizontally below the base of the postorbital process, and bordered ventrally by what is probably the ectopterygoid facet. However, the nature of the jugal-ectopterygoid contact is far from clear. Further anteriorly, a sub-triangular concavity, open anteriorly (Figs 9D₂, 12B), corresponds to the region overlying the maxilla. The concavity is bordered ventrally by a crest that



Fig. 12. *Osmolskina czatkowicensis* Borsuk-Białynicka *et* Evans, 2003, Early Triassic of Czatkowice 1, Poland. Jugal fragments. A. Central portion with maxillary facet (left upper angle), and the base of a postorbital process ZPAL RV/274. B. Central portion with bases of both postorbital and quadratojugal processes ZPAL RV/277. C. Postorbital process with fragment of the main body ZPAL RV/275. D. Quadratojugal and postorbital processes ZPAL RV/273. E. Posterior part of jugal ZPAL RV/270 combined with quadratojugal ZPAL RV/394. F. Quadratojugal ZPAL RV/53. Lateral view (A, C₂, D, F) and medial view (B, C₁, E). Left bones, SEM stereo-pairs.

probably contacted the anterior flange of the ectopterygoid, overlying the maxilla medial to the jugal. A ventral incision separates the maxillary facet from the posterior part of the jugal (Fig. 12A).

As a rule, the anterior ramus is convex laterally in transverse section. Directly anterior to the postorbital process, and posterior to this process, the jugal wall is concave. Some specimens differ in having an evenly convex lateral surface with no concavities in the vicinity of the postorbital process. They are otherwise quite similar to the main type and are provisionally considered as variants. However, some very flat specimens (ZPAL RV/ 279 and 280), with a more vertical postorbital process (angle 72–78°), may belong to another animal.

PALATAL COMPLEX

Palatine. — As reconstructed on the basis of specimens ZPAL RV/33 and 34 (Figs 13A, B, 14A, B), the palatine is an elongated plate roughly rectangular in outline and approximately twice as long as wide (Fig. 13D). A V-shaped notch in its anterolateral end marks the posterior limit of the choana. The exact length and morphology of the anteromedial process are unknown, as are the posterior extent and outline of the bone and

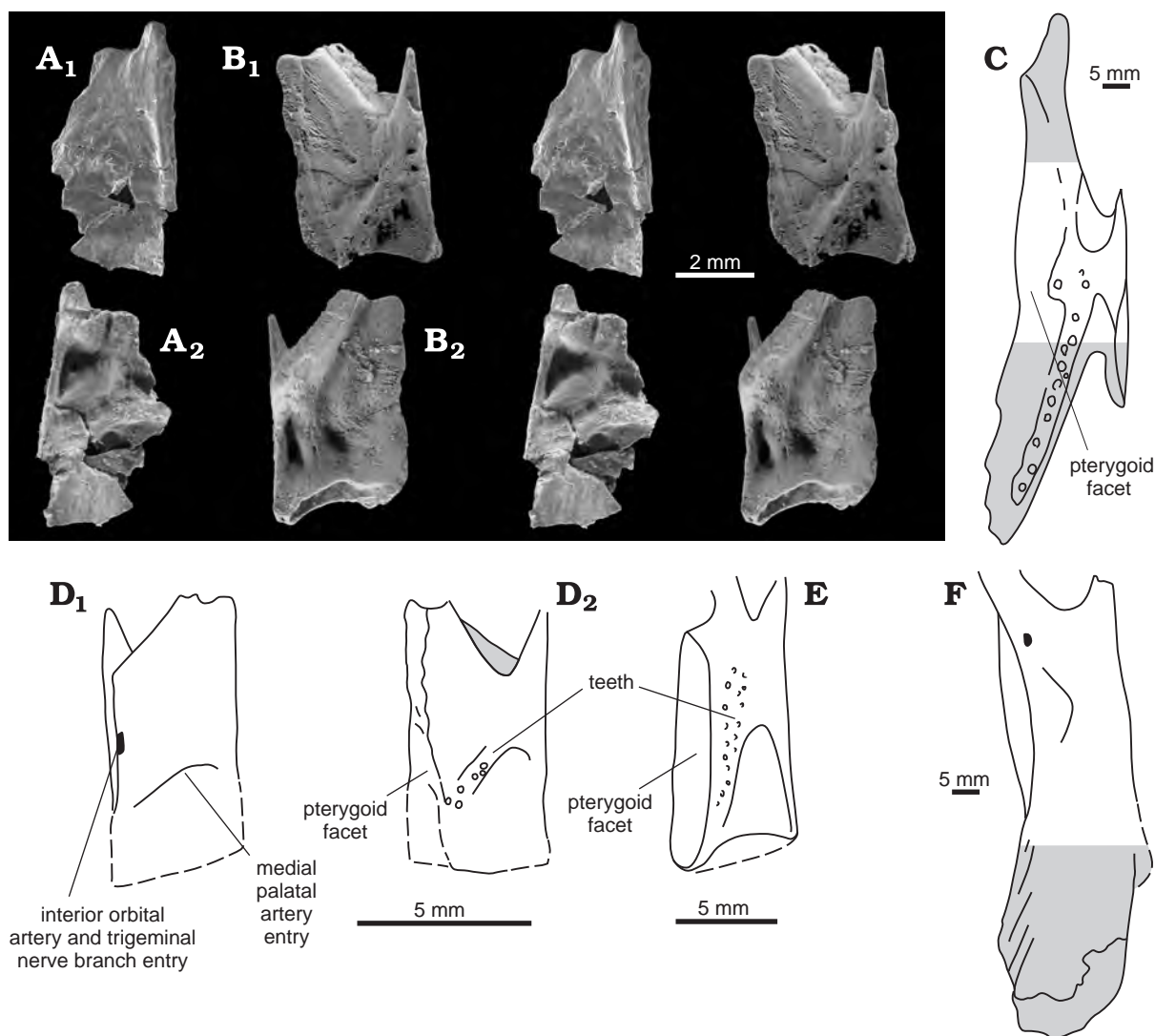


Fig. 13. *Osmolskina czatkowicensis* Borsuk-Białynicka *et* Evans, 2003, Early Triassic of Czatkowice 1, Poland. **A.** Left palatine fragment ZPAL RV/34. **B.** Left palatine fragment ZPAL RV/33. **C–F.** Partial reconstructions of left palatines. **C.** *Sarmatosuchus otschevi* (after Gower and Sennikov 1997). **D.** *Osmolskina czatkowicensis*. **E.** *Euparkeria capensis* (after Ewer 1965, fig. 27). **F.** *Batrachotomus kupferzellensis* (after Gower 1999, fig. 14). All but A₂, B₂, D₁ in ventral view. Shaded areas show the missing parts. A, B, SEM stereo-pairs.

the shape of the sub-orbital fossa. As a whole the dorsal surface is concave because of the upward curvature of both the choanal border and the medial one, but the main portion is flat. A sharp arcuate, posteriorly concave crest borders a sub-transverse slit giving entry perhaps to branches of the medial palatal artery. Another foramen or foramina, situated at the lateral border of the bone, probably served for the entry of a passage used by the inferior orbital artery and a palatine branch of the trigeminal nerve (Fig. 13D₁). The general position of this passage in the palatine should correspond with that of the posterior opening of the superior alveolar canal of the maxilla (the posterior alveolar foramen of Oelrich 1956; see also Evans 1980, figs 21–25) which determines the mutual position of the bones. The maxillary facet is double and extends from the tip of the anterolateral process of the bone backwards (Fig. 14A, B). Ventrally, an elongated, ridged surface extends along the entire length of the bone. Close to the posterior border of the choana, this surface passes dorsally into a triangular facet along the medial border of the upturned flange of the palatine. The two parts enclose a longitudinal furrow that more or less matches the palatine facet of the maxilla (Fig. 14D). This places the palatine in position within the palate (Fig. 1A).

The ventral surface of the bone is bordered medially by a narrow pterygoid surface tapering forwards and extending medially in its posterior part. An oblique crest extends posteromedially almost in line with the lat-

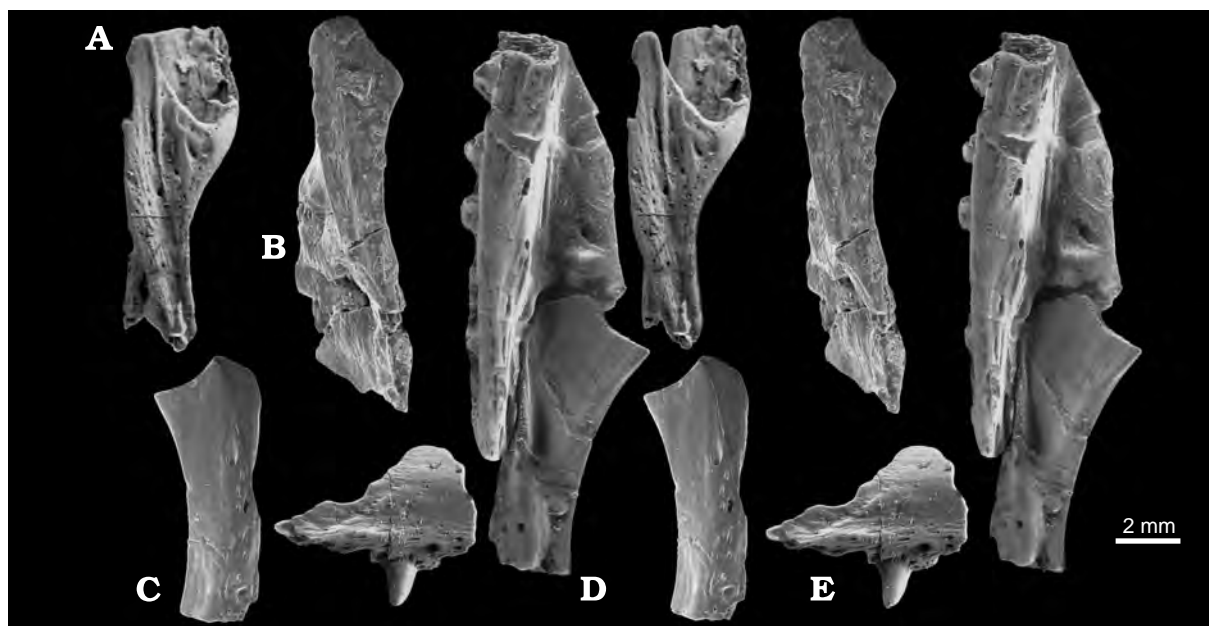


Fig. 14. *Osmolskina czatkowicensis* Borsuk-Białynicka *et* Evans, 2003, Early Triassic of Czatkowice 1, Poland. Left palatines in lateral view exposing maxillary facet (anterior to the top): ZPAL RV/34 (A) and ZPAL RV/33 (B). C. Jugal fragment ZPAL RV/281, in lateral view. D. Posterior fragment of maxilla ZPAL RV/484 combined with the anterior part of the jugal ZPAL RV/281, in medial view. E. Posterior fragment of maxilla ZPAL RV/1371. SEM stereo-pairs.

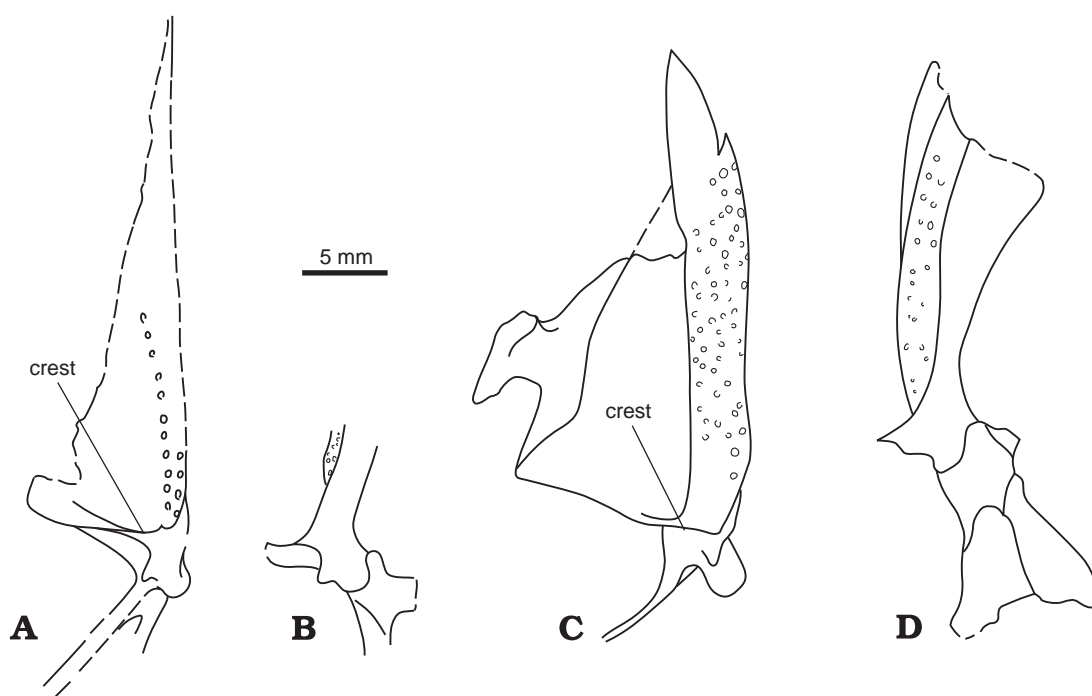


Fig. 15. Reconstructions of right pterygoids. A, B. *Osmolskina czatkowicensis*. C, D. *Euparkeria capensis* (a drawing after Ewer's 1965, fig. 26; stereo-photographs). Ventral (A, C) and medial (B, D) views.

eral border of the choanal notch. The crest bears traces of a tooth row that was probably continuous with that of the pterygoid. A triangular section of palatine blade, posterolateral to this crest, ascends obliquely toward the maxillary border.

The attribution of this type of palatine to *Osmolskina* is based primarily on its having a size that best fits the largest and most numerous bones of the assemblage. The possibility of procolophonid provenance has been considered, but seems unlikely because of its elongated and rectangular outline, with the choanal notch occupy-



Fig. 16. *Osmolskina czatkowicensis* Borsuk-Białynicka *et* Evans, 2003, Early Triassic of Czatkowice 1, Poland. A–C. Central portions of left pterygoids. A. ZPAL RV/74. B. ZPAL RV/72. C. Basipterygoid facet and base of the quadrate process ZPAL RV/73. D. Right pterygoid combined with ectopterygoid ZPAL RV/604. E. Lateral part of the left pterygoid wing with ectopterygoid facet ZPAL RV/605. F. Left ectopterygoid ZPAL RV/465. G. Right ectopterygoid ZPAL RV/408. Ventral (A₁, B, D, G), medial (A₂), ventromedial (C), and dorsal (F) views. All but B, D, E SEM micrographs; all stereo-pairs.

ing a short margin. This differs from the short, sub-rhomboid palatine of procolophonians that bears articular facets on all margins, with the choanal notch situated in one corner (Carroll and Lindsay 1985, fig. 6E). As preserved the bone corresponds to the middle portion of the palates in *Sarmatosuchus otschevi* (Fig. 13C; Gower and Sennikov 1997, fig. 4B), *Batrachotomus kupferzellensis* (Fig. 13F; Gower 1999, fig. 14), and *Euparkeria capensis* (Fig. 13E; Ewer 1965, fig. 1), while corresponding to the latter species in detail (Fig. 13C–E).

Pterygoid. — The pterygoid consists of two wings, palatal and quadrate, united by a short neck. In dorsal aspect, the main part of the palatal wing is fan-shaped and convex in transverse section. However, towards the medial side, the convexity passes into a radially oriented furrow that, in turn, is bordered by the prominent dorsomedial border. The posterior angle of the palatal wing, between the fairly deep medial wall and the thick laterally directed posterior border, is ca. 80°. The ventral surface of the palatal wing is separated from the neck by a sharp crest (Figs 15A, 16B), and similar crest occurs in *Euparkeria capensis* (Fig. 15C). The lateral part of the palatal wing is ventrally concave and funnel-shaped. Sharply delimited on both sides, the dentigerous zone is flat, and bears about 4 longitudinal rows of small teeth. The anterior part of the pterygoid is never preserved, and was reconstructed (Fig. 15A) on the basis of the space left by the palatines and maxillae. The lateral extreme is a fairly stout, laterally thickened sub-quadrangular blade bearing a flat incision for the ectopterygoid (Fig. 16D, E). The ectopterygoid facet is never complete in existing material.

The pterygoid neck has a ventromedially protruding hooked process (Fig. 16A, C) which contributes to the basiptyergoid articulation. Situated on the posterior face of this process, the articular surface is sub-perpendicular to the plane of the palatal wing. It continues onto the medial surface of the ventral twig of the quadrate process (Fig. 16A, C). A tuber for insertion of the pterygoideus muscle (Schumacher 1973) or for ligament attachment is situated about the middle of the neck. Its size is variable, and the apex is directed laterally. At the very base of the quadrate ramus is a bone blade that is flat both ventrally and dorsally. Distally, it divides into two processes and extends obliquely posterolaterally.

Ectopterygoid. — The ectopterygoid is a strongly curved bone with a relatively small hook-shaped lateral head and a body that extends strongly to a sub-triangular medial conch. The latter is dorsally convex (Fig. 16F) and ventrally concave (Fig. 16G). The concave surface is probably continuous with the concavity of the ventral surface of the pterygoid, and it is bordered by a V-shaped crest that opens medially. The pterygoid facets it bears are obscure, and contact must be reconstructed on the basis of the facet on the lateral margin of the pterygoid (Fig. 16D). The lateral head (turned down in Fig. 16F, G) bears an articular facet here interpreted as the jugal facet, but the nature of its contact with neighbouring bones is conjectural.

BRAINCASE

The braincase is represented by all constituent elements, with the exception of a laterosphenoid, the presence of which is conjectural. The braincase material is disarticulated except for the parabasisphenoid, which is a fully integrated element, and the exoccipitals that are almost always fused with the opisthotic (*e.g.*, ZPAL RV/115, 422). A few specimens also have the supraoccipital or prootic, or both (ZPAL RV/419), fused with the opisthotic, but in existing material, the *Osmolskina* exoccipitals are never fused with the basioccipital. The base of the cranial cavity is, as a rule, covered by unfinished bone, except for the ossified basal grooves for the metotic foramen, and occasionally the abducens grooves (ZPAL RV/424), as well as the articular facets for neighbouring bones in a few larger specimens.

Basioccipital. — The basioccipital (Fig. 17A, B) is a thick bone that is cordate in shape, with the apex forming the majority of the occipital condyle. It contacts the basisphenoid by means of two sub-circular surfaces facing anteriorly and separated from each other by a notch (Fig. 17A₃, B₂). More laterally, an ovoid surface probably received the tip of the ventral ramus of the opisthotic that fitted between the basioccipital and the posterolateral parabasisphenoid wing. The surface is situated on the anterolateral face of each basal tuber. The exoccipital facets are symmetrical, flattened, and posterolaterally inclined. They almost touch one another in the midline, but do not completely exclude the basioccipital from the foramen magnum. Anteriorly, the exoccipital facets diverge, and the basioccipital contributes a narrow zone to the braincase floor. However, the contribution of the basioccipital to the braincase floor may have decreased in ontogeny with progressing co-ossification of the bones. An elongated furrow of finished bone, corresponding to the base of the embryonic metotic fissure (nerves IX and X), lies anterior to the exoccipital facets, and posterolateral to the opisthotic facet of both sides. The apices of the basal tubera are situated at about the anterior one third of the basioccipital length. Medially they meet the crests that border the V-shaped ventral concavity of the braincase floor posteriorly.

Supraoccipital. — The supraoccipital (Fig. 18) is a hexagonal plate that is thickened ventrally on both sides. The thickened parts bear oblique articular facets, for the prootic anterolaterally and for the opisthotic posterolaterally. The former is pierced by the entrance of the anterior semicircular canal, the latter by that of the posterior canal. The canals converge medially as more or less open furrows, and are sometimes separated from each other by a transverse septum (Fig. 18C₁). Their eventual fusion into a *crus communis* must have occurred below the ossified part. Between the lateral otic facets, the ventral surface of the supraoccipital provides a concave, fully ossified ceiling to the brain cavity. Its posterior border is laterally incised by surfaces for the exoccipitals. Between them, the border of the supraoccipital contributes to the foramen magnum. On the ventral surface of the bone, medial to the semicircular canal regions, the anterior margin bears symmetrical triangular incisions (Fig. 18A₁, C₁). The incisions display a surface of finished bone and extend laterally to the cavities continuous with the space for the dural venous sinus draining the prootic (see below) or for the endolymphatic ducts. The cavities most probably had their exits on the dorsal surface of the bone (Fig. 25B, C).

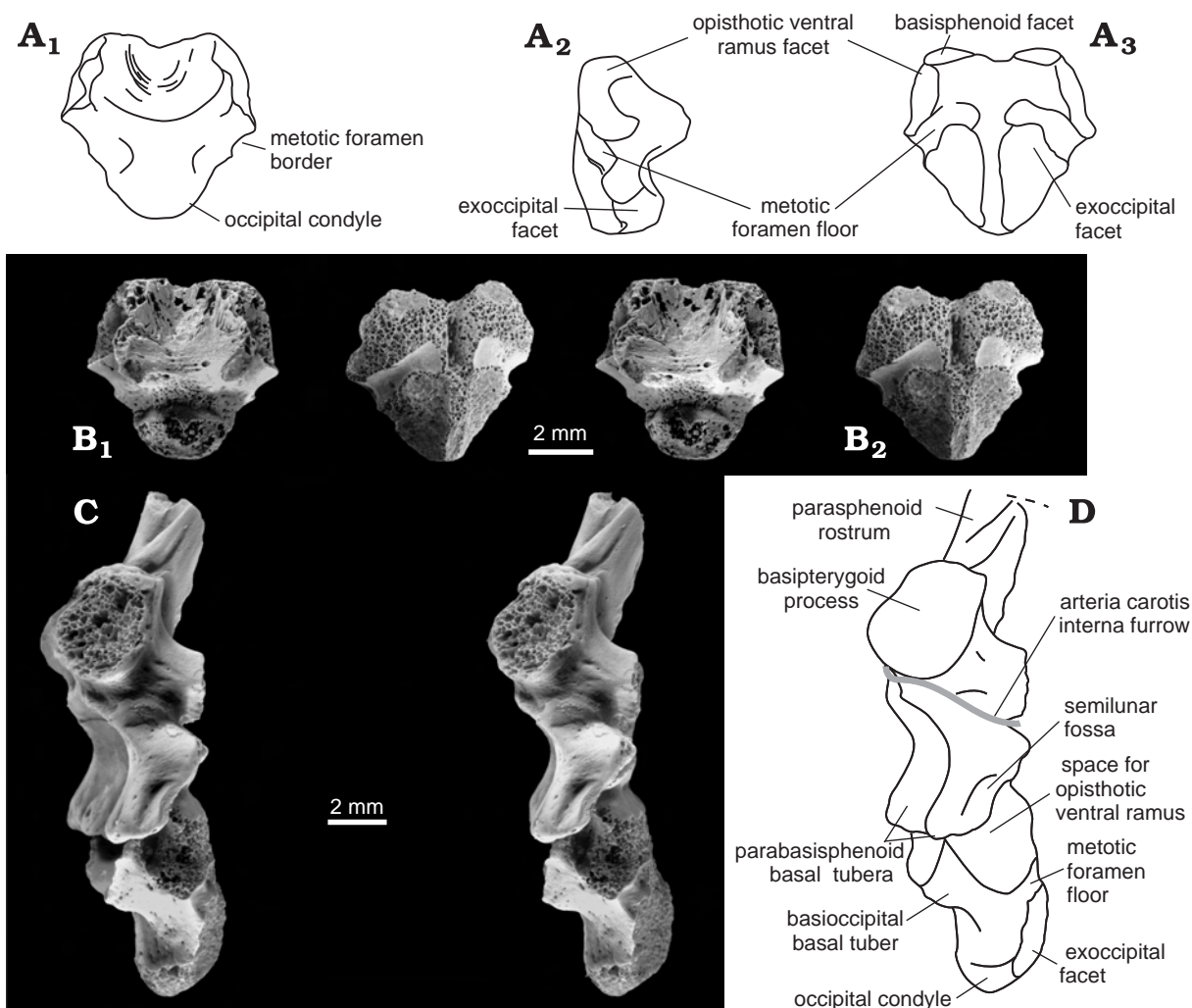


Fig. 17. *Osmolskina czatkowicensis* Borsuk-Białynicka *et* Evans, 2003, Early Triassic of Czatkowice 1, Poland. **A, B.** Basioccipital ZPAL RV/114, in ventral (**A₁**, **B₁**), lateral (**A₂**), and dorsal (**A₃**, **B₂**) views. **C, D.** Parabasisphenoid with basioccipital ZPAL RV/413 combined from two specimens, in left lateral view. **B, C,** SEM micrographs; **B, C,** stereo-pairs.

The supraoccipital displays a fairly consistent structure, but the stage of ossification and the level of co-ossification with neighbouring bones vary with respect to the details of the posterior margin. The triangular surfaces for the exoccipitals are more or less widely spaced (Fig. 18B, D), sometimes separated by an acute roof above the foramen magnum incised in the sagittal axis, in some others the exoccipital facets are close together and blend to produce a small finger-shaped process (Fig. 18B). The specimens do not differ from one another in other aspects.

Exoccipital. — The exoccipitals (Fig. 19) are hour-glass shaped bones with enlarged upper and lower ends contacting the opisthotic, supraoccipital, and basioccipital respectively. The exoccipitals diverge dorsally and contribute to the lateral borders of the foramen magnum (Fig. 25), but do not usually make contact above it. Two hypoglossal foramina pierce the exoccipital pillar. The exits lie on the lateral side, with the larger one postero-dorsal to the smaller one, which almost touches the suture with the basioccipital. Two acute sub-vertical crests border the posterior foramen from both anterior and posterior sides (Fig. 24A). The anterior crest forms the posterior border of the metotic fissure while the opisthotic ventral ramus makes up the anterior wall of the fissure, and the basioccipital the furrow-like floor. The sutures between the exoccipital and the basioccipital close later in ontogeny than those between the exoccipital and the opisthotic, the latter two frequently being preserved as a single element (Fig. 25).

Opisthotic. — The opisthotic (Fig. 19) is a pyramidal bone that makes up the main body of the paroccipital process. The tip is bilaterally flattened and distally bears a dorsal ridge for the parietal contact. In

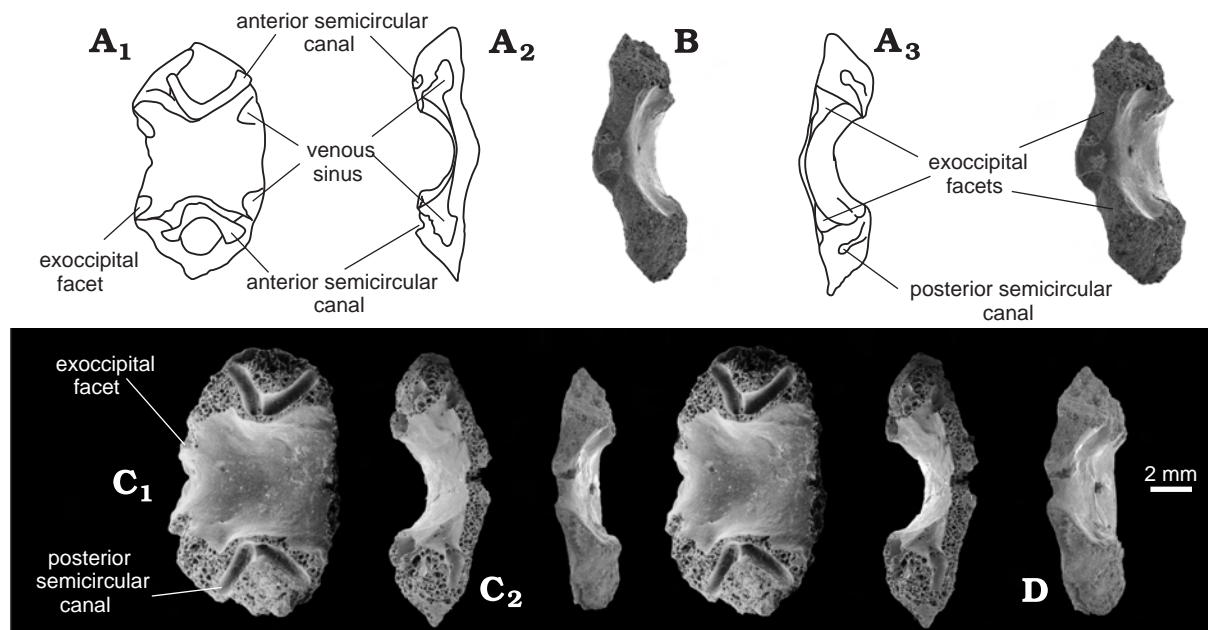


Fig. 18. *Osmolskina czatkowicensis* Borsuk-Białynicka *et* Evans, 2003, Early Triassic of Czatkowice 1, Poland. Supraoccipital: ZPAL RV/125 (A, C), ZPAL RV/420 (B), and ZPAL RV/417 (D). Ventral (A₁, C₁), anterior (A₂, C₂), and posterior (A₃, B) views. B–D, SEM stereo-pairs.

life, the paroccipital processes of both sides extend posteriad enclosing an angle of about 55° (Fig. 25B). The ventral surface bears three longitudinal crests (Fig. 19B₁). The blunt medial crest is continuous with the posterior wall of the exoccipital. Topographically, it roughly corresponds to the tuberal crest *sensu* Säve-Söderbergh (1947, see also Oelrich 1956) but is medial instead of lateral to the hypoglossal foramina. The lateral crest extends half way along the paroccipital process and is continuous with the main line of the prootic crest. Intermediate in position, the third, most acute, crest extends along the posterior side of the ventral ramus of the opisthotic. It roughly corresponds to the interfenestral crest of lizards (Oelrich 1956) in that it separates the region of fenestra ovalis from that corresponding to the embryonic metotic fissure. In *Osmolskina*, the metotic fissure is largely open, and no separate compensatory window is formed exactly as in the case of *Euparkeria* (Gower and Weber 1998). The “interfenestral crest” borders a stapedia fossa, which leads to the fenestra ovalis, widely open in *Osmolskina*.

The ventral ramus of the opisthotic has a twofold structure (Fig. 19A). It is composed of two elongated processes, the posterior one is fused along its anterior margin with a second process protruding from the ventral border of the posterior vestibular recess. The suture between the two parts remains visible in all specimens having the ventral ramus preserved. It produces a blunt ridge cutting the stapedia groove sub-perpendicular to its axis. The ridge produces a semicircle partly surrounding the fenestra ovalis. Anterior to it is a pit, possibly for the ligament supporting the stapes. The anterior margin of the ventral ramus is pierced proximally by a tiny canal extending posteriad (Fig. 19A). On the other side of the process it opens into the dorsal part of the metotic foramen, possibly carrying the glossopharyngeal nerve (IX), or a part of it.

The heavy proximal end of the opisthotic (Fig. 19A) bears articular facets for neighbouring bones: exoccipital, supraoccipital, and prootic, as well as for the basioccipital and possibly for the parabasisphenoid which it contacts by means of its ventral ramus. The contact between the opisthotic and exoccipital is subhorizontal, the latter extending ventromedially. Dorsolateral to it, and facing antero-medially, is the supraoccipital facet. This is slightly convex, and pierced by the circular opening of the posterior semicircular canal that penetrates the posterolateral margin of the supraoccipital after having left the opisthotic (Fig. 19A). The prootic facet cuts obliquely across the proximal end of the opisthotic. This surface is overlapped laterally by the posterior process of the prootic and is pierced by the horizontal semicircular canal. Below this, the opisthotic contains a large ventral cavity for the posteroventral part of the vestibule, with the exit of the horizontal semicircular canal and a posterior ampullary recess (Fig. 23A) into which the posterior semicircular canal opens. The lagenar recess must have been located medial to the ventral ramus (Fig. 23A).

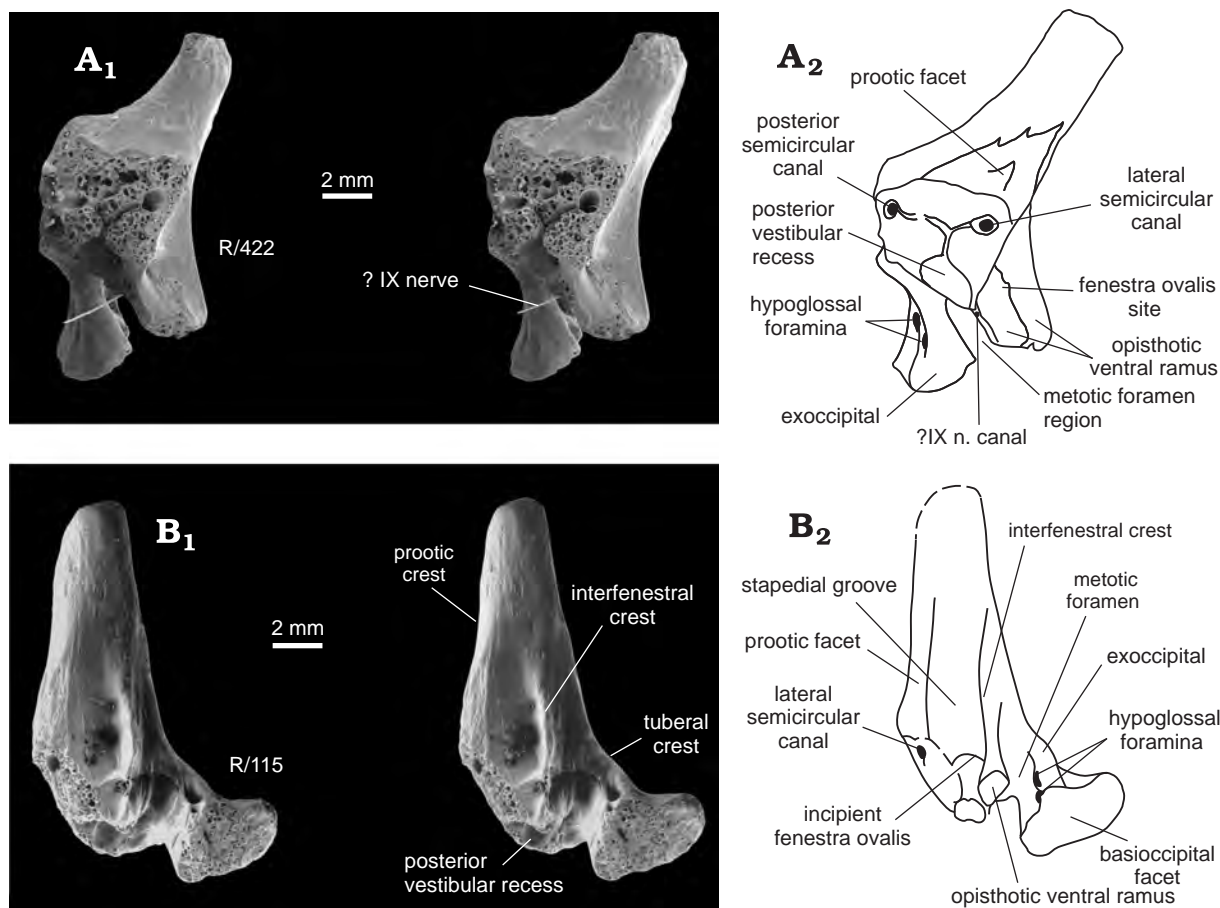


Fig. 19. *Osmolskina czatkowicensis* Borsuk-Białynicka *et* Evans, 2003, Early Triassic of Czatkowice 1, Poland. **A.** Left opisthotic + exoccipital ZPAL RV/422, in antero-lateral view. White line in A shows the possible course of the IXth nerve canal. **B.** Left opisthotic + exoccipital ZPAL RV/115, in ventral view. A₁, B₁, SEM stereo-pairs. Shortened catalogue numbers indicate the specimens on which the reconstruction is based.

Parabasisphenoid. — Some specimens from Czatkowice 1 (*e.g.*, ZPAL RV/412) display a clear division of the parabasisphenoid (Fig. 20C₂) into a spongy endochondral, probably basisphenoid part, and a thin sheet of finished dermal bone, probably corresponding to the parasphenoid. The parasphenoid rostrum is roughly U-shaped in transverse section. It bears a blunt sagittal crest ventrally and a longitudinal dorsal furrow. Although the exact life position is unknown, an oblique, anterodorsal orientation of the parasphenoid rostrum (Fig. 17C) is suggested by that of the neighbouring bones. As a whole, the parabasisphenoid is a triangular bone with the apex extended into an elongated parasphenoid rostrum and the body divided dorsally into anterior and posterior parts by clinoid processes united by a transverse crest (*crista sellaris*). The parasphenoid sheet extends posteriad over the ventral surface of the basisphenoid to produce large posterolateral flanges that cover the basisphenoid–basioccipital contact from below (Fig. 21C₁). They protrude well beyond the basisphenoid. Their tips have been referred to as parabasisphenoid basal tubera (Gower and Weber 1998), but in *Osmolskina* they seem to be produced by the parasphenoid. The flanges are separated from each other by a roughly V-shaped incision, the margin of which is very thin and usually badly damaged. It is therefore difficult to say how large the parasphenoid overlap was on the surface of the basioccipital. A pitted surface on the ventral aspect of the basioccipital (Fig. 17B₁) suggests that the parasphenoid retained a posteromedial flange similar to that of *Prolacerta*. There is however no evidence of a transverse thickening homologous to that in erythrosuchids (Parrish 1992, fig. 4) and described as an intertuberal plate by Gower and Sennikov (1996).

The braincase floor of *Osmolskina* is organised on two levels, the floor of the braincase cavity being situated significantly higher than the parasphenoid rostrum and more or less parallel to the latter. Between them the basisphenoid body is essentially vertically aligned. The anteriorly directed surface is occupied by the hypophysial fossa below and the dorsum sellae above it. The *crista sellaris* separates the dorsum sellae from

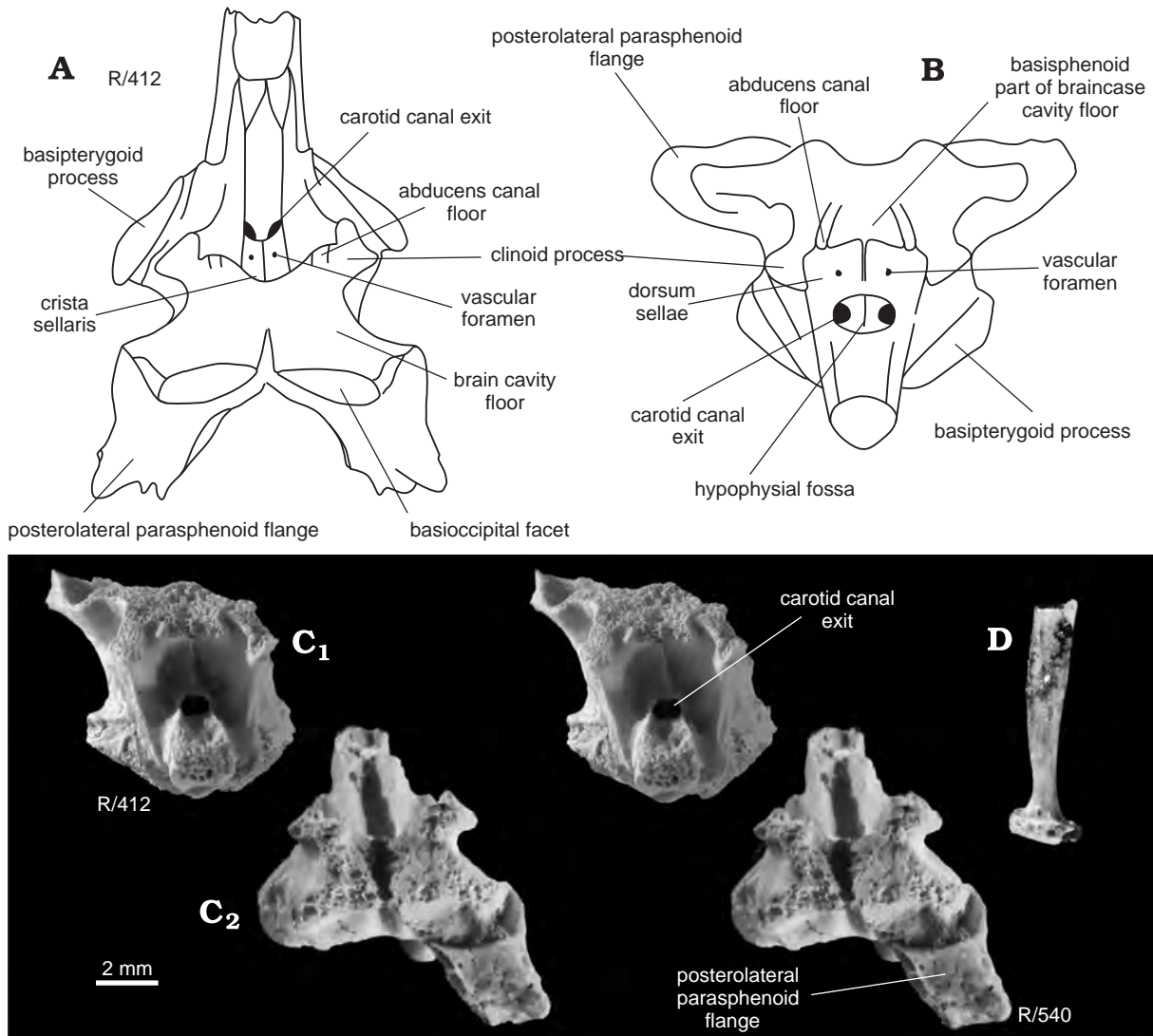


Fig. 20. *Osmolskina czatkowicensis* Borsuk-Białynicka *et* Evans, 2003, Early Triassic of Czatkowice 1, Poland. **A**, **B**. Parabasisphenoid reconstruction based on specimen ZPAL RV/412, in dorsal (**A**) and anterior (**B**) views. **C**. Parabasisphenoid ZPAL RV/412, in anterior (**C**₁) and dorsal (**C**₂) views. **D**. Stapes ZPAL RV/59. **C**₁, **C**₂, stereo-pairs. Shortened catalogue numbers indicate the specimens on which the reconstruction is based.

the basisphenoid part of the braincase floor. Some specimens (Fig. 20A, C) preserve paired furrows of finished bone that cut through the crista sellaris and represent the floor of the abducens canals, the roof being made by the anterior inferior prootic processes. The hypophysial fossa is a small concavity continuous with the dorsal furrow of the rostrum (Fig. 20B, C₁). It is pierced by paired foramina for the cerebral branches of the carotid artery, but some additional vascular foramina produced by superficial bone bridges may also appear. A sagittal crest divides the dorsum sellae into bilateral concavities for eyeball muscles (*m. retractor bulbi* and *m. bursalis*) and the venous system (Säve-Söderbergh 1946). It is bordered on each side by an acute lateral crest, and is pierced by tiny vascular foramina. The dorsal surface of the basisphenoid is essentially X-shaped. The clinoid processes diverge anteriorly. They are separated from the posterolateral parts of the basisphenoid by deep bilateral incisions. Each incision corresponds to the lateral depression of Gower and Weber (1998), and is a sub-vertical furrow on the lateral face of the parabasisphenoid destined for the palatal branch of the facial nerve that descended from the prootic. The internal carotid artery probably also used this passage to reach the entrance foramen on the ventral side of the parabasisphenoid between the basipterygoid processes.

Posteriorly, the basisphenoid bears paired ovoid surfaces for basioccipital contact. These are covered by a thin layer of finished bone. Lateral to them, small surfaces, one on each side, might have received the

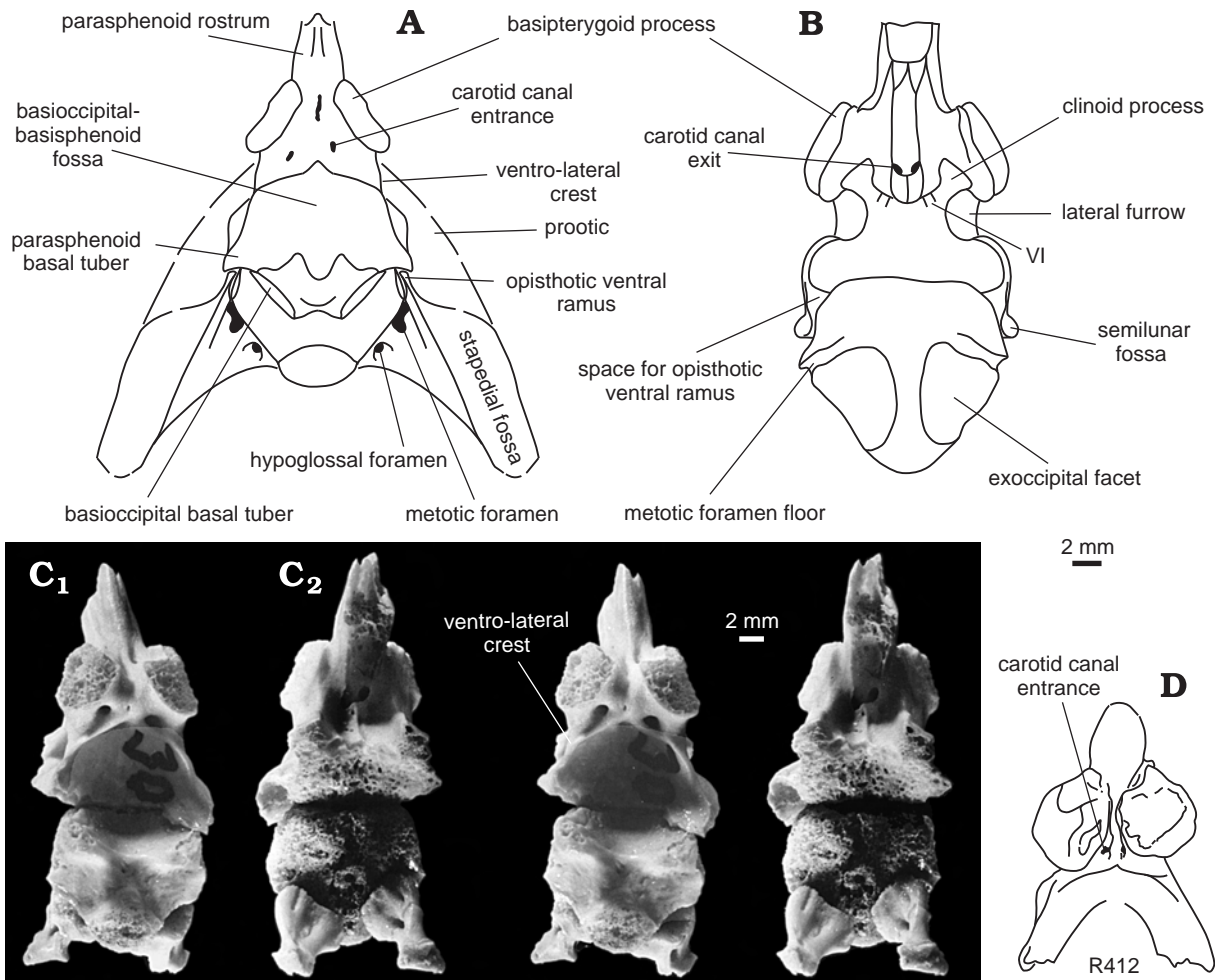


Fig. 21 *Osmolskina czatkowicensis* Borsuk-Białynicka *et* Evans, 2003, Early Triassic of Czatkowice 1, Poland. **A.** Braincase reconstruction, in ventral view. **B.** Reconstruction of parabasisphenoid combined with basioccipital, in dorsal view. **C.** Partial braincase ZPAL RV/413 combined from different individuals, in ventral (C_1) and dorsal (C_2) views. **D.** Parabasisphenoid ZPAL RV/412, in ventral view. C, stereo-pairs.

opisthotic ventral rami. The surfaces are bordered ventrally by well-ossified parasphenoid laminae extending posterolaterad (parasphenoid flanges), and facing dorsally.

The lateral wall of the parabasisphenoid (Fig. 24A) turns anteroventrally into the neck of the basipterygoid process. The dorsal border of the lateral wall extends between the clinoid process and the apex of the posterolateral parasphenoid flange, its posterior corner bearing a semilunar fossa (Fig. 24A) facing laterally. The anterior border of the wall is the lateral crest of the dorsum sellae, whereas the posterior one is the ventrolateral crest. Posterior to the basipterygoid process, the lateral wall of the parabasisphenoid bears a sub-vertical furrow (Figs 17C, D, 24A) for the palatine branch of the facial nerve and the internal carotid artery. At the contact with the prootic, the furrow is deep, and is bordered anteriorly by a distinct prootic crest (Fig. 24A). Both furrow and crest fade out ventrally. The nerve and artery must have wound around the posterior angle of the basipterygoid stalk, with the artery then dividing into two parts. As recognized by earlier authors (Evans 1986; Gower and Sennikov 1998), the cerebral part entered the foramen on the ventral side of the braincase (Fig. 21A), while the anterior, palatal branch, along with the palatine branch of the facial nerve, could have followed the sub-horizontal furrow on the ventral side of the parasphenoid rostrum (the palatine branch is lost in adult crocodiles; personal communication from the referee D. Gower).

Ventrally, the braincase is excavated by a deep fossa (Fig. 21C₁), referred to as basioccipital-basisphenoid fossa by Gower and Sennikov (1996). The fossa extends posteriorly to the apices of the parasphenoid flanges and is bordered laterally by the acute ventrolateral crests which fuse with each other posterior to the basipterygoid processes.

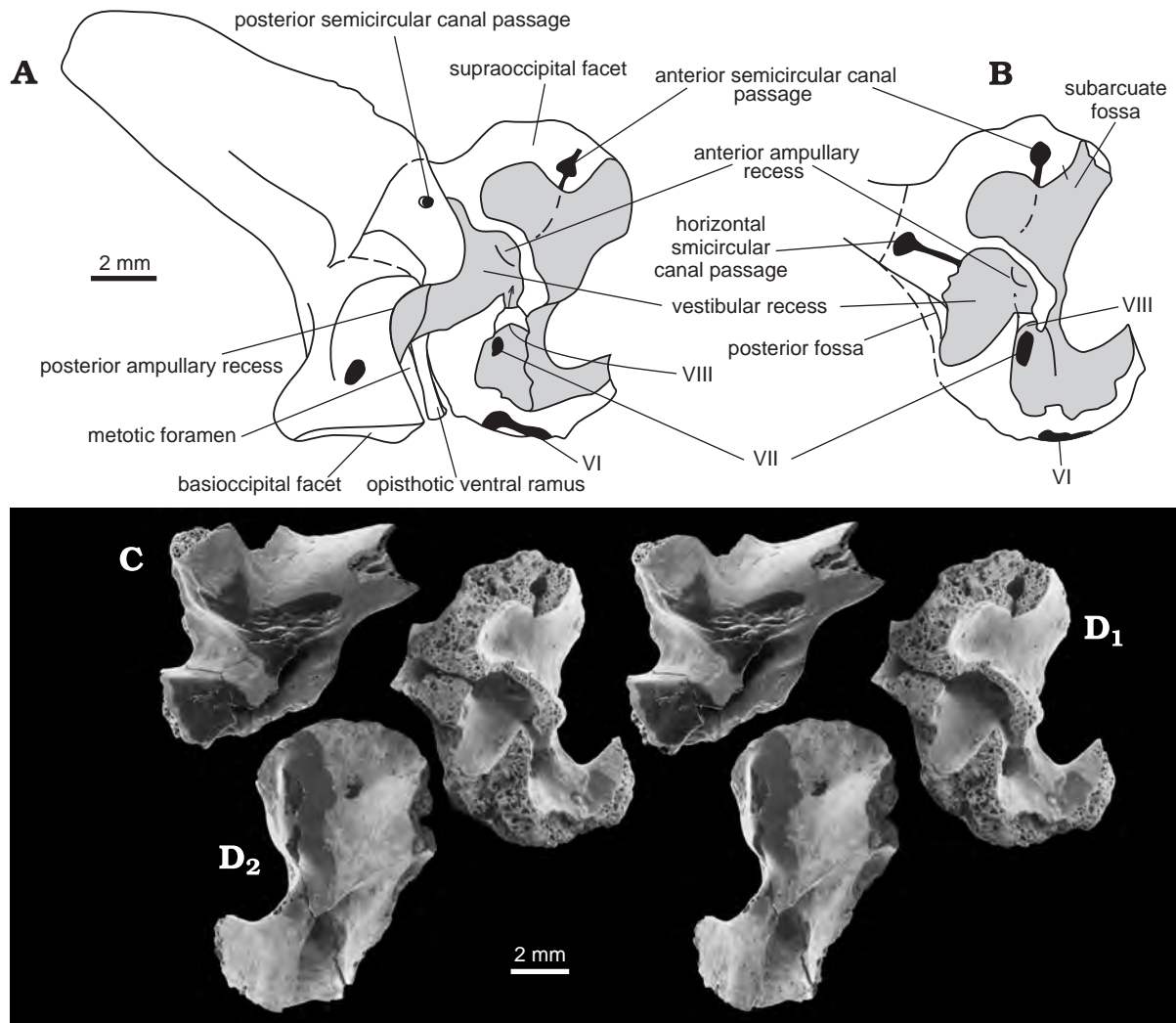


Fig. 22. *Osmolskina czatkowiczensis* Borsuk-Białynicka *et* Evans, 2003, Early Triassic of Czatkowice 1, Poland. **A**. Reconstruction of the opisthotic and exoccipital combined with the prootic, in medial view. **B**, **D**. Prootic ZPAL RV/124, in medial (**B**, **D**₁) and lateral (**D**₂) views. **C**. Prootic ZPAL RV/123, in lateral view. **C**, **D**, SEM stereo-pairs.

The basiptyergoid processes are thick rounded bodies on short stout stalks that are mainly directed ventrally. An articular surface of finished bone is preserved in only a few specimens (*e.g.*, ZPAL RV/412), but usually the whole distal part is damaged. The mutual relations of the basiptyergoid processes show some variability. This variability also affects the position of the carotid foramina, but, as a rule, they are situated on the ventral surface of the parabasisphenoid, posterior to the basiptyergoid stalks and in front of the arched crest produced by fused anterior sections of the ventrolateral crests.

Prootic. — The prootic (Fig. 22) encloses the main part of the osseous labyrinth of the inner ear. Its lateral surface is dominated by elongated swellings corresponding to the anterior and lateral semicircular canals and ampullae (Figs 22, 23A, B). The position of the lateral canal determines the orientation of the long axis of the bone and this appears to be sub-vertical (Fig. 22A, B, D). Posteriorly, the main part of the prootic extends into a triangular process that overlaps the opisthotic, and is usually broken off. Anteriorly, the otic region is separated from the anterior inferior process by an open U-shaped trigeminal notch. The notch is partially divided by a protruding part of its margin into two parts (Fig. 24A), the upper part for the exit of the medial cerebral vein, and the lower part, the trigeminal notch proper, for the trigeminal nerve. On the lateral side of the bone (Fig. 22C, D), the trigeminal notch extends into a large sub-horizontal furrow under the prominence corresponding to the anterior ampullary recess. The furrow fades out posteriad where it is crossed by a sub-vertical anterior section of the prootic crest. The extension of the crest onto the opisthotic borders the stapedia fossa and forms the lat-

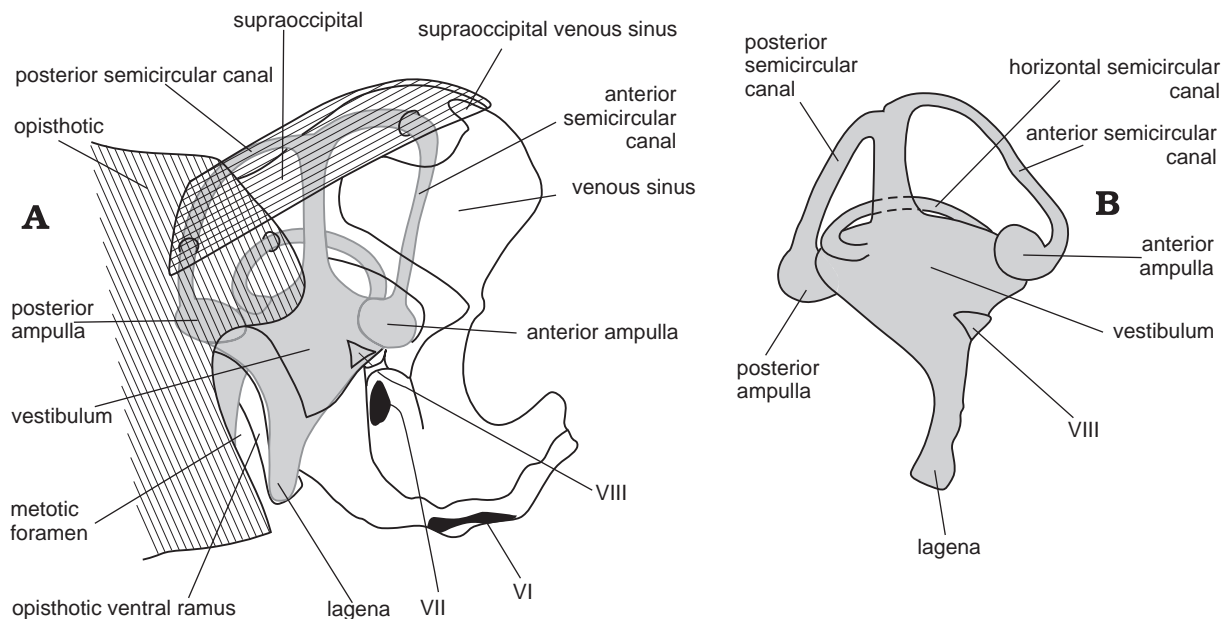


Fig. 23. *Osmolskina czatkowicensis* Borsuk-Białynicka *et* Evans, 2003, Early Triassic of Czatkowice 1, Poland. **A.** Reconstruction of a labyrinth based on the bones illustrated in Fig. 22B, D₁. **B.** Labyrinth in *Alligator mississippiensis* (according to Wever 1978, fig. 24-15). Not to scale.

eral wall of the tympanic cavity. Anteriorly, it provided attachment for the aponeurosis of origin of the protractor pterygoideus muscle (Oelrich 1956). A single large circular foramen for the facial nerve (VII) is situated in a deep concavity posterior to the prootic crest (Fig. 22A) and is overhung by the crest. The groove for the palatine branch of the facial nerve, and for the carotid artery, extends anteroventrally from the facial foramen region. It passes from the prootic onto the basisphenoid, thus determining their mutual contact. The second furrow, for both the hyomandibular branch of the facial nerve and the carotid artery fades out posteriad. There is no distinct partition of the furrow into nervous and vascular parts.

The lateral surface of the anterior inferior process is flat, and bordered dorsally by a faint blunt horizontal crest (possibly for the protractor pterygoidei muscle: Oelrich 1956; Gower and Sennikov 1996; Gower 2002), and bordered posteriorly by the prootic crest. The anterior end of the process bears a slightly concave, anteroventrally directed facet of finished bone (ZPAL RV/532), the only possible trace of the laterosphenoid (if present). The abducens nerve presumably passed through the basisphenoid-prootic suture leaving shallow furrows in both elements (Fig. 20A, B, C₁). The canals certainly cut through the crista sellaris to open directly above the dorsum sellae. The ventral border of the anterior inferior process bears an elongated ventromedially facing facet for the clinoid process of the basisphenoid, but this is usually poorly preserved. When oriented, the prootics converge slightly anteroventrad. As preserved, they do not meet each other in the midline, but the lack of contact is probably only a matter of preservation or of poor ossification in immature animals.

In medial aspect (Fig. 22A, B, D₁), the prootic is excavated by a complicated system of concavities separated from each other by blunt ridges of unfinished bone that were probably extended by connective tissue in life. The supraoccipital and opisthotic facets contribute to the posterodorsal borders of the cavities. They face medially and bear a circular opening for the anterior semicircular canal near the anterior end, and a trace of the lateral canal along the posterior opisthotic process. The largest and most posterior of the cavities enclosed the lower lateral part of the vestibule. The lateral semicircular canal begins with the anterior ampullary recess in the deepest, most dorsal part of the concavity, and extends into the posterior process. It has its circular exit at the end of this process where it penetrates the lateral face of the opisthotic. The anterior semicircular canal extends directly dorsad to exit through the supraoccipital facet. Towards the posteroventral margin of the bone, the vestibular concavity has a funnel-shaped ventral prolongation that continues into the opisthotic (Fig. 22A) and includes the posterior ampullary recess with the entrance of the posterior semicircular canal. The funnel-shaped space (Fig. 22B, D₁, vestibular recess) must have housed the ventralmost part of the labyrinth that passed into the lagena (Fig. 23A, B; Wever 1978). There is no crest to separate the lagena from the main vestibular part. In contrast, a crest has been described in at least some archosaurs (Gower 2002; crista

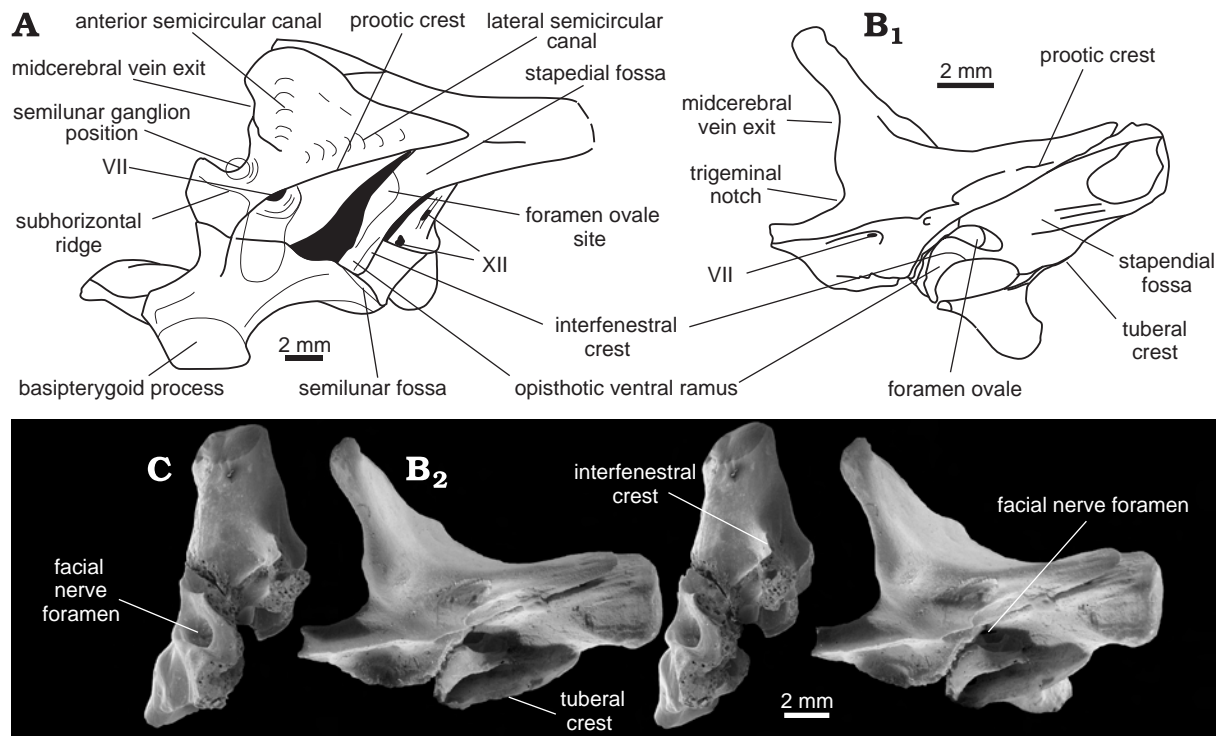


Fig. 24. *Osmolskina czatkowicensis* Borsuk-Białynicka *et* Evans, 2003, Early Triassic of Czatkowice 1, Poland. **A.** Reconstruction of the braincase, in lateral view. **B.** *Varanus griseus* braincase, Recent, in lateral view. **C.** Opisthotic associated with fragmentary prootic ZPAL RV/540, in ventral view. B₂, C, stereo-pairs.

vestibuli). The lagena must have lain ventrally within the unossified part of the braincase wall. Ventral to the base of the posterior process, and posterior to the vestibular concavity, there is a triangular shelf (posterior fossa; Fig. 22B, D₁; see also ZPAL RV/532) facing posteromedially. It contributes a small anterolateral part to the stapedial groove.

Dorsal to the vestibular recess and separated from it by a ridge, and medial to the anterior semicircular canal, there is a shallow concavity corresponding to the subarcuate fossa (Fig. 22B). This is more or less circular in outline but opens into a wide funnel-shaped mouth anteriorly. It probably housed a cerebellar flocculus (concerned with the maintenance of equilibrium), and a dural venous sinus as in *Youngina capensis* and *Prolacerta broomi* according to the interpretation by Evans (1986, 1987). The venous sinus could have extended into a lateral cavity in the anterior border of the supraoccipital (Fig. 18A₁, A₂, C₂). The furrow perforated by the facial nerve (VII) forms a third anteroventral concavity in the medial face of the prootic. Anteriorly, this concavity opens towards the trigeminal notch. Posterodorsally a furrow, possibly for the vestibulocochlear nerve (VIII), leads into the vestibular cavity and is medially closed by a narrow bridge of bone.

Laterosphenoid. — As yet, the laterosphenoid has not been recognized in *Osmolskina*, and evidence for its presence is inconclusive. Regions of possible contact can be suggested on the basis of Clark's *et al* (1993, fig. 2) description of *Proterosuchus fergusi* in which the laterosphenoid articulates with the alar process (dorsal wing) of the prootic and with the tip of the anterior inferior process of the same bone (thus enclosing the trigeminal foramen). Dorsally, it meets the skull roof, articulating with a facet/recess on the under surface of the parietal wing (medial to the postfrontal articulation) as well as with the descending crest of the frontal. In *Osmolskina*, the dorsal wing of the prootic shows a small descending extension to the supraoccipital facet (Fig. 22) while the tip of the anterior inferior process, sometimes bears a small surface of finished bone that may be for the laterosphenoid. It should be stressed, however, that the trigeminal notch is much more open than it is in *Proterosuchus fergusi*. On the other hand, the underside of the lateral wing of the parietal bears a rugose surface, immediately medial to the postfrontal facet that matches the position of the laterosphenoid attachment surface in *Proterosuchus* (Clark *et al.* 1993, fig. 2).

In extant crocodiles, the laterosphenoid ossifies early in embryogenesis (Iordansky 1973, p. 252, fig. 13), and was probably ossified in *Osmolskina* despite the possible immaturity of the preserved bones.

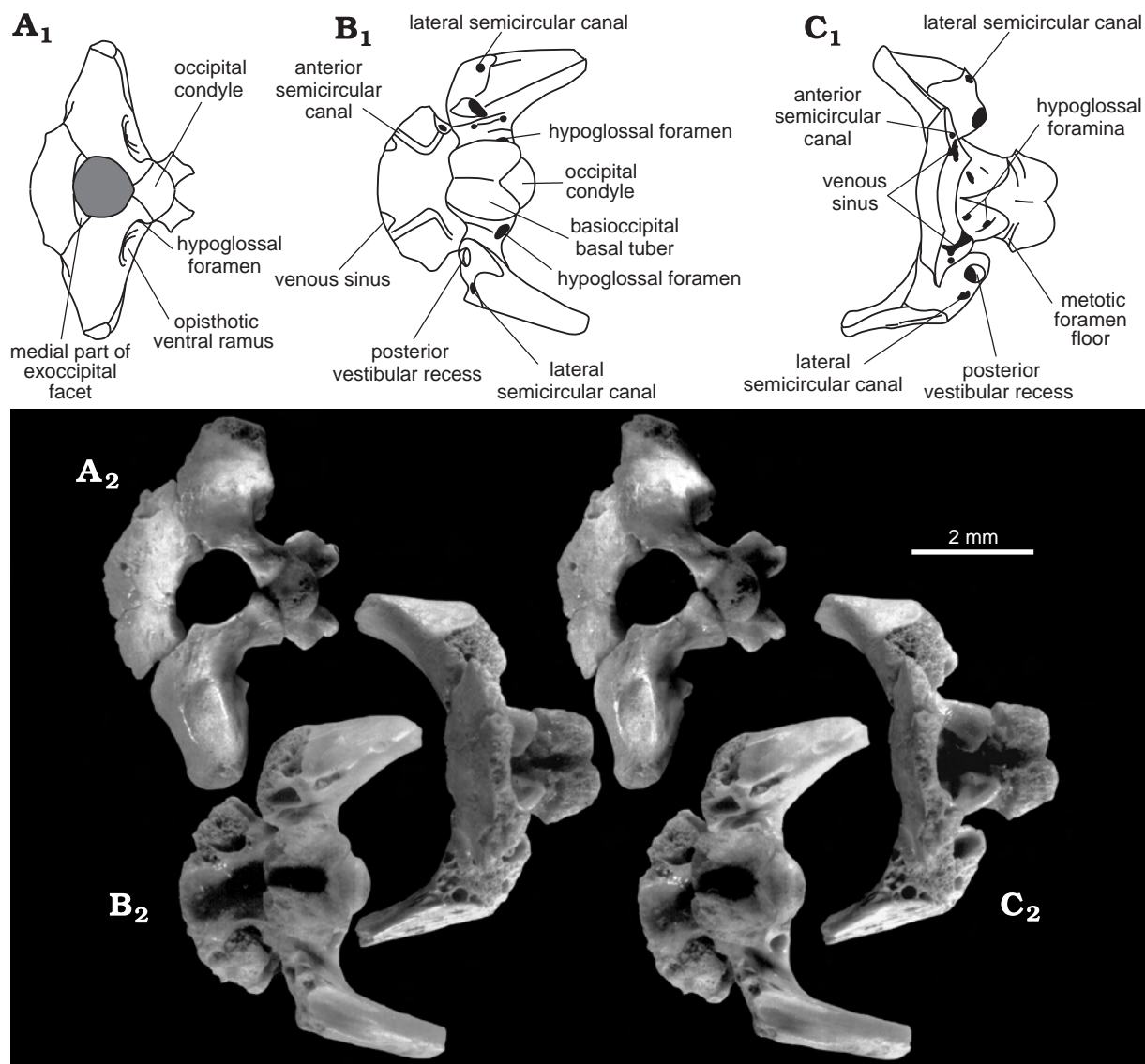


Fig. 25. *Osmolskina czatkowicensis* Borsuk-Białynicka *et* Evans, 2003, Early Triassic of Czatkowice 1, Poland. Posterior part of the braincase ZPAL RV/424 combined from different individuals, in occipital (A), ventral (B), and anterior (C) views. A₂, B₂, C₂, stereo-pairs.

MANDIBLE

Dentary. — As reconstructed, the dentary (Fig. 26A) is approximately six times longer than deep, slightly deeper at the posterior end. The posterior margin is always damaged, and shows neither facets for the posterior mandibular bones, nor the anterior border of the mandibular fenestra. The lateral face is convex in transverse section, uneven and permeated by nutrient foramina that are distributed mainly along the dorsal margin of the bone and in the mental region. As a rule, one of the foramina, situated at the level of the second tooth position, is much larger than the others. Some of the posterior foramina extend posteriad into furrows. Lingually, the Meckelian fossa is long and low, expanding slightly in the vertical plane towards the rear. It bears three foramina that probably carried the inferior alveolar nerve and its branches. The posteriormost foramen is situated slightly behind the mid-length of the bone and may have allowed the alveolar nerve to pass from the Meckelian fossa into the inferior alveolar canal. The Meckelian fossa is bordered by two ridges, both bearing faint traces of the splenial. The sub-dental ridge is sub-equal in depth to the fossa, and is deeper than the sub-Meckelian ridge. Anteroventrally, at about the fifth tooth position (Fig. 26C, D), it is obliquely cut by the splenial facet. The shape and anterior limit of the splenial (Fig. 26B) has been reconstructed from

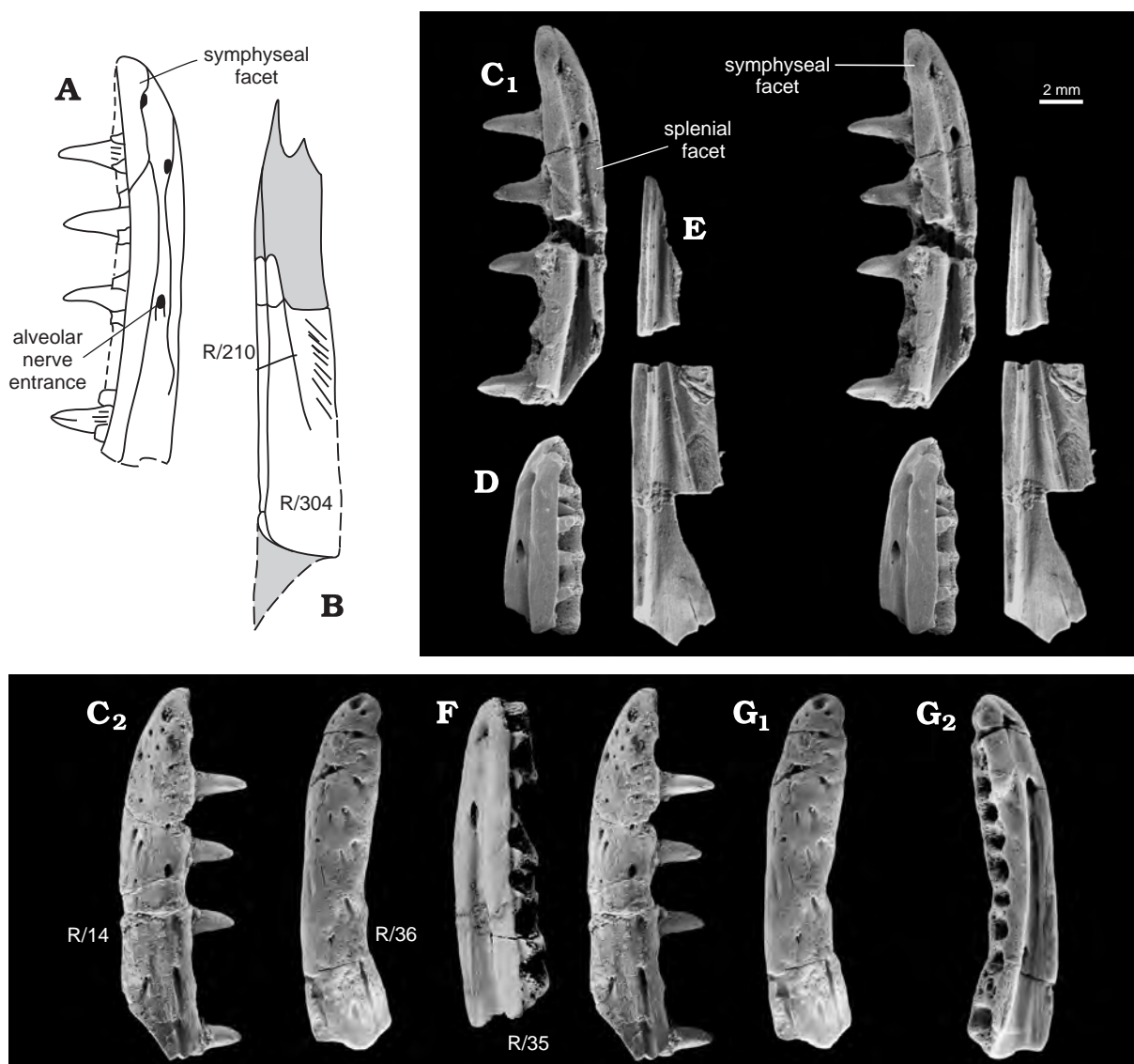


Fig. 26. *Osmolskina czatkowicensis* Borsuk-Białynicka *et* Evans, 2003, Early Triassic of Czatkowice 1, Poland. **A**. Dentary reconstruction. **B**. Right splenial reconstruction based on ZPAL RV/210 and 304. **C**. Left dentary ZPAL RV/14. **D**. Anterior part of right dentary ZPAL RV/562. **E**. Right splenial ZPAL RV/304 (below) and ZPAL RV/210 (above). **F**. Right dentary ZPAL RV/35. **G**. Left dentary ZPAL RV/36. Lingual (A, B, C₁, D, E, F, G₂) and labial (C₂, G₁) views. C–G₂, SEM micrographs; all but F and G₂ stereo-pairs. Shortened catalogue numbers indicate the specimens on which the reconstruction is base.

these traces. The symphyseal surface is barely delimited, but seems to extend posteriorly to the fourth alveolus. The alveolar border is subdivided by interdental septa into alveoli that are usually preserved empty. Interdental plates border the lingual side of each alveolus at the front and rear (Fig. 30D, E). When the teeth are preserved they are fastened by spongy bone of attachment. The longest preserved specimen, ZPAL RV/36 (Fig. 26G₂), bears 12.5 alveoli. There is variation in the robusticity of the dentaries and in the corresponding shape of their anterior ends (Fig. 26C₂, F). This is considered to represent individual and ontogenetic variation.

Surangular. — The surangular is represented by numerous fragments (Fig. 27A, D, E), of which the most complete are from the posterior region. The bone usually breaks into pieces, particularly in its very fragile anteroventral portion. No part of the anteroventral border is ever preserved, and the presence of the mandibular fenestra may only be deduced from the dorsal border of the angular (see below). The outline of the fenestra (Fig. 1F, G) is conjectural, but the lateral wall of the surangular is quite deep at its contact with the dentary, suggesting a fairly low position for the inferred fenestra.

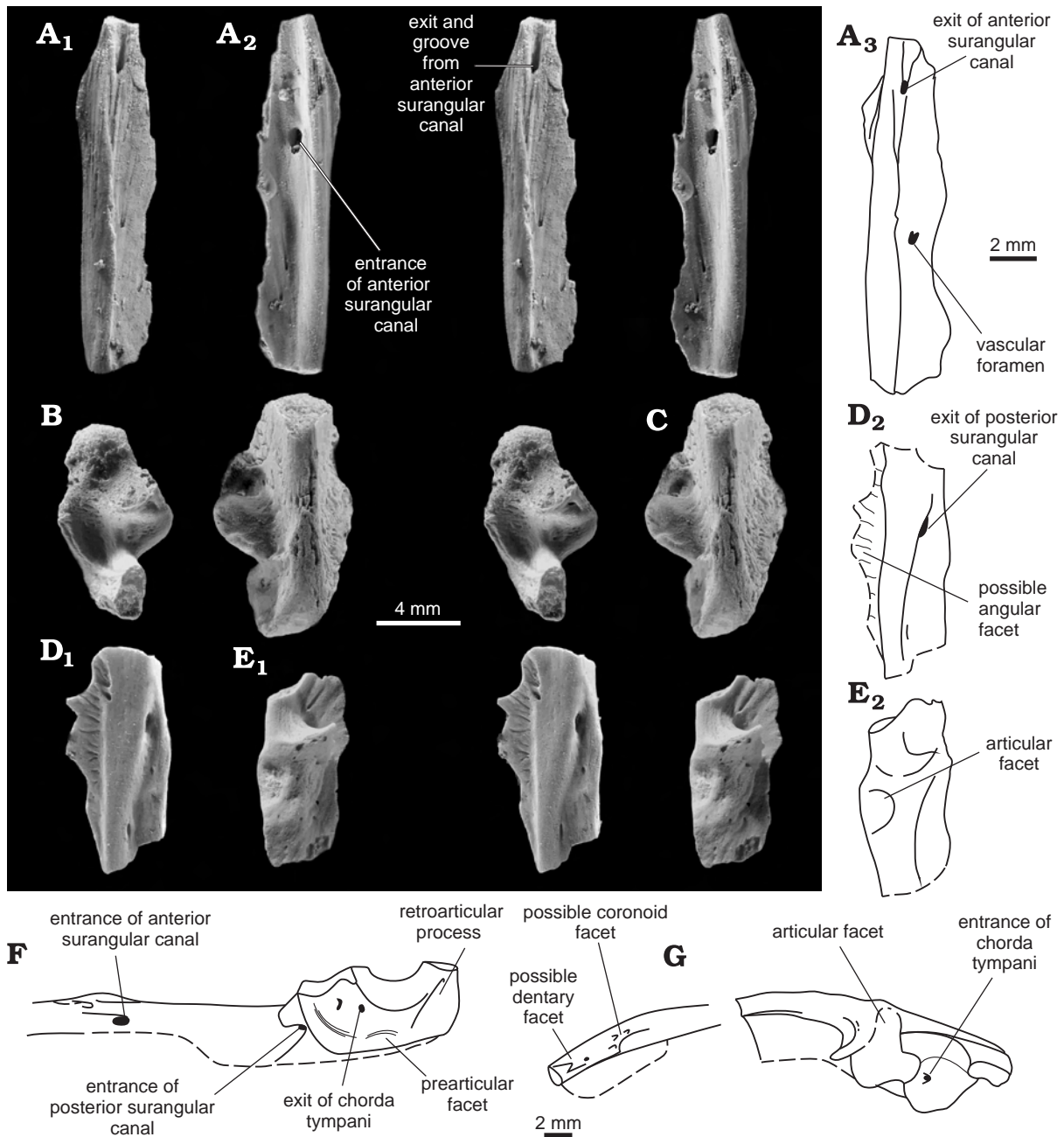


Fig. 27. *Osmolskina czatkowicensis* Borsuk-Białynicka *et* Evans, 2003, Early Triassic of Czatkowice 1, Poland. **A.** Anterior fragment of right surangular ZPAL RV/551, in dorso-lateral (A₁, A₃) and medial (A₂) views. **B.** Left articular ZPAL RV/549, in dorsal view. **C.** Left articular ZPAL RV/321, in ventral view. **D.** Posterior end of the left surangular ZPAL RV/550, in ventral view. **E.** Posterior end of the left surangular ZPAL RV/548, in dorsal view. **F, G.** Reconstruction of the surangular and articular, in medial (**F**), and dorsal (**G**) views. A₁, A₂, B, C, D₁, E₁, SEM stereo-pairs.

The bone is a flat elongated plate that is laterally convex along the longitudinal axis. It is overhung, both laterally and medially, by a thick dorsal ridge. In the posterior portion of the bone, the dorsal ridge produces a hook-like medial projection that forms an anterior buttress for articulation with the articular bone. This part is pierced by two foramina (Fig. 27D–F) probably corresponding to the entrance (the medial one) and the exit (the lateral one) of the posterior surangular canal (Oelrich 1956). Posterior to the hook-like projection, the surangular extends into a long pyramidal process, its ventrolateral wall (Fig. 29A₁) tapering posteriad. The longitudinal convexity of the dorsomedial wall of the pyramid (Fig. 27E) matches the concavity of the ventrolateral face of the articular (Fig. 27C). The third wall of the pyramid (Fig. 29A₃) is an elongated triangular continuation of the thick dorsal ridge of the anterior portion.

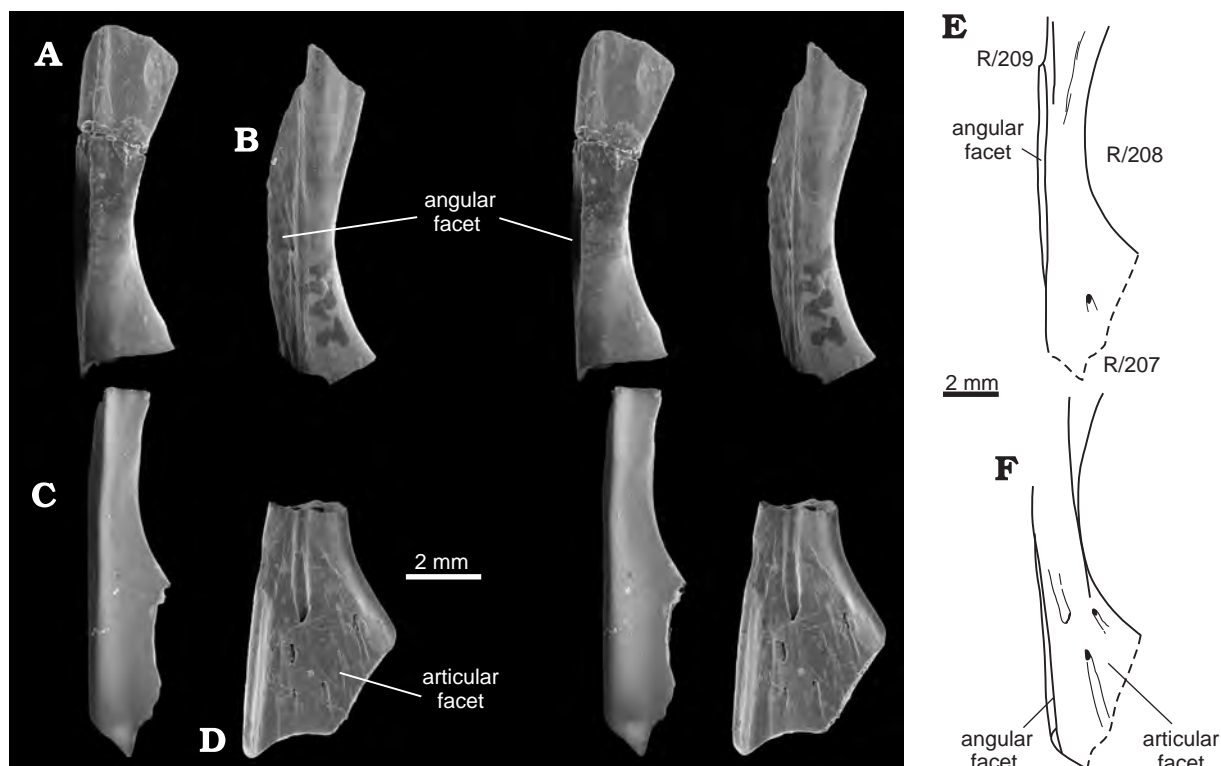


Fig. 28. *Osmolskina czatkowicensis* Borsuk-Białynicka *et* Evans, 2003, Early Triassic of Czatkowice 1, Poland. Prearticular: ZPAL RV/208 (A), ZPAL RV/214 (B), ZPAL RV/209 (C), and ZPAL RV/207 (D). A–C. Right bones, in medial view. D. Right bones, in lateral view. E, F. Reconstructions of the bone, in medial (E) and lateral (F) views. A–D, SEM stereo-pairs. Shortened catalogue numbers indicate the specimens on which the reconstruction is base.

Anterior to the hook-like projection, the dorsal ridge is bordered by two crests, a lateral one that overhangs the lateral face of the bone (Fig. 27A₁), and a medial one (Fig. 27A₂) that passes gently into the concave dorsomedial surface of the mandibular fossa. The lateral crest probably corresponds to the structure described as an external flange of the surangular. This marks the origin of the lamina lateralis of the tendon supporting pterygoideus posterior muscle in extant crocodiles (Busbey 1989) and birds (Lakjer 1926). Clark *et al.* (1993) considered it to be characteristic of basal archosauriforms.

The anterior end of the dorsal ridge is produced into a small dorsal tuber, in front of which is a ridged surface (Fig. 27A₂) for possible articulation with the coronoid, although it might be, partly or entirely, a trace of the attachment of the mandibular adductor tendon. More anterior and slightly medial to this surface is the dentary facet. This part of surangular is pierced by foramina for branches of the mandibular artery and the mandibular division of the trigeminal nerve entering the mandibular fossa. This probably corresponds to the anterior surangular foramen (Oelrich 1956). The medial surface of the surangular (Fig. 27A₁, F) is a possible entrance, the lateral a possible exit (Fig. 27A₁, A₃) for the anterior surangular canal. The main plate of the surangular forms the lateral wall of the mandibular fossa and the posterodorsal border of a probable lateral mandibular fenestra. Where preserved, the lateral surface of the posteromedial border of the surangular bears an obliquely ridged facet for the overlapping angular (Fig. 27D₁, D₂).

Splenial (Fig. 26B, E). — The best-preserved splenials (PAL RV/210, 211, and 304) are too large to match the preserved dentaries, and are assigned only tentatively. This bone may be reconstructed from facets on the medial surface of the dentary (Fig. 26C₁) and angular (Fig. 29E). Based on the best-preserved specimen (ZPAL RV/210), the splenial was an elongate sub-triangular bone contacting the dentary ridges bordering the Meckelian fossa (see above). It must have extended to at least the fourth tooth position, its anterior border descending obliquely to a point between the third and second tooth position, before turning down around the level of the middle inferior alveolar nerve foramen, to the level of the second tooth position. Medially, the splenial is flat, except for the ventral border that curves towards the dentary. The lateral (internal) surface is correspondingly concave ventrally. Its lower border is overhung in a step-like manner by a hori-

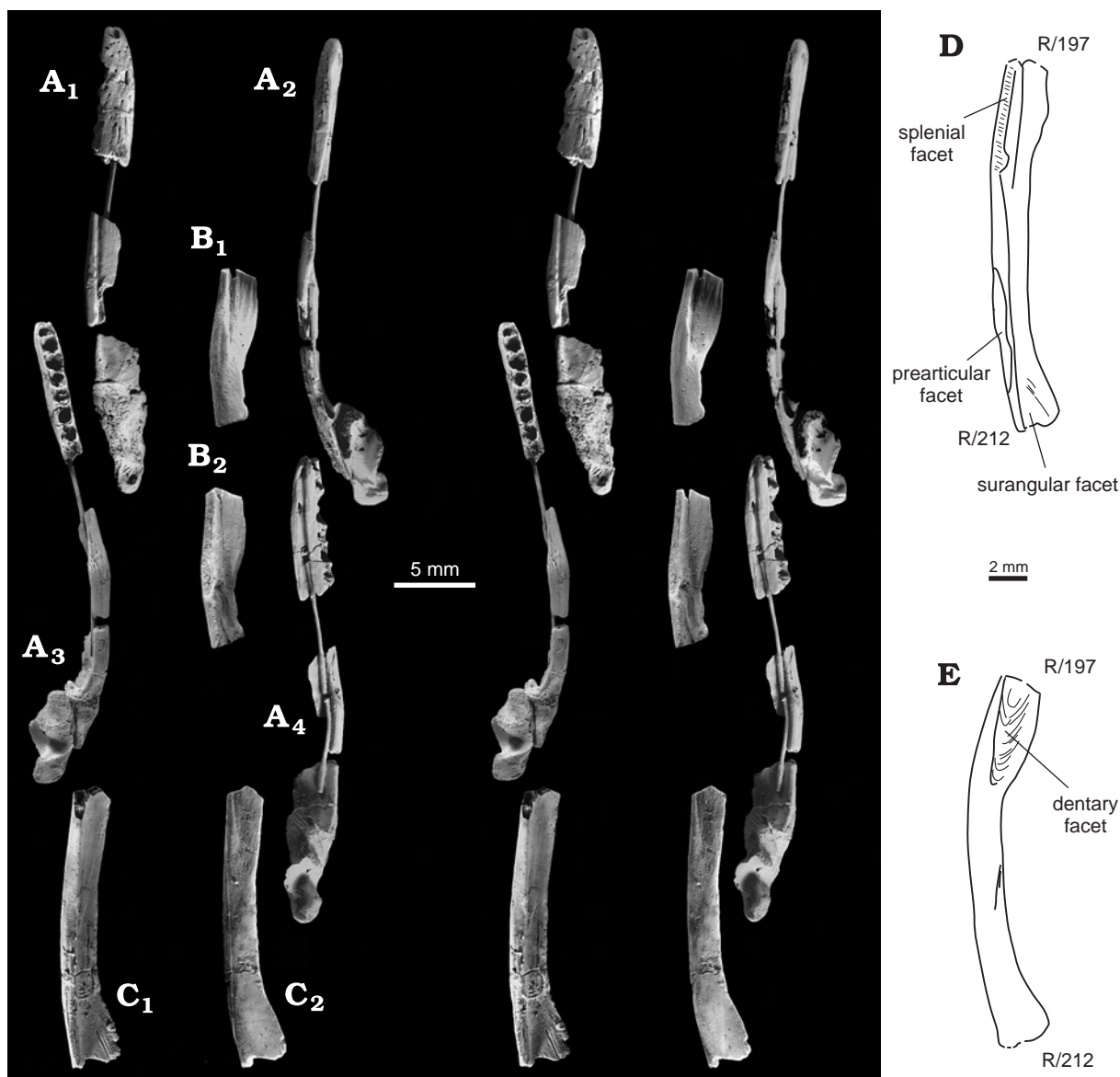


Fig. 29. *Osmolskina czatkowicensis* Borsuk-Białynicka *et* Evans, 2003, Early Triassic of Czatkowice 1, Poland. **A.** Right mandible ZPAL RV/ 35+35a combined from different individuals, in lateral (A₁), ventral (A₂), dorsal (A₃), and medial (A₄) views. **B.** Anterior portion of right angular ZPAL RV/197, in lateral (B₁) and medial (B₂) views. **C.** Posterior portion of angular ZPAL RV/212, in lateral (C₁) and medial (C₂) views. **D, E.** Reconstructions of right angular, in medial (D) and lateral (E) views. A–C, SEM stereo-pairs. Shortened catalogue numbers indicate the specimens on which the reconstruction is based.

zontal shelf that must have met the dorsomedial surface of the dentary sub-meckelian ridge (see above), whereas the ventral margin of the splenial contacted the medial surface of the ridge. The lateral (intra-mandibular) concavity of the splenial is subdivided by a longitudinal anteroventral crest.

Articular (Figs 27B, C, F, G, 29A). — In the Czatkowice material, the articular is never co-ossified with the surangular. This may be a genuine character or a reflection of immaturity. The articular is a fairly massive, ventrally crested, and dorsally tripartite bone. The anteriormost part of the dorsal face is occupied by articular cotyles for the quadrate condyles, and is divided posteriorly by a prominence (Fig. 27B). It is covered by unfinished and usually damaged bone, but was probably completed by a laterally protruding part. The central and posterior parts of the articular contribute to the retroarticular process. The central part displays a saddle-shaped dorsal surface divided into two concavities by a sagittal crest. The posterior part is a heavy, laterally compressed process (Fig. 27B) referred to as a “hooked ascending process” in *Batrachotomus kupferzellensis* (Gower 1999). It was probably for the attachment of the depressor mandibulae muscle tendon, as in extant croc-

odiles. When the surangular is oriented in a possible life position, the hooked ascending process of the articular is inclined medially. This inclination is similar to that in *Batrachotomus* (Gower 1999), but differs from that of crocodiles. The ventrolateral aspect of the articular bears a concavity (Fig. 27C) matching the convexity of the posterior process of the surangular to which it is applied (Fig. 27E). The medial surface is overhung by a protruding semi-circular shelf, and is pierced by a foramen (Fig. 27B, C, G). A similarly located foramen in extant crocodiles is an entrance into a blind pneumatic space (foramen aerum Iordansky 1973). In *Osmolskina*, the foramen leads to a canal that opens on the dorsomedial surface of the articular, exactly as it does in numerous rauisuchians and is similarly interpreted as a chorda tympani canal (Gower 1999). The structure of the retroarticular process is closely comparable to that of an extant crocodile, but is shorter and broader. It is longer than in *Batrachotomus* (Gower 1999).

Prearticular. — As reconstructed (Fig. 28E, F) from fragmentary remains (ZPAL RV/207–209, 213–215), the prearticular consists of an elongated body joining two sub-triangular ends. Ventrally, the bone angles laterally along a straight ridge to form a horizontal step-like shelf extending toward the angular. The dorsal border of the bone is arcuate. It bordered the medial entrance to the mandibular fossa. The posterior end probably had a wide contact with the articular, and the anterior end ascended slightly towards the splenial and coronoid, but the structure of these contacts is unknown. The internal surface of the bone that walls the mandibular fossa medially is slightly concave in transverse section, and is richly permeated by neurovascular canals.

Angular. — This element is usually preserved in pieces (Fig. 29B–E). The longest specimen (ZPAL RV/212) demonstrates that the posterior end of the angular is slightly larger than the rest, and was covered by traces of radiating blood vessels on its inner, concave surface. The dorsal part of this surface probably overlapped the ventromedial margin of the surangular (Fig. 27D₂), but the surface does not reach far anteriorly. The more anterior dorsal border of the angular bears no trace of facets for the surangular and, thus, probably bordered the mandibular fenestra.

Along the ventral border of the bone there is an elongated surface that should have matched the one on the prearticular shelf, but the match is not perfect. Specimen ZPAL RV/197 is an anterior fragment of a right bone (Fig. 29B). A long triangular lateral facet (Fig. 29E), open dorsally but ending ventrally in a deep sub-horizontal furrow, probably received a posterior process of the dentary that is not preserved in the material, whereas an elongated ventral step in the medial surface probably met the splenial (Figs. 29D, 36E–G). The position of the angular in relation to the other mandible bones, and particularly to the surangular, is far from clear.

Coronoid. — The coronoid has not been identified and the only information on this bone is a possible trace of this bone (Fig. 27G) at the anterior end of the dorsal ridge of the surangular (see above). Its position is reconstructed (Fig. 1G) on the basis of crocodile structure.

DENTITION

General remarks. — *Osmolskina* is well represented by jaw elements and many isolated teeth, but no specimen has a complete dentition preserved. This causes some difficulty in determining regional variation (see below). Those jaw fragments retaining teeth, firmly held by bone of attachment, are mostly large and perhaps closer to maturity. The teeth are typically worn, lack surface features, and may represent an adult morphology somewhat different from that of the majority of isolated teeth in the deposit.

Basic tooth morphology. — In describing a typical tooth, we are focusing on isolated, unankylosed, and therefore immature examples from the mid-part of the tooth series. A typical tooth of this type (*e.g.*, Fig. 30B) has a root and crown of roughly equal proportions. The tooth is widest at the gingival boundary. The root tapers only slightly towards the tip, but the crown does so sharply. The surface of the root is generally marked by parallel longitudinal striae reflecting the development of periodontal connective tissue holding the tooth in place; the cross-section remains ovoid (long axis anteroposterior). The crown is labio-lingually compressed and has a posteriorly recurved tip (convex anterior margin, concave distal one). The surface of the crown is shiny and smooth except for keeled and serrated anterior and posterior edges. The posterior margin bears a row of around 25 denticles (independent of tooth size) along the entirety of its edge. The anterior margin usually bears denticles on only the apical half (although the row may be longer), but these denticles are borne on a distinct, lingually inflected keel that may continue further than the serrations themselves. A broad furrow separates this

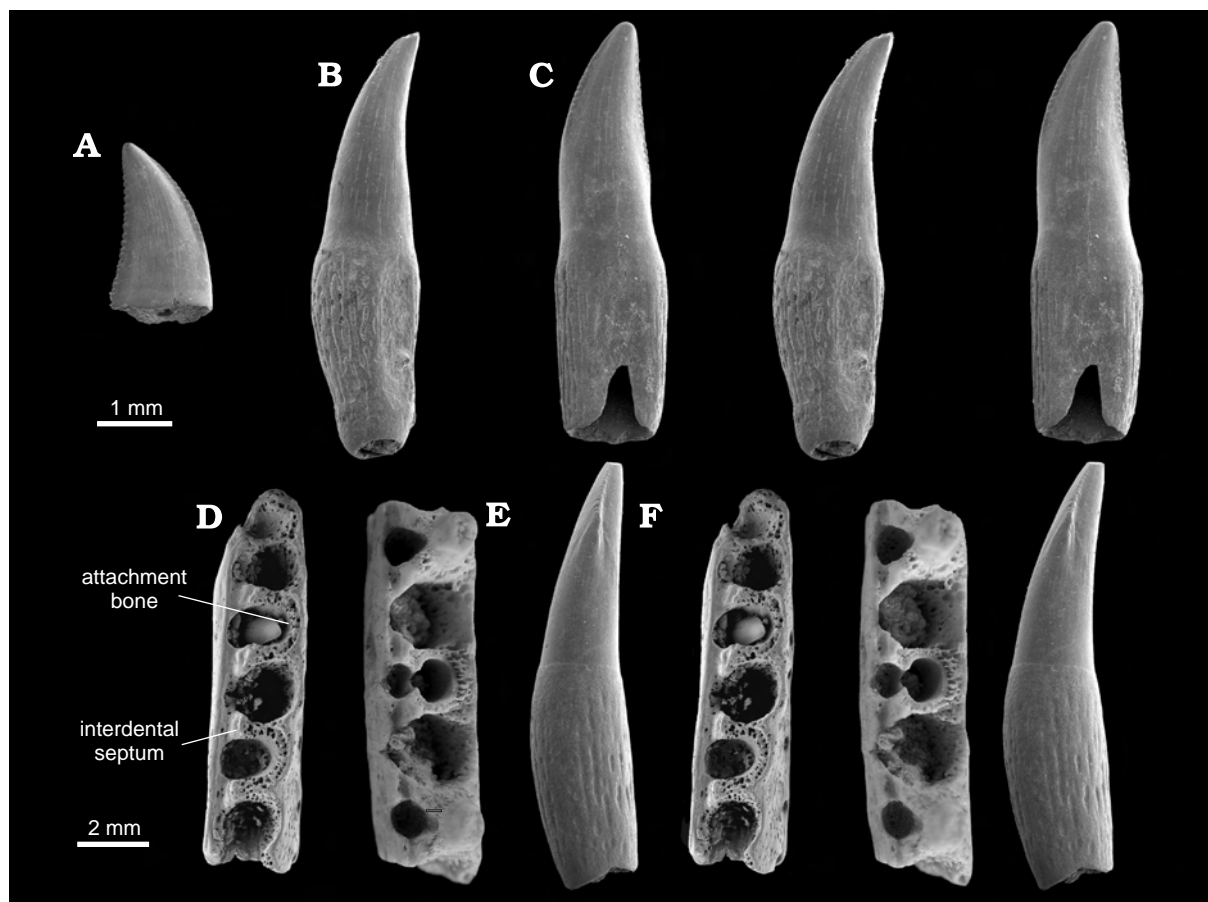


Fig. 30. *Osmolskina czatkowicensis* Borsuk-Białynicka *et* Evans, 2003, Early Triassic of Czatkowice 1, Poland. A–C, F. Isolated teeth. A. Juvenile tooth crown ZPAL RV/565. B. ZPAL RV/564. C. ZPAL RV/566. F. ZPAL RV/567. D. Anterior part of right dentary ZPAL RV/562. E. Middle part of right maxilla ZPAL RV/563. Lingual (A–C, F) and occlusal (D, E) views. SEM micrographs; all but A stereo-pairs.

anterior keeled margin from the remainder of the tooth surface on the lingual side (the labial side of the tooth curves uniformly) (*e.g.*, Fig. 30F). The denticles themselves are close set with parallel, weakly grooved margins and square or slightly rounded apices. Together they form a sharp, serrated cutting edge.

Implantation and replacement. — The implantation is fully thecodont. In a typical mid-jaw tooth, the root and the crown are of roughly equal length. The alveolar margin of each tooth-bearing element is divided into a series of rounded alveoli by a combination of lingual interdental plates and interdental septa (a combination referred to as an interdental unit by Senter 2003) composed mainly of bone of attachment (Fig. 30D, E). The attachment bone forms a thin layer on the internal wall of the alveolus in juveniles or where the teeth are not yet fully implanted (Fig. 30D), but fills the alveolus and blends with the surface of the tooth itself where the teeth are mature (Fig. 30E). During replacement, the lingual side of the alveolar bone is eroded first then the attachment bone, and finally the root. Once the functional tooth is lost, the replacement tooth fills a socket, but is only weakly attached. Only once the root is fully formed does bone of attachment become deposited around it. The high incidence, therefore, of isolated unerupted crowns (Fig. 30A), and complete but not yet fully attached, teeth, suggests that replacement was rapid. The rarity of fully attached teeth may suggest that much of the material is immature.

Two specimens (ZPAL RV/ 562 and 563) provide a good demonstration of the stages of implantation, attachment, and replacement. The juvenile jaw ZPAL RV/562 (Fig. 30D) contains no implanted teeth, but there is a single unerupted tooth crown in tooth position three. The alveoli have only a thin layer of attachment bone on the walls. The unerupted tooth crown is pristine and the anterior and posterior serrations are clearly visible. This is a labio-lingually compressed tooth of the type described above as typical. ZPAL RV/563 (Fig. 30E) is the central part of an older maxilla, preserving five tooth positions from the level of the

anterior maxillary pillar backwards. It shows alternate tooth replacement. Positions one, three and five (as preserved) contain mature teeth (broken tooth bases), while positions two and four are empty and presumably held developing teeth. Again, the structure of the interdental septa (interdental plate and bone of attachment) is clearly visible. All three implanted teeth are firmly attached, but all are undergoing replacement from the lingual side, as shown by the cavities that notch both the alveolar margin of the maxilla and the alveolar attachment bone. The cavities must have contained very small loose replacement teeth now lost. Presumably once the mature teeth had finally been eroded, lost, and replaced, the developing teeth in positions two and four would have been firmly implanted.

Variation. — As far as can be judged from the jaw elements themselves, the teeth vary in size and, to some degree, morphology along the jaws, and show some differences between elements.

Each premaxilla contains four teeth housed in large rounded sockets (Fig. 2). The teeth are relatively longer and narrower than those on the dentary and maxilla, and are more rounded in cross-section. None of the teeth preserved in situ bears serrations, but some isolated teeth of otherwise similar morphology bear serrations on a sharp keel along the posterior margin only, the anterior margin of the tooth being rounded. In ZPAL RV/88 (Fig. 2B), only the most medial premaxillary tooth is preserved. It is fully rounded in cross-section with no trace of keels. In contrast, ZPAL RV/83 (Figs 2A, 3D) preserves the last premaxillary tooth, and, although broken, the cross-section shows a clear posterior keel and a slight anterior ridge.

Each maxilla bears an estimated 13 teeth. These vary in size with the largest teeth in positions four to eight, in the region of the nasal process and anterior pillar. This is reflected by an increased depth of the supra-alveolar ridge (Fig. 6C–E). Behind this point the teeth decrease in size, with the most posterior teeth being tiny denticles. On the limited evidence available, the most anterior maxillary teeth resemble those of the premaxilla in being rather more rounded in cross-section.

At least 13 teeth were present in the dentary which is never complete. Overall, the dentary teeth seem to have been slightly smaller than those on the maxilla. The dentary ZPAL RV/14 demonstrates that teeth in positions four to eleven were subequal in size. Judging by alveolar size and depth, the first two positions were held by relatively small teeth and this may reflect the slightly overhanging position of the premaxilla reconstructed for this animal.

DISCUSSION

As revised by Juul (1994), the diagnosis of archosauriforms (Gauthier *et al.* 1988) has been reduced to two well supported synapomorphies, the possession of an antorbital fenestra and an ossified laterosphenoid (see also Clark *et al.* 1993), supplemented by a third, the possession of a mandibular fenestra (Parrish 1992; Juul 1994). Of these, only the antorbital fenestra has been confidently reconstructed in *Osmolskina*, while the presence of the laterosphenoid was deduced on the basis of the prootic and the skull roof morphology, and that of the mandibular fenestra was reconstructed from the outline of the angular margin. The presence of all the above synapomorphies would be expected in *Osmolskina*, because this genus presents a combination of many other archosauriform features such as the very small postfrontal (character 1 of Gauthier 1988, and of Benton and Clark 1988), the tall columnar quadrate (Romer 1956), and deep rooted (thecodont) teeth (characters 8 and 18 Gauthier *et al.* 1988) showing lateral compression and serrated margins (character 12 of Benton and Clark 1988, and character 7 of Gauthier *et al.* 1988 respectively), as well as characters relegated by Juul (1994) to some less inclusive groups.

The absence of teeth on the transverse flange of the pterygoid (character 21 of Gauthier *et al.* 1988) is consistent with a position crownward of proterosuchids, while the retention of toothed zones along the medial margin of the pterygoid and on the palatine (the vomer is not identified) tends to exclude *Osmolskina* from the crown-group. The presence of interdental plates tends to locate *Osmolskina* more crownwards than the erythrosuchids. They are perfectly developed also in *Euparkeria* (Senter 2003). According to Juul (1994), the interdental plates are characteristic of some basal archosaurs (rauisuchians, *Herrerasaurus*, *Ornithosuchus*), while being absent from non-archosauriform Archosauromorpha (rhynchosaurs and *Prolacerta*), proterosuchids (Cruickshank 1972, Gower and Sennikov 1997), and erythrosuchids (Parrish 1992, Gower 2003). However, the relationship between *Osmolskina* and the Erythrosuchidae is far from clear. *Osmolskina*

differs in its much smaller size and lighter build as well as in having a ventral maxillary margin that is straight instead of convex. Some characters considered derived within the non-archosaurian archosauriforms (Juul 1994, p. 38), such as a fairly large antorbital fenestra with an antorbital fossa around it, and the absence of a parietal foramen cannot discriminate between the above taxa. The antorbital fossa does occur in erythrosuchids (Juul 1994, p. 6; Gower 2003), and both its size and the structure of its anterior border are similar in *Erythrosuchus* (Parrish 1992, fig. 6), *Osmolskina*, and *Euparkeria* (Ewer 1965, fig. 22). The parietal foramen is retained only in *Garjainia* (Parish 1992, p. 96).

The above discussion shows only that *Osmolskina* is a non-archosaur archosauriform situated more crownward than the proterosuchids in the phylogeny.

In the Appendix 2, *Osmolskina* has been added to the data matrix of braincase characters of Gower and Sennikov (1996), although this has been restricted to those characters and taxa relevant to the present case. The characters discussed below are numbered and scored according to Gower and Sennikov (1996) unless otherwise indicated.

Character 1. — Position of the entry foramina for the cerebral branches of the internal carotid artery: ventral or ventrolateral = 0, lateral = 1 (according to Gower and Sennikov 1996). Gower (2002) updated this character, and recognized three states: foramina posterior = 0; posterolateral = 1, and anterolateral = 2. Our scoring is different: foramina lateral to the ventrolateral crests = 0; directly ventral, anterior to the fused ventrolateral crests = 1; lateral to basiptyergoid stalks = 2. *Osmolskina* is scored 1.

According to Gower (2002), the foramina on the posterior surface of the parabasisphenoid occur in non-crown-group archosaurs, *Proterosuchus*, *Garjainia*, and *Euparkeria*, so this state is probably equal to the ventral or ventro-lateral position of Gower and Sennikov (1996).

In our opinion, all the genera included in our matrix (Appendix 2) have the carotid foramina situated close to the ventral surface of the parabasisphenoid, and also posterior to the basiptyergoid processes, and so qualifications such as just ventral or posterior are not informative enough. Our position is that there is a difference between *Proterosuchus* and *Euparkeria*–*Osmolskina* that should be expressed in scoring. The illustrations of braincases in *Prolacerta* and *Proterosuchus* (Gow 1975, figs 35A, 36C; Evans 1986) suggest they are similar in having the foramina located lateral to the ventrolateral crests of the parabasisphenoid, which is probably also true of *Fugusuchus* given the reconstruction of Gower and Sennikov (1996, fig. 4D). The anteriormost parts of the crests converge gradually over a long distance and at a small angle to each other, whereas in *Osmolskina* they turn abruptly mediad and fuse with each other. This change in the course of the ventrolateral crests associated, for simple geometrical reasons, with both a sub-vertical position of the basisphenoid (character 7), and a more vertical position of the basiptyergoid processes (character 7a), both derived according to Gower and Sennikov (1996), is considered derived as well. If it is correct, the directly ventral position of the carotid foramina, anterior to the fused ventrolateral crests (we score 1 herein) should also be considered derived with respect to their primitive lateral position in proterosuchids, *Prolacerta*, and a prolacertiform grade animal from Czatkowice 1 (Borsuk-Białynicka and Evans 2009, fig. 8E₁). *Osmolskina* shares the position “directly ventral, and anterior to the fused ventrolateral crests” with *Euparkeria* (Gower and Weber 1998, fig. 4), *Dorosuchus* (Sennikov personal communication), *Garjainia* (Gower and Sennikov 1996, fig. 1), *Xilousuchus* (Gower and Sennikov 1996, fig. 5), and probably *Turfanosuchus* (Wu and Russell 2001, fig. 5). The directly ventral position of the foramina (1) in the rhynchosaurs (*Mesosuchus*, Dilkes 1998; *Hyperodapedon*, Benton 1983, figs 10, 11), which are among the outgroups of archosauriforms, is probably homoplastic in view of the highly specialized skull.

The lateral position of the carotid foramina has been considered a synapomorphy of proterochampsids + crown-group archosaurs (Parrish 1993), or of the crown-group alone (Gower and Weber 1998). The Crurotarsi (at least *Postosuchus*, *Batrachotomus*, *Parasuchus*, and *Stagonolepis*) have these foramina in a lateral position (Chatterjee 1978; Gower and Sennikov 1996; Gower 2002), and the same is true of early ornithomirans (*Marasuchus*, Sereno and Arcucci 1994; prosauropods, Galton and Upchurch 2004; and basal Saurischia, Langer 2004). However, the Middle Triassic *Arizonasaurus babbitti* from the United States (Gower and Nesbitt 2006), and the Late Triassic dinosauriform, *Silesaurus opolensis*, from Poland (Dzik 2003) have the carotid foramina directly ventral.

Character 2. — Basisphenoid intertuberal plate: present = 0; absent = 1. *Osmolskina* is scored 1. The basisphenoid intertuberal plate is a transverse septum separating the parabasisphenoid from the basioccipital part of the ventral concavity. Parrish (1992) proposed that it was an autapomorphy of erythrosuchids. Ac-

According to Gower and Sennikov (1996), it was shared not only by *Proterosuchus* and *Fugusuchus* but also by *Prolacerta*, and on this basis has been considered plesiomorphic of archosauriforms. In our opinion, this would suggest that what is labelled basisphenoid intertuberal plate might be homologous with the posterior margin of the parasphenoid, at least in some taxa.

According to Gow (1975, figs 35, 36), the parasphenoid of early diapsids was long and bridged the gap between the overlying basisphenoid and basioccipital. It has subsequently shortened, in parallel and at different rates, in different diapsid clades, although its posterolateral corners continued to contribute to the basal tubera, and the posteromedial part retained a horizontal flange protruding posteriad to overlap the basioccipital. This horizontal flange is variable in size and shape, and its presence is here considered as a primitive character state. It occurs in *Prolacerta* (Gow 1975, figs 35; Evans 1986, figs 4, 5) and in *Osmolskina*, (according to impressions left on the basioccipital surface Fig. 33B), and probably corresponds to the thickened border of the parasphenoid in *Proterosuchus* (Gow 1975, fig. 36). The erythrosuchid intertuberal plate unites the basal tubera of the parabasisphenoid, but extends clear of the posterior border of this bone (as demonstrated by *Garjainia* and *Xilousuchus*, Gower and Sennikov 1996, figs. 2, 5; and *Erythrosuchus*, Gower 1997, fig. 2). It does not seem to be homologous with the posteromedial parasphenoid flange of other archosauriforms and *Prolacerta*, but was probably added to it. If this interpretation is correct, its presence would be derived as originally stated by Parrish (1992). Its absence in *Prolacerta* and non-erythrosuchid archosauriforms, including both *Osmolskina* and *Euparkeria*, would be primitive (contra Gower and Sennikov 1996). However, this problem requires further study and this equivocal character is removed from the matrix (see Appendix 2).

Character 3. — Abducens canal position: between the basisphenoid and prootic = 0, within prootic only = 1. *Osmolskina* is scored 0. In early amniotes, as exemplified by *Captorhinus* and *Milleretta* (Evans 1986), the abducens canals are located within the basisphenoid. A canal situated within the prootic-basisphenoid suture is characteristic of the immediate outgroups of the Archosauriformes (*Prolacerta*, Evans 1986; *Hyperodapedon*, Benton 1983), as well as of *Proterosuchus* (Cruickshank 1972) and *Euparkeria* (Gower and Weber 1998). In some erythrosuchids, at least, the canal has shifted into the prootic (Gower and Sennikov 1996). However, in basal archosaurs it seems to remain within, or return to, the basisphenoid (e.g., the phytosaurian *Parasuchus*, Chatterjee 1978; and the prosauropod *Thecodontosaurus*, Benton *et al.* 2000). If properly reconstructed (Figs 20A, 21B), *Osmolskina* shares the primitive archosauromorph condition, but the polarity of this character, and its developmental basis, remain unclear.

Character 5. — Ventral ramus of the opisthotic: prominent = 0; recessed = 1. *Osmolskina* is scored 0.

Character 6. — Ridge on the anterior inferior prootic process below the trigeminal notch: present = 0; absent = 1. *Osmolskina* is scored 0.

Character 7. — Basisphenoid orientation: horizontal = 0, sub-vertical = 1. *Osmolskina* is scored 1.

Character 7a. — Basipterygoid processes directed laterally = 0, ventrolaterally = 1. *Osmolskina* is scored 1. Based on the work of Gower and Sennikov (1996, description and fig. 4C, D) the braincase of *Fugusuchus* is primitive not only in having a horizontal basisphenoid, but also in having laterally directed basipterygoid processes and carotid foramina lying lateral to the ventrolateral crests (though ventrolateral with respect to the whole braincase). In contrast, erythrosuchids (*Erythrosuchus*, *Garjainia*, and *Xilousuchus*) display a high braincase with a very short, sub-vertically oriented parabasisphenoid (Gower 1997; Gower and Sennikov 1996). In *Xilousuchus* (Gower and Sennikov 1996, fig. 5), the processes are slightly more lateral, whereas in *Garjainia* (Gower and Sennikov 1996, fig. 1) and *Erythrosuchus* (Gower 1997, figs 2, 11) they are directed more ventrally. As a result, the carotid foramina are further apart in *Xilousuchus* and less so in the illustrated representatives of *Garjainia* and *Erythrosuchus*. *Euparkeria* has a sub-vertical parabasisphenoid (Ewer 1965, Gower and Weber 1998, p. 385). The basioccipital-basisphenoid fossa seems to be wedged slightly between the carotid foramina (Gower and Weber 1998, fig. 4) as it is in *Osmolskina*, and in both genera the foramina are located close to one another posteromedial to the basipterygoid processes on the ventral surface of the parabasisphenoid (Fig. 21A, E). The whole pattern seems to fall within the range of variability manifested by the erythrosuchids, which was probably the range of the non-archosaurian archosauriforms crownward of *Proterosuchus*. However, the braincase of *Sarmatosuchus otschevi* from the Anisian of Russia, considered to be a proterosuchid Gower and Sennikov 1997, is strikingly derived in having essentially vertical alignment, with a ventrolateral orientation of the basipterygoid processes as well as ventral orientation of the internal carotid foramina.

Clark *et al.* (1993) considered that the verticalization of the parabasisphenoid, which occurred during the early course of archosauriform evolution, resulted in an increase in the space available for the adductor mus-

cles. According to these authors, this was an adaptation towards macropredaceous habits. A reorientation of the basiptyergoid processes to a more vertical position, closer to each other, may have been a response to the same selective agent. As hypothesised above, the changes in the basisphenoid configuration influenced the position of the anteriormost parts of the ventrolateral crests so that they were pushed back and became confluent. They eventually fused across the midline to form a sharp border to the basisphenoid fossa. As the basiptyergoid processes were pushed together towards the midline, the entry foramina for the cerebral branches of the internal carotid artery followed them onto the ventral side of the braincase, into the space anterior to the basioccipital-basisphenoid fossa. The internal carotid artery extends down the dorsomedial wall of the tympanic fossa in lizards at least (Oelrich 1956) or along the ventrolateral crests (Evans 1986; Gower 2002). Its cerebral branch would have passed from the lateral to the ventral face of the parabasisphenoid to reach the entry foramen. The ventral position of the foramina required that the artery wound ventrally around the posterior surface of the basiptyergoid process. This probably accounts for the S-shaped path of the carotid artery (Gower and Weber 1998) associated with verticalization of the basisphenoid. The return of the foramina to the lateral side of the parabasisphenoid, which occurred in crown-group archosaurs, probably eliminated this convolution to make the path of the artery more direct.

Character 9. — Prootic midline contact on the endocranial floor: absent = 0; present = 1. *Osmolskina* is scored 1.

The lack of a midline contact of the prootics on the endocranial floor might be correlated with an exposure of the basisphenoid in the midline (character 10), but according to Gower and Sennikov (1996), this is not always the case. Apart from *Parasuchus* (Chatterjee 1978), *Osmolskina* probably has the prootic contact (limited to the crista sellaris region) and, at the same time, the midline exposure of the basisphenoid in the braincase floor.

Character 10. — Basisphenoid midline exposure on endocranial cavity floor: present = 0; absent = 1. *Osmolskina* is scored 0.

Character 11. — Semilunar depression: present = 0; absent = 1. *Osmolskina* is scored 0.

Further character states preserved in *Osmolskina* (Appendix 2) and scored “0” on the basis of Gower and Sennikov (1996) are as follows:

Character 16. — Number of hypoglossal foramina: two = 0; one = 1. *Osmolskina* is scored 0. The character may be uninformative because it shows some variability *e.g.*, *Hyperodapedon* can have two or three foramina (Benton 1983) and the number supposedly changes with age in *Sphenodon* (SEE). If Gower and Sennikov’s (1996) scoring is correct, both *Euparkeria* and *Osmolskina* and some archosaurs (see Appendix 2) show the primitive state, whereas the condition in erythrosuchids and *Fugusuchus* which have only a single foramen is derived.

Character 17. — Ventral contact of the exoccipitals in the sagittal plane: absence = 0; presence = 1. *Osmolskina* is scored 1. This character appears to be quantitative and gradual rather than qualitative. In both *Osmolskina* (Figs 17, 25) and *Euparkeria* (Ewer 1965, p. 391; Gower and Weber 1998, fig. 4) the basioccipital is almost excluded from the border of the foramen magnum. The state in these taxa is far from primitive and close to the derived condition, and so is scored as such (Appendices 1 and 2).

Character 25. — Fusion of opisthotic with exoccipital: absent = 0; present = 1. *Osmolskina* is scored 1. The elements are suturally distinct in *Prolacerta* (Evans 1986), but the condition is variable in rhychoosaurs Benton 1983, p. 632). In *Osmolskina* the exoccipital is consistently tightly fused with the opisthotic, even in smaller (probably younger) individuals, in contrast to the condition in a prolacertiform-grade reptile (Borsuk-Białynicka and Evans 2009) represented in the Czatkowice 1 assemblage.

Character 26. — Medial wall of the vestibule (character 7 of Gower 2002): unossified = 0; ossified = 1. *Osmolskina* is scored 0. This character discriminates, more or less, between non-crown group archosauriforms and archosaurs, although some archosaurs (phytosaurus) display the primitive state, and the character should be scored on adult individuals as it is age dependent.

Character 30. — Supraoccipital contribution to the foramen magnum: no contribution = 0; supraoccipital contributes to foramen magnum = 1. This character may be subject to ontogenetic variation, as is character 17, because fusion involves enlargement of bones. In *Osmolskina* the exoccipital facets are variably spaced on the supraoccipital margin (Fig. 18). In *Euparkeria capensis* the exoccipital facets are separated as shown by Ewer 1965, fig. 2b). *Prolacerta* is polymorphic in this respect (Evans 1986).

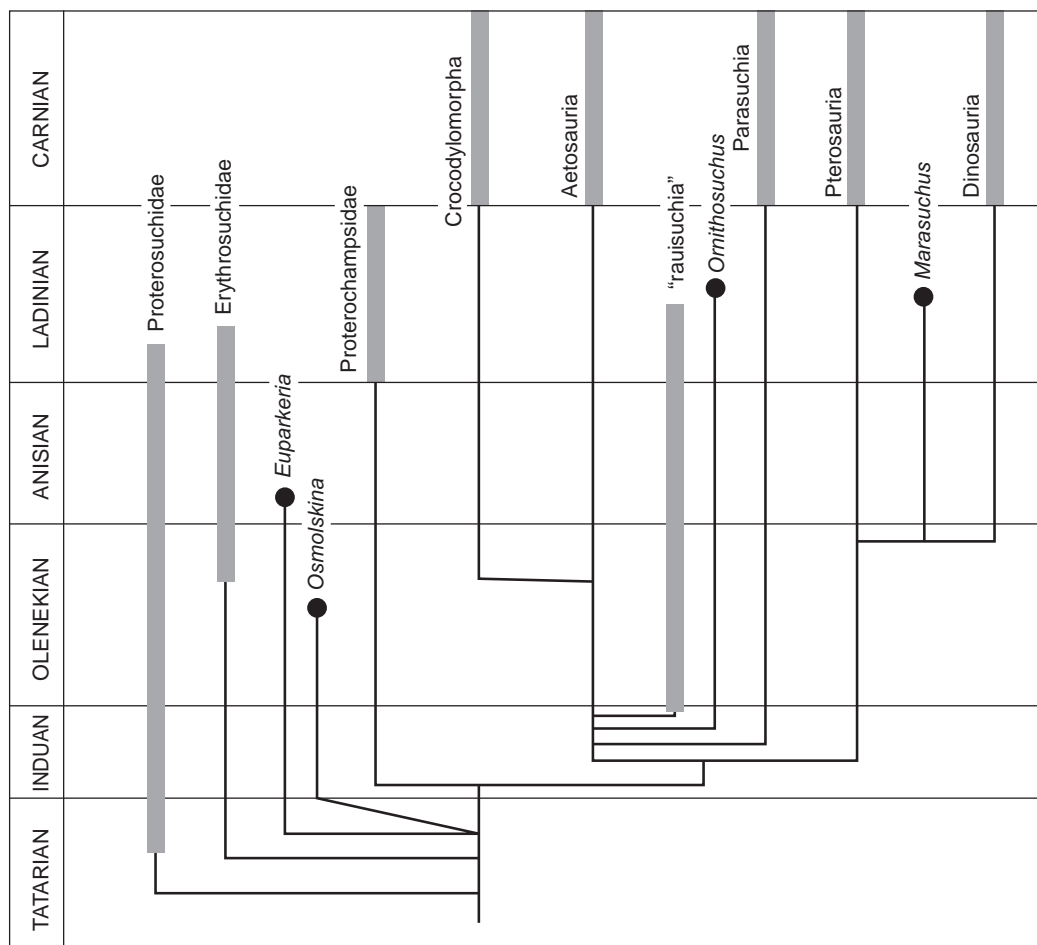


Fig. 31. Pattern of early archosauriform evolution based on Gower and Wilkinson's (1996, fig. 4) cladogram plotted against biochronology mainly after Gower and Sennikov (2000). Position of Aetosauria modified according to Gower and Walker (2002).

The following non-braincase characters might be of some phylogenetic value. They are added to those of Gower and Sennikov (1996), and are numbered consecutively here.

Character 33. — Snout position: snout not downturned = 0; snout downturned due to internal geometry of the premaxilla = 1; snout downturned due to angulation of premaxilla-maxilla contact = 2. *Osmolskina* is scored 1. The downturned appearance of the snout was originally considered as a proterosuchid character (Charig and Sues 1976), but occurs in some other archosauriforms and is not always homologous. Two factors may contribute to this character: the internal geometry of the premaxilla, with the ventrolateral border descending anteroventrally so that its anterior end lies below the horizontal palatal process, as in *Proterosuchus* Cruickshank (1972) and *Sarmatosuchus* (Gower and Sennikov 1997, p. 62), and the oblique orientation of the premaxilla resulting from its joint with the maxilla. The downturned snout we reconstruct for *Osmolskina* results from the second factor (Fig. 3B, C₂), and this is also the case for some other stem-group archosauriforms and early archosaurs, as exemplified by *Erythrosuchus* (Gower 2003) and *Riojasuchus* (Parrish 1993, fig. 4A) respectively. It may suggest a degree of kinesis at this joint. In *Osmolskina* a small additional antorbital foramen may have opened within the premaxilla-maxilla suture (Figs 1B, 3B) as a by-product of this loose contact.

Character 34. — Ventral pterygoid crest on the posterior border of the palatal wing of the pterygoid: absent = 0, present = 1. *Osmolskina* is scored 1 (Fig. 15A). In *Euparkeria* (Ewer 1965, fig. 1b), *Sarmatosuchus* (Gower and Sennikov 1997, fig. 4A), *Gracilisuchus* (Romer 1972b, fig. 3), and seemingly *Proterosuchus* (Cruickshank 1972, fig. 3), the palatal wings of the pterygoids are also bordered posteriorly by a distinct, anteriorly concave, crest but this is not the case in *Prolacerta* (Gow 1975, fig. 17, see also Borsuk-Białynicka and Evans 2009). The crest is a potential synapomorphy of the Archosauriformes, but requires further comparative studies.

Summing up the results of the above discussion, *Osmolskina* is identical to *Euparkeria* in all 12 characters that can be scored (Appendix 2). Given this correspondence, a phylogenetic analysis of *Osmolskina* seems redundant at the present time as this genus would take exactly the same position in the archosauriform phylogeny, crownward of proterosuchids and close to the crown group (Fig. 31), as does *Euparkeria* (Gower and Wilkinson 1996). Several of their character states (characters 3, 5, 6, 10, 16) suggest a position stem-ward of erythrosuchids, from which *Osmolskina* and *Euparkeria* also differ in overall skeleton and vertebrae proportions. This position is firmly supported by three of 13 braincase character states (1, 7, 7a). They are mostly those of the braincase verticality complex discussed above. The unique combination of primitive and derived character states of the whole skeleton (Appendices 1 and 2; Borsuk-Białynicka and Sennikov 2009) shared by *Osmolskina* and *Euparkeria*, as well as a general similarity of the body form, leads us, with reservation, to accord them family status within Euparkeriidae Huene, 1920 although as yet no unique shared derived character states have been identified to support the monophyly of Euparkeriidae Huene 1920 (Charig and Sues 1976).

Osmolskina (Borsuk-Białynicka and Evans 2003) is differentiated from *Euparkeria* at a generic level based mainly on skull proportions. *Osmolskina* has the preorbital part of the skull less elongated than *Euparkeria*, a difference that is best expressed in maxilla proportion, the maximum length to depth being 5:1 and 7:1 respectively, but the maxillary tooth count is estimated as 13 in both genera. According to our reconstruction, the premaxilla is downturned in *Osmolskina*, and it is probably separated from the maxilla by an additional antorbital foramen. Its body is shallower (maximum length to depth 10:3) than in *Euparkeria* (10:4), and its posterolateral process slopes at an angle of about 50° in contrast to the near vertical orientation in *Euparkeria*. Orbit shape also differs. In *Osmolskina*, the ventral border of the orbit is smoothly concave due to the widely divergent processes of the jugal, whereas the same region is more angular in *Euparkeria*. Finally, unlike the mandible of *Euparkeria*, that of *Osmolskina* does not increase in depth posteriorly. We acknowledge that many of these differences could be artifacts of reconstruction. However, in the absence of articulated material, these reconstructions represent the best approximation of the real state.

CONCLUSIONS

Osmolskina czatkowicensis is a non-archosaur archosauriform situated more crownward than the proterosuchids in the phylogeny of Archosauriformes (Fig. 31), in exactly the same position on the cladogram as is usually accorded to *Euparkeria capensis* (Gower and Wilkinson 1996).

Osmolskina and *Euparkeria* share a unique combination of primitive and derived archosauriform character states of the braincase (see above) and postcranium (Borsuk-Białynicka and Sennikov 2009). On this basis, they are tentatively placed as sister taxa within a monophyletic Euparkeriidae Huene, 1920, although no synapomorphy has been found to support the clade.

The differences between *Osmolskina* and *Euparkeria* are here regarded as generic. Among them, only one, the localization of the coracoid foramen (Borsuk-Białynicka and Sennikov 2009), is uncontroversial. Some differences in skull morphology, and notably skull proportions, are dependent on the accuracy of the reconstructions. Nonetheless, given the geographical (Europe *versus* South Africa) and stratigraphical (earliest Late Olenekian *versus* Anisian) differences, although these do not represent valid criteria in themselves, it seems preferable to retain generic distinction pending the recovery of further material from other localities.

REFERENCES

- Battail, B. 1993. On the biostratigraphy of Triassic therapsid-bearing formations. In: S.G. Lucas and M. Morales (eds), *The Nonmarine Triassic. New Mexico Museum of Natural History & Science Bulletin* 3, 31–35. University of New Mexico Printing Services. Albuquerque.
- Benton, M.J. 1983. The Triassic reptile *Hyperodapedon* from Elgin: functional morphology and relationships. *Philosophical Transactions of the Royal Society of London B* 302, 605–717.
- Benton, M.J. 1985. Classification and phylogeny of the diapsid reptiles. *Zoological Journal of the Linnean Society* 84, 97–164.

- Benton, M.J. 1999. *Scleromochlus taylori* and the origin of dinosaurs and pterosaurs. *Philosophical Transactions of the Royal Society of London B* **354**, 1423–1446.
- Benton, M.J. and Clark, J.M. 1988. Archosaur phylogeny and the relationships of the Crocodylia. In: M.J. Benton (ed.) *The Phylogeny and Classification of the Tetrapods. 1. Amphibians, Reptiles, Birds. Systematic Association Special Volume 35A*, 295–338. Clarendon Press, Oxford.
- Benton, M.J., Shishkin, M.A., Unwin, D., and Kurochkin, E.N. (eds) 2000. *The Age of Dinosaurs in Russia and Mongolia*. 697 pp. Cambridge University Press, Cambridge.
- Borsuk-Białynicka, M. and Evans S.E. 2002. The scapulocoracoid of an Early Triassic stem-frog from Poland. *Acta Palaeontologica Polonica* **47**, 79–96.
- Borsuk-Białynicka, M. and Evans S.E. 2003. A basal archosauriform from the Early Triassic of Poland. *Acta Palaeontologica Polonica* **48**, 649–652.
- Borsuk-Białynicka, M. and Evans, S.E. 2009. A long-necked archosauromorph from the Early Triassic of Poland. *Palaeontologia Polonica* **65**, 203–234.
- Borsuk-Białynicka, M. and Lubka, M. 2009. Procolophonids from the Early Triassic of Poland. *Palaeontologia Polonica* **65**, 107–144.
- Borsuk-Białynicka, M. and Sennikov, A.G. 2009. Archosauriform postcranial remains from the Early Triassic karst deposits of southern Poland. *Palaeontologia Polonica* **65**, 283–328.
- Borsuk-Białynicka, M., Cook, E., Evans, S.E., and Maryńska, T. 1999. A microvertebrate assemblage from the Early Triassic of Poland. *Acta Palaeontologica Polonica* **44**, 167–188.
- Borsuk-Białynicka, M., Maryńska, T., and Shishkin, M.A. 2003. New data on the age of the bone breccia from the locality Czatkowice 1 (Cracow Upland, Poland). *Acta Palaeontologica Polonica* **48**, 153–155.
- Brochu, C.A. 1996. Closure of neurocentral sutures during crocodylian ontogeny: implications for maturity assessment in fossil archosaurs. *Journal of Vertebrate Paleontology* **16**, 49–62.
- Broom, R. 1913. Note on *Mesosuchus browni* Watson and on a new South African Triassic pseudosuchian (*Euparkeria capensis*). *Records of the Albany Museum* **2**, 394–396.
- Busbey, A.B. III 1989. Form and function of the feeding apparatus of *Alligator mississippiensis*. *Journal of Morphology* **202**, 99–127.
- Charig, A.J. and Sues, H.-D. 1976. Suborder Proterosuchia Broom 1906. In: O. Kuhn (ed.) *Handbuch der Palaeoherpetologie, Vol. 13*, 11–39. Gustav Fischer Verlag, Stuttgart.
- Chatterjee, S. 1978. A primitive parasuchid (phytosaur) reptile from the Upper Triassic Maleri Formation of India. *Palaeontology* **21**, 83–127.
- Clark, M.J., Welman, J., Gauthier, J.A., and Parrish, J.M. 1993. The laterosphenoid bone of early Archosauriformes. *Journal of Vertebrate Paleontology* **13**, 48–57.
- Cook, E. and Trueman, C. 2009. Taphonomy and geochemistry of a vertebrate microremains assemblage from the Early Triassic karst deposits at Czatkowice 1, southern Poland. *Palaeontologia Polonica* **65**, 17–30.
- Cruickshank, A.R.I. 1972. The proterosuchian thecodonts. In: K.A. Joysey and T.S. Kemp (eds) *Studies in Vertebrates Evolution*, 89–119. Oliver & Boyd, Edinburgh.
- Dzik, J. 2003. A beaked herbivorous archosaur with dinosaur affinities from the early Late Triassic of Poland. *Journal of Vertebrate Paleontology* **23**, 556–574.
- Evans, S.E. 1980. The skull of a new eosuchian reptile from the Lower Jurassic of South Wales. *Zoological Journal of the Linnean Society* **70**, 203–264.
- Evans, S.E. 1986. The braincase of *Prolacerta broomi* (Reptilia, Triassic). *Neues Jahrbuch für Geologie und Paläontologie* **173**, 181–200.
- Evans, S.E. 1987. The braincase of *Youngina capensis* (Reptilia: Diapsida; Permian). *Neues Jahrbuch für Geologie und Paläontologie* **4**, 193–203.
- Evans, S.E. 1988. The early history and relationships of the Diapsida. In: M.J. Benton (ed.) *The Phylogeny and Classification of the Tetrapods. 1. Amphibians, Reptiles, Birds. Systematic Association Special Volume 35A*, 221–260. Clarendon Press, Oxford.
- Evans, S.E. 2009. An early kuehneosaurid reptile (Reptilia: Diapsida) from the Early Triassic of Poland. *Palaeontologia Polonica* **65**, 145–178.
- Evans, S.E. and Borsuk-Białynicka, M. 1998. A stem-group frog from the Early Triassic of Poland. *Acta Palaeontologica Polonica* **43**, 573–580.
- Evans, S.E. and Borsuk-Białynicka, M. 2009a. A small lepidosauromorph reptile from the Early Triassic of Poland. *Palaeontologia Polonica* **65**, 179–202.
- Evans, S.E. and Borsuk-Białynicka, M. 2009b. The Early Triassic stem-frog *Czatkobatrachus* from Poland. *Palaeontologia Polonica* **65**, 79–105.
- Ewer, R.F. 1965. The anatomy of the thecodont reptile *Euparkeria capensis* Boom. *Philosophical Transactions of the Royal Society of London B* **248**, 379–435.
- Galton, P.M. and Upchurch, P. 2004. Prosauropoda. In: D.B. Weishampel, P. Dodson, and H. Osmolska (eds) *The Dinosauria*, 232–258. University of California Press, Berkeley.
- Gauthier, J. 1986. Saurischian monophyly and the origin of birds. In: K. Padian (ed.) *The Origin of Birds and the Evolution of the Flight. Memoirs, California Academy of Sciences* **8**, 1–58.
- Gauthier, J., Kluge, A.G., and Rowe, T. 1988. Amniote phylogeny and the importance of fossils. *Cladistics* **4**, 105–209.
- Gow, C.E. 1970. The anterior of the palate in *Euparkeria*. *Palaeontologia Africana* **13**, 61–2.

- Gow, C.E. 1975. The morphology and relationships of *Youngina capensis* Broom and *Prolacerta broomi* Parrington. *Palaeontologia Africana* **18**, 89–131.
- Gower, D.J. 1997. The braincase of the early archosaurian reptile *Erythrosuchus africanus*. *Journal of Zoology, London* **242**, 557–576.
- Gower, D.J. 1999. Cranial osteology of a new rauisuchian archosaur from the Middle Triassic of Southern Germany. *Stuttgarter Beiträge zur Naturkunde B* **280**, 1–49.
- Gower, D.J. 2000. Rauisuchian archosaurs (Reptilia, Diapsida): An overview. *Neues Jahrbuch der Geologie und Paläontologie, Abhandlungen* **218**, 447–488.
- Gower, D.J. 2002. Braincase evolution in suchian archosaurs (Reptilia: Diapsida): evidence from the rauisuchian *Batrachotomus kupferzellensis*. In: D.B. Norman and D.J. Gower (eds) Archosaurian Anatomy and Palaeontology. Essays in Memory of Alick D. Walker. *Zoological Journal of the Linnean Society* **136**, 49–76.
- Gower, D.J. 2003. Osteology of the early archosaurian reptile *Erythrosuchus africanus* Broom. *Annals of the South African Museum* **111**, 1–88.
- Gower, D.J. and Nesbitt, S.J. 2006. The braincase of *Arizonasaurus babbitti* — further evidence for the non-monophyly of “rauisuchian” archosaurs. *Journal of Vertebrate Paleontology* **26** (1), 79–87.
- Gower, D.J. and Sennikov, A.G. 1996. Morphology and phylogenetic informativeness of early archosaur braincases. *Palaeontology* **39**, 883–906.
- Gower, D.J. and Sennikov, A.G. 1997. *Sarmatosuchus* and the early history of the Archosauria. *Journal of Vertebrate Paleontology* **17**, 60–73.
- Gower, D.J. and Sennikov, A.G. 2000. Early archosaurs from Russia. In: M.J. Benton, M.A. Shishkin, D. Unwin, and E.N. Kurochkin (eds) *Dinosaur Age in Russia and Mongolia*, 120–139. Cambridge University Press, Cambridge.
- Gower, D.J. and Walker, A.D. 2002. New data on the braincase of the aetosaurian archosaur (Reptilia: Diapsida) *Stagonolepis robertsoni* Agassiz. In: D.B. Norman and D.J. Gower (eds) Archosaurian Anatomy and Palaeontology. Essays in Memory of Alick D. Walker. *Zoological Journal of the Linnean Society* **136**, 7–23.
- Gower, D.J. and Weber, E. 1998. The braincase of *Euparkeria*, and the evolutionary relationships of birds and crocodylians. *Biological Reviews* **73**, 367–411.
- Gower, D.J. and Wilkinson, M. 1996. Is there any consensus on basal archosaur phylogeny. *Proceedings of the Royal Society of London B* **263**, 1399–1406.
- Hancox, P.J., Shishkin, M.A., Rubidge, B.S., and Kitching, J.W. 1995. A threefold subdivision of the *Cynognathus* assemblage Zone (Beaufort Group, South Africa) and its palaeogeographical implications. *South African Journal of Science* **91**, 143–144.
- Haughton, S.H. 1922. On the reptilian genera *Euparkeria* Broom and *Mesosuchus* Watson. *Transactions of the Royal Society, South Africa* **10**, 81–88.
- Huene, F. v. 1920. Osteologie von *Aetosaurus ferratus* O. Fraas. *Acta Zoologica* **1** (3), 465–491.
- Iordansky, N.N. 1973. The skull of Crocodylia. In: C. Gans and Th.S. Parsons (eds) *Biology of the Reptilia, Vol. 4*, 201–262. Academic Press, London.
- Juul, L. 1994. The phylogeny of basal archosaurs. *Palaeontologia Africana* **31**, 1–38.
- Langer, M.C. 2004. Basal Saurischia. In: D.B. Weishampel, P. Dodson, and H. Osmólska (eds) *The Dinosauria*, 25–46. University of California Press, Berkeley.
- Lucas, S.L. 1993. Vertebrate biochronology of the Triassic of China. In: S.E. Lucas and M. Morales (eds) The Nonmarine Triassic. *New Mexico Museum of Natural History & Science Bulletin* **3**, 301–306.
- Ochev, V.G. 1993. Early Triassic tetrapod biogeography. In: S.E. Lucas and M. Morales (eds) The Nonmarine Triassic. *New Mexico Museum of Natural History & Science Bulletin* **3**, 375–377.
- Ochev, V.G. and Shishkin, M.A. 1989. On the principles of global correlation of the continental Triassic on the tetrapods. *Acta Paleontologica Polonica* **34**, 149–173.
- Oelrich, Th.M. 1956. The anatomy of the head of *Ctenosaura pectinata* (Iguanidae). *Miscellaneous Publications. Museum of Zoology, University of Michigan* **94**, 1–122.
- Parrish, J.M. 1992. Phylogeny of the Erythrosuchidae (Reptilia: Archosauriformes). *Journal of Vertebrate Paleontology* **12**, 93–102.
- Parrish, J.M. 1993. Phylogeny of the Crocodylotarsi with reference to archosaurian and crurotarsan monophyly. *Journal of Vertebrate Paleontology* **13**, 287–308.
- Paszkowski, M. 2009. The Early Triassic karst of Czatkowice 1, southern Poland. *Palaeontologia Polonica* **65**, 7–16.
- Paszkowski, M. and Wiczorek, J. 1982. Fossil karst with Mesozoic bone breccia in Czatkowice (Cracow Upland, Poland). *Kras i Speleologia* **3**, 32–38.
- Romer, A.S. 1956. *Osteology of the Reptiles*. 772 pp. The University Chicago Press, Chicago.
- Romer, A.R. 1971. The Chanares (Argentina) Triassic Reptile fauna XI. Two long-snouted thecodonts, *Chanaresuchus* and *Gualosuchus*. *Breviora of the Museum of Comparative Zoology* **379**, 1–22.
- Romer, A.R. 1972a. The Chanares (Argentina) Triassic Reptile fauna XII. The postcranial skeleton of the thecodont *Chanaresuchus*. *Breviora of the Museum of Comparative Zoology* **385**, 1–21.
- Romer, A.R. 1972b. The Chanares (Argentina) Triassic Reptile fauna XIII. An early ornithosuchid pseudosuchian, *Gracilisuchus stipanicorum* gen. et sp. nov. *Breviora of the Museum of Comparative Zoology* **389**, 1–24.
- Säve-Söderbergh, G. 1946. The fossa hypophyseos and the attachment of the retractor bulbi group in *Sphenodon*, *Varanus* and *Lacerta*. *Arkiv for Zoologii* **38A** (11), 1–24.

- Säve-Söderbergh, G. 1947. Notes on the brain-case in *Sphenodon* and certain Lacertilia. *Zoologiska Bidrag från Uppsala* **25**, 489–516.
- Schumacher, G.-H. 1973. The head and hyolaryngeal skeleton of turtles and crocodiles. In: C. Gans and Th.S. Parsons (eds) *Biology of the Reptilia, Vol. 4*, 101–199. Academic Press, London.
- Sennikov, A.G. [Сенников, А.Г.] 1989. Новый эупаркерид (Thecodontia) из среднего триаса Южного Приуралья [A new euparkerid (Thecodontia) from the Middle Triassic of the Southern Cis-Urals]. *Палеонтологический журнал* **2**, 71–78.
- Sennikov, A.G. [Сенников, А.Г.] 1995. Ранние текодонты Восточной Европы [Early thecodonts of Eastern Europe]. *Труды Палеонтологического Института* **263**, 1–139.
- Senter, Ph. 2003. New information on cranial and dental features of the Triassic archosauriform reptile *Euparkeria capensis*. *Palaeontology* **46**, 613–621.
- Sereno, P.C. 1991. Basal archosaurs: phylogenetic relationships and functional implications. *Journal of Vertebrate Paleontology* (Supplement) **11**, 1–53.
- Sereno, P.C. and Arcucci, A.B. 1990. The monophyly of crurotarsi archosaurs and the origin of bird and crocodile ankle joints. *Neues Jahrbuch für Geologie und Palaeontologie. Abhandlungen* **180**, 21–52.
- Sereno, P.C. and Arcucci, A.B. 1994. Dinosaur precursors from the Middle Triassic of Argentina: *Marasuchus lilloensis* gen. nov. *Journal of Vertebrate Paleontology* **14**, 53–73.
- Shishkin, M.A. and Ochev, V.G. [Шишкин, М.А. и Очев, В.Г.] 1985. Значение наземных позвоночных для стратиграфии триаса Восточно-Европейской платформы [Significance of land vertebrates for stratigraphy of Triassic of East European Platform]. In: А.В. Востряков [A.V. Vostriakov] (ed.) *Триасовые отложения Восточно-Европейской платформы [Triassic Deposits of East European Platform]*, 28–43. Издательство Саратовского Университета, Саратов.
- Shishkin, M.A. and Ochev, V.G. 1993. The Permo-Triassic transition and the early Triassic history of the Euramerican tetrapod fauna. In: S.E. Lucas and M. Morales (eds) *The Nonmarine Triassic. New Mexico Museum of Natural History & Science Bulletin* **3**, 301–306.
- Shishkin, M.A. and Sulej, T. 2009. The Early Triassic temnospondyls of the Czatkowice 1 tetrapod assemblage. *Palaeontologia Polonica* **65**, 31–77.
- Shishkin, M.A., Ochev, V.G., and Tverdohlebov, V.P. [Шишкин, М.А., Очев, В.Г. и Твердохлебов, В.П.] (eds) 1995. *Биостратиграфия континентального южного Приуралья [Biostratigraphy of the Triassic of the Southern Cis-Urals]*. 205 pp. Наука, Москва.
- Shishkin, M.A., Ochev, V.G., Lozovsky, V.R., and Novikov, I.V. 2000. Tetrapod biostratigraphy of the Triassic of Eastern Europe. In: M. Benton, M.A. Shishkin, D. Unwin, and E.N. Kurochkin (eds) *Dinosaur Age in Russia and Mongolia*, 120–139. Cambridge University Press, Cambridge.
- Sill, W.D. 1967. *Proterochampsia barrionuevoi* and the early evolution of the Crocrodilia. *Bulletin of the Museum of Comparative Zoology* **135**, 415–446.
- Tatarinov, L.P. [Татаринов, Л.П.] 1960. Материалы псевдозухий в берхней перми СССР [Discovery of pseudosuchians in the Upper Permian of SSSR]. *Палеонтологический журнал* **4**, 74–80.
- Wever, E.G. 1978. *The Reptile Ear — Its Structure and Function*. 1024 pp. Princeton University Press, Princeton.
- Wu, X.-Ch. 1981. The discovery of a new thecodont form North-East Shensi. *Vertebrata Palasiatica* **19**, 122–132.
- Wu, X.-Ch. 1982. Two pseudosuchian reptiles from Sha-Gan-Ning Basin (in Chinese with English summary). *Vertebrata Palasiatica* **20**, 289–301.
- Wu, X.-Ch. and Russell, A.P. 2001. Redescription of *Turfanosuchus dabanensis* (Archosauriformes) and new information on its phylogenetic relationships. *Journal of Vertebrate Paleontology* **21**, 40–50.
-

APPENDIX 1

Character list based mainly on Gower and Sennikov (1996). Character numbering according to the same authors.

1. Cerebral branches of the internal carotid entrances: lateral to the ventrolateral crests = 0; directly ventral, anterior to the fused ventrolateral crest = 1; lateral to basipterygoid stalks = 2
3. Abducens canal: between the basisphenoid and prootic = 0; within prootic only = 1
5. Ventral ramus of the opisthotic: prominent = 0; recessed = 1
6. Ridge on lateral surface of anterior inferior prootic process below the trigeminal notch: present = 0; absent = 1
7. Basisphenoid: oriented horizontally = 0; or more vertically = 1
- 7a. Basispterygoid processes: directed laterally = 0; ventrolaterally = 1
9. Prootic midline contact on endocranial cavity floor: absent = 0; present = 1
10. Basisphenoid midline exposure on endocranial cavity floor: present = 0; absent = 1
11. Semilunar depression: present = 0; absent = 1
16. Number of hypoglossal foramina: two = 0; one = 1
17. Midline contact of the exoccipitals in braincase floor: absent = 0; present = 1
25. Fusion of opisthotic-exoccipital: absent = 0; present = 1
26. Medial wall of vestibulum: open = 0; ossified = 1

APPENDIX 2

Character state matrix for selected Archosauromorpha with *Osmolskina* included.

Character no	1	1	3	5	6	7	7a	9	10	11	16	17	25	26
<i>Prolacerta</i>	0	0	0	0	0	0	0	0	0	0	0	0	0	0
<i>Hyperodapedon</i>	1	0	0	0	0	0	0	0	0	1	0	1	1	0
<i>Proterosuchus</i>	0	0	0	0	0	0	0	?	?	0	?	?	?	0
<i>Erythrosuchus</i>	1	1	1	1	1	1	1	1	1	0	1	1	1	0
<i>Euparkeria</i>	1	1	0	0	0	1	1	1	?	0	0	1	1	0
<i>Osmolskina</i>	1	1	0	0	0	1	1	1	0	0	0	1	1	0
<i>Dorosuchus</i>	1	?	?	0	?	1	1	?	?	?	?	?	0	?
<i>Turfanosuchus</i>	1	?	?	0	?	1	1	?	?	1	0	?	1	?
<i>Chanaresuchus</i>	2	2	?	?	?	?	0	0	?	?	?	?	?	?
<i>Parasuchia</i>	2	2	0	1	1	?	1	1	0	1	0	1	?	0
<i>Batrachotomus</i>	2	2	?	0/1	0	1	1	1	1	1	1	1	1	1
<i>Stagonolepis</i>	2	2	?	0	1	1	?	?	?	1	0	?	?	1

Batrachotomus according to Gower (2002)

Dorosuchus according to Sennikov (1989, 1995)

Euparkeria according to Gower and Weber (1998)

Hyperodapedon after Benton (1983)

Proterochampsia according to Romer (1971)

Prolacerta according to Gow (1975, fig. 35)

Stagonolepis according to Gower and Walker (2002)

Turfanosuchus according to Wu and Russell (2001, p. 43, figs 3, 5)

